NEW INSIGHTS INTO CRYSTALLIZATION:

FROM THERMODYNAMICS TO POLYMORPHISM AND KINETICS

HAN GUANGJUN

M. ENG., NUS, SINGAPORE

A THESIS SUBMITTED FOR
THE DEGREE OF DOCTOR OF PHILOSOPHY

DEPARTMENT OF CHEMICAL & BIOMOLECULAR ENGINEERING

NATIONAL UNIVERISTY OF SINGAPORE

2007

Acknowledgements

With deep sense of gratitude and profound respect, I sincerely thank my supervisor Prof Reginald B. H. Tan. His resourcefulness, enthusiasm, professional guidance and excellent supervision created a very favorable environment for my research work and got me increasingly interested in the research. Such an encouraging environment definitely inspired me to come out with new ideas one after another, which accounted for the great success of the challenging research in a broad area covering thermodynamics, polymorphs and kinetics of crystallization. Indeed, it was an important and enriching experience under his supervision that had positive and significant effects on my career development.

I would like to thank my former colleagues Mdm Li Xiang and Mdm Li Fengmei (the Dept of Chemical and Biomolecular Eng, NUS) for supporting my job and my research. Without their assistance, my research work would not have been done that efficiently.

I am thankful to the following undergraduate students for their assistance with some of my experimental and numerical work during the period of carrying out their Final Year Projects: Tian Fanghui, Ang Yixuan, Ng Suat Ling Vivien, Ng Wei Jun Andy, Heng Wei Jie, Chen Sue Ann, Ong Shu Ling, Han Yong Yuan, Ang Yong Wei, Leong

Guorong, Kwan Li Min Beatrice, Wu Xinpei, Lim Lihua Charlotte, Teo Lizhu, Zheng Zi Jian, Ng Boon Foong, Lee Syin Dee, Ong Geok Hoon and Ng Huiting.

I am grateful to Dr Yu Zaiqun (Institute of Chemical and Engineering Sciences, Singapore). The discussion with him about the crystal growth kinetics and its experimental measurement was very useful, which helped me carry out the project of kinetics more efficiently.

As a part-time PhD candidate, weekends and public holidays were often the time for me to do the research. Without the full support of my family, it would not have been possible for me to complete my PhD study. Dedicating this thesis to my wife Zeng Yingzhi is a minor recognition of her full support, great encouragement, taking good care of my sons and assuming housekeeping while she did a full-time research work with IHPC (Institute of High Performance Computations).

Table of Contents

Summary

In this study, a new and simple technique, namely **Steady State Shifting Technique,** has been developed to overcome the difficulty in measuring thermodynamic activity for supersaturated electrolyte-containing solutions to provide an in-depth insight into crystallization. The successful application of the proposed technique to thermodynamic studies of a few ternary electrolyte+nonelectrolyte+H_2O systems has been demonstrated, in a wide range of solution concentrations from dilute up to the onset of nucleation. New thermodynamic data in the supersaturated region were obtained and interesting phenomena were found. The supersaturated activity data enabled the good thermodynamic consistency between activity and solubility to be confirmed. With the activity data for the ternary systems and solubility data of the nonelectrolytes, activity data for binary supersaturated nonelectrolyte aqueous solutions were derived. It is expected that the new technique can be applicable to many other systems, based on the experimental framework established in this study.

The obtained activity data, particularly those for NaCl+glycine+H_2O, were well analyzed and interpreted by the proposed molecular interaction and the formation of different ion-glycine complexes. More importantly, the analysis implied that the introduction of univalent ions (e.g. Na^+ and Cl^-) from a 1:1 electrolyte would significantly disrupt the formation of glycine cyclic dimers which are building units of α-glycine polymorph, while it would generate building units (singly-charged ion-glycine complexes) of γ-glycine polymorph. Therefore, it would be a general phenomenon that

univalent ions inhibit α-glycine and promote γ-glycine. This naturally led to the systematic exploration of the impacts of different electrolytes on glycine polymorphs.

The experimental investigation of glycine polymorphs formed from different electrolyte solutions revealed an interesting pattern: 1:1 (e.g. KCl) and 1:2 (e.g. $(NH_4)_2SO_4$) electrolytes substantially inhibit α-glycine and promote γ-glycine, while 2:1 (e.g. $CaCl_2$) and 2:2 (e.g. MgSO4) electrolytes have a higher tendency to induce α-glycine. The mechanisms have been proposed based on molecular interaction, ion-glycine complex formation and chemistries of glycine polymorphs. They suggested that the valence(s), rather than other properties of the ions from an electrolyte primarily determine the outcome of glycine polymorphs formed from electrolyte solutions, as the valences of electrolyte ions affect the formation of ion-glycine complexes and they eventually exert substantial impacts on the anisotropic growth rates from the facets of polymorphic glycine nuclei. It was then logical to quantify glycine crystal growth rates from electrolyte solutions.

The kinetic study of γ-glycine crystals from different electrolyte solutions has been done using a batch isothermal crystallizer. As it can be expected, 1:1 and 1:2 electrolytes tremendously enhance the growth rates of γ-glycine crystals, while 2:1 and 2:2 electrolytes have a much weaker influence on the enhancement of γ-glycine growth. Though different ions affect the growing faces of γ-glycine crystals differently, the obtained kinetic data lend additional support to the mechanisms proposed for glycine polymorphs from electrolyte solutions.

List of Tables

List of Figures

Nomenclature

a – thermodynamic activity

a^{Sat} – thermodynamic activity at saturation point

A_0 – initial crystal surface area, m^2

A – crystal surface area, m^2

amrd – absolute mean relative difference

EDB – electrodynamic balance

emf – electromotive force, mV

g – power of the power low for crystal growth

ISE – ion selective electrode

K_{SP} – solubility product of a nonelectrolyte

k_g – growth rate coefficient

k_v – volume shape factor

k_a – surface shape factor

L – crystal size, meter

L_0 – initial crystal size, meter

m – unit of concentration, molality (i.e. mol/kg-H_2O)

m_A – nonelectrolyte (e.g. glycine) concentration, molality

m_S – electrolyte (e.g. NaCl) concentration, molality

m^{Sat} – nonelectrolyte (e.g. glycine) solubility in a solution, molality

$m_A^{I,Sat}$ – nonelectrolyte (e.g. glycine) solubility in pure H_2O, molality

$m_A^{II,Sat}$ – nonelectrolyte (e.g. glycine) solubility in an electrolyte solution, molality

mV – milli volt

R_A – mass growth rate, kg/m^2/s

R_G – linear growth rate, m/s

$R_{G,N}$ – normalized linear growth rate, m/s

S – slope of Nernst equation, mV

T – measurement temperature, ^oC

T_R – reference temperature, ^oC

T_S – saturated temperature, ^oC

W_0 – initial crystal mass, kg

W – crystal mass, kg

ΔE^0 – the intercept of the Nernst equation, mV

ΔE^I – type I cell potential, mV

ΔE^{II} – type II cell potential, mV

ΔL – increment of crystal size, meter

Δt – time interval, second

σ – relative supersaturation, defined as $\sigma = (m_A - m_A^{Sat})/m_A^{Sat}$

$\Delta\mu$ – difference in chemical potential, J/mol

μ_A^0 – chemical potential of a nonelectrolyte at its reference state, J/mol

μ_A – chemical potential of a nonelectrolyte in a solution, J/mol

μ_A^{Sat} – chemical potential of a nonelectrolyte in a solution saturated with the nonelectrolyte, J/mol

$\mu_A^{I,Sat}$ – chemical potential of a nonelectrolyte at the saturation point $m_A^{I,Sat}$ in its binary nonelectrolyte+H_2O solution, J/mol

$\mu_A^{II,Sat}$ – chemical potential of a nonelectrolyte at electrolyte m_S and saturation point $m_A^{II,Sat}$ in its ternary electrolyte+nonelectrolyte+H_2O solution, J/mol

μ_A^{Crys} – chemical potential of a nonelectrolyte solid crystal, J/mol

γ_A^I – activity coefficient of a nonelectrolyte at m_A in its binary nonelectrolyte+H_2O solution

$\gamma_A^{I,Sat}$ – activity coefficient of a nonelectrolyte at the saturation point $m_A^{I,Sat}$ in its binary nonelectrolyte+H_2O solution

γ_A^{II} – activity coefficient of a nonelectrolyte at electrolyte m_S and nonelectrolyte m_A in its ternary electrolyte+nonelectrolyte+H_2O solution

$\gamma_A^{II,Sat}$ – activity coefficient of a nonelectrolyte at m_S and solubility $m_A^{II,Sat}$ in its ternary electrolyte+nonelectrolyte+H_2O solution

$\frac{\gamma_A^{II}}{\gamma_A^I}$ – activity coefficient ratio of a nonelectrolyte at a given nonelectrolyte molality m_A

$\gamma_\pm^I$ – mean ionic activity coefficient of an electrolyte (e.g. NaCl) at m_S in its binary electrolyte+H_2O solution

$\gamma_\pm^{II}$ – mean ionic activity coefficient of an electrolyte (e.g. NaCl) at electrolyte m_S and nonelectrolyte m_A in its ternary electrolyte+nonelectrolyte+H_2O solution

$\frac{\gamma_\pm^{II}}{\gamma_\pm^I}$ – mean ionic activity coefficient ratio of an electrolyte (e.g. NaCl) at a given electrolyte molality m_S

$(\frac{\gamma_{\pm}^{II}}{\gamma_{\pm}^{I}})_{exp}$ – experimental mean ionic activity coefficient ratio of an electrolyte (e.g. NaCl) at a given electrolyte molality m_S

$(\frac{\gamma_{\pm}^{II}}{\gamma_{\pm}^{I}})_{corr}$ – correlated mean ionic activity coefficient ratio of an electrolyte (e.g. NaCl) at a given electrolyte molality m_S

ν – stoichiometric number per mole of electrolyte

Chapter 1 Introduction

In many industries, one of the most important methods for separation and purification of valuable crystalline chemicals is crystallization from solution (Mohan and Myerson, 2002). Crystallization phenomena, such as nucleation, polymorphism and crystal growth are vital to industries, especially to pharmaceutical industry, as the failure to control polymorphism of a drug can lead to a disastrous consequence (Davey et al., 1997; Desiraju, 1997; Ferrari and Davey, 2004; Knapman, 2000; Mohan and Myerson, 2002; Qiu and Rasmuson, 1990; Roelands et al., 2007). This is because the behavior of a drug can be drastically affected by its polymorphs, causing the rate of uptake in the body to change considerably and making the biological activity out of the desired range. In extreme cases (e.g. chloramphenicol-3-palmitate), the danger of fatal dosages can be created if a wrong polymorph is administrated (Knapman, 2000). Therefore it is required to gain a full understanding of these crystallization phenomena.

As solution crystallization which can only take place in supersaturated solutions is a molecular recognition process, it is understandable that molecular interaction and complex formation in a solution can influence the crystallization phenomena tremendously. Therefore, it is of practical importance to probe how molecules to interact and what complexes to form in supersaturated solutions, especially when an impurity, either desired or undesired, is introduced.

It has been recognized that thermodynamics of supersaturated solutions can play a significant role in the fundamental exploration of these crystallization phenomena, since the thermodynamic activity coefficients of a solute are related to molecular interaction, complex and cluster formation etc. In fact, study on thermodynamics of supersaturated solutions in modeling and fundamental understanding of the crystallization phenomena has been an active research area of both experimental and theoretical interests (Izmailov and Myerson, 1999; Koop et al., 2000; Mohan and Myerson, 2002; Mullin and Sohnel, 1977; Na et al., 1994; Öncül et al., 2005).

For thorough kinetic studies on nucleation and crystal growth from supersaturated solution, the thermodynamic driving force (i.e. chemical potential difference, $\Delta\mu$) should be used, and therefore solute activity coefficients in the supersaturated region are required (Garside et al., 2002; Granberg et al., 2001; Grant, 2000; Koop et al., 2000; Mohan and Myerson, 2002; Mullin and Sohnel, 1977; Öncül et al., 2005). Unfortunately, thermodynamic activity data of supersaturated solutions are generally not readily available (Mohan and Myerson, 2002), mainly due to the lack of proper experimental methods (Han and Tan, 2006). As a result, the thermodynamic driving force for nucleation or crystal growth is often approximated by the solute concentration difference. For special cases (e.g. ideal solutions), such an approximation may be adequate. However, as pointed out by Mohan et al. (2000) and Mohan and Myerson (2002), expressing the driving force for nucleation and crystal growth in terms of solute concentration difference is inadequate for many real systems, and it can lead to large

discrepancies which in turn may incorrectly bias the analysis of the crystal growth rate and the interpretation of the kinetic mechanisms.

Due to the general unavailability of the thermodynamic activity data for supersaturated solutions, the actual applications of thermodynamics to the exploration of the crystallization phenomena are very limited. Nevertheless, studies on a few special cases have shown how powerful the thermodynamics of supersaturated solutions can be.

Koop et al. (2000) studied the homogeneous ice nucleation rates from a broad spectrum of binary inorganic and organic aqueous solutions. When the authors used the thermodynamic driving force derived from freezing-point depression, they obtained a universal expression for homogeneous ice nucleation rates. They found, surprisingly, that the nucleation rate coefficient for homogeneous ice nucleation depends on the water activity alone and is independent of the nature of the solute in the binary aqueous solutions.

Izmailov and Myerson (1999) investigated the effects of Cr^{+3} ions (as an impurity, a few ppm) on crystallization of ammonium sulfate [$(NH_4)_2SO_4$] from its highly supersaturated aqueous solutions. In their investigation, the water (solvent) activity was directly measured using the electrodynamic balance (EDB) method (Cohen et al., 1987; Knezic et al., 2004) while the solute $(NH_4)_2SO_4$ activity was calculated by Gibbs-Duhem relationship, with the assumption that the activity coefficient of the impurity Cr^{+3} is unity. The result they presented was provoking. From point of view of thermodynamics, Cr^{+3}

ions seem to promote the nucleation of $(NH4)_2SO_4$, which is opposite to the observations made by another research group (Kobota and Mullin, 1995). It should be pointed out that the activity coefficient of the impurity Cr^{+3} may not be unity and therefore a rigorous method needs to be developed for accurately calculating the impurity activity (Mohan and Myerson, 1999).

Veverka et al. (1991) analyzed the thermodynamics of continua and they showed that a concentration gradient always develops in a vertical column of a stagnant supersaturated solution under the influence of a gravitational field when the difference in the partial specific volumes of solute and solvent is not zero. Interestingly, though they did not assume any cluster formation, their thermodynamic analysis is consistent with the concept of cluster formation in supersaturated solutions.

Na et al. (1994) experimentally measured the activities for two binary supersaturated aqueous solution systems glycine+H_2O and NaCl+H_2O, using the electrodynamic balance (EDB) method. The activity data were then used to determine the size of the critical clusters at a given concentration, which provided a more quantitative analysis of nucleation.

Although the importance of thermodynamics in polymorph control was highlighted (Davey et al., 1997; Desiraju, 1997), the advanced applications of thermodynamics to reliably predict and control the outcome of polymorphs were hardly reported. In general, many more applications of thermodynamics of supersaturated

solutions to exploration of crystallization phenomena need to be fulfilled. In fact, in order to provide an in-depth insight into the nucleation, polymorphism and kinetics, reliable and accurate thermodynamic activity data of supersaturated solutions are required while they are difficult to be obtained. Therefore, the obstacle in obtaining the thermodynamic activities for supersaturated solutions has to be overcome.

Experimentally, there are several traditional methods available for measuring activity coefficients (Rard and Platford, 1991). These methods include the diffusivity-based method, the freezing-point depression measurement, the boiling-point elevation measurement, the isopiestic method and the potentiometric method. As it was noted, the isopiestic method and the potentiometric method (i.e. electrochemical method) are the major conventional techniques commonly used for measuring activity coefficients of under-saturated solutions (Khoshkbarchi and Vera, 1996b; Rard and Platford, 1991). In general, all these traditional methods mentioned above are unlikely to be suitable for supersaturated solutions, due to their features. Consequently the experimental activity data can normally be obtained only up to the saturation limits (Cohen et al., 1987). More detailed explanation of why these methods fail to work in the supersaturated region will be elaborated in **Chapter 2**.

In order to overcome this experimental difficulty which arises when a solution is supersaturated, the electrodynamic balance (EDB) method was developed and used to measure the activity coefficient for a supersaturated aqueous solution droplet (Chan et al., 2005; Cohen et al., 1987; Knezic et al., 2004; Na et al., 1994; Peng et al., 2001). The

electrodynamic balance was usually made by individual researchers to measure the solution droplet concentration at a given vapor pressure, normally with an assumption that the solute was not volatile. The solute activities were then calculated using the Gibbs-Duhem equation.

The EDB method allowed a very high level of supersaturation to be reached without resulting in nucleation. However, for under-saturated solutions or solutions with a low level of supersaturation, the required time for reaching the equilibrium could be prohibitively long (Cohen et al., 1987) and experimental measurements failed (Chan et al., 2005; Na et al., 1995). Further more, the uncertainties in controlling or determining the quantities (e.g. relative humidity RH, solution concentration) were quite large (Chan et al., 2005; Na et al., 1995). Especially when the solutes were volatile, the uncertainty in determining mass fraction of a solution droplet became even larger (Chan et al., 2005; Na et al., 1995). Though efforts were made to reduce this uncertainty, the accuracy in determining concentration was still questionable as the evaporation loss of a solute could be up to 5% (Chan et al., 2005).

Using thermodynamic models is one alternative for obtaining activity coefficients. Although currently available thermodynamic models (e.g. NRTL, UNIQUAC, UNIFAC) and quantum mechanics (Sum and Sandler, 1999; Sandler, 2003) for predicting activity coefficients in solute-solvent systems may be generally useful for under-saturated solutions, their applicability to supersaturated solutions has yet to be confirmed by validation with experimental activity data. Without accurate experimental activity data,

the applicability of these standard thermodynamic models to supersaturated solutions remains questionable. In fact, the behavior of under-saturated solutions and supersaturated solutions may be vastly different. Bui et al. (2003) showed that the water activities in $CaCl_2$ solutions change significantly around the solubility point. Ginde and Myerson (1991) experimentally demonstrated that, for solution systems glycine+H_2O and KCl+H_2O, the viscosity and diffusivity vary substantially with solute concentration around the solubility point. Such a behavior has been attributed to significant cluster formation (Larson and Garside, 1986; Mohan et al., 2000; Ohgaki et al., 1991, 1992). Cluster formation may also partly explain the unsatisfactory performance of the UNIFAC equation for activity prediction in the supersaturated domain (Peng et al., 2001).

It can be seen that the unavailability of accurate and reliable experimental activities for supersaturated solutions is mainly due to the lack of suitable experimental methods. Even if the EDB method can be applied to highly supersaturated solutions, without other suitable methods, it is difficult to verify the activity data obtained by EDB. Moreover, when the solute is volatile, the accuracy of concentration determination is a big concern due to the evaporation loss of solute, which would lead to erroneous activity and hence undermine the EDB method. Furthermore, systematic and rigorous studies on solute activities for multi-component supersaturated solutions are hardly found, though biochemicals are often crystallized from multi-component supersaturated solutions (e.g. aqueous electrolyte-containing solutions. Khoshkbarchi and Vera, 1996b).

In this work, a new technique, **Steady State Shifting Technique**, for the conventional potentiometric method was developed for measuring the thermodynamic activities of supersaturated solutions. As this new technique only requires the change of the operation procedure for the conventional potentiometric method and additional hardware is not necessary, practically it is as simple as the conventional potentiometric method.

The new technique was applied to measure thermodynamic activities for three ternary NaCl+amino acid+H_2O systems (namely NaCl+glycine+H_2O, NaCl+DL-serine+H_2O and NaCl+DL-alanine+H_2O). These obtained activity data in the supersaturated region enabled the complexes which are formed by electrolyte ions (Na^+ and Cl^-) and amino acid dipolar ions (i.e. zwitterions) to be analyzed more thoroughly. The outcome of this analysis naturally guided the research to further explore the phenomena of glycine polymorphs and its crystal growth from solutions with presence of different electrolytes.

In the presentation of this research work, literature review is given in **Chapter 2**, covering three major aspects of crystallization: 1) the traditional experimental methods for measuring activities for solutions and their difficulties when the solutions are supersaturated; 2) crystal polymorphs; 3) crystal growth kinetics. In **Chapter 3**, the fundamental of the transport phenomena occurring in an electrochemical cell used for the poteniometric method is analyzed. The development of the new technique (namely Steady State Shifting Technique**)** for activities of supersaturated solutions is presented.

The experimental verification of the new technique is elaborated. Using the new technique, thermodynamic activity data for the three ternary systems (NaCl+glycine+H_2O, NaCl+DL-serine+H_2O and NaCl+DL-alanine+H_2O) are obtained in both under-saturated and supersaturated regions. The new technique is further extended to nonelectrolyte binary aqueous solutions (i.e. nonelectrolyte+H_2O).

In **Chapter 4**, it is showed how the obtained activity data for the glycine+NaCl+H_2O solutions in the glycine supersaturated region lead to the implications that any 1:1 electrolytes (the same type as NaCl) would induce γ-glycine polymorph and would enhance γ-glycine growth. Naturally, the impacts of many electrolytes including NaCl on glycine polymorphs and crystal growth rate are systematically investigated and the very interesting results are presented in **Chapters 5** (for glycine polymorphs) and **Chapter 6** (crystal growth) respectively.

In **Chapter 7**, conclusions are drawn and recommendations are made for the future work.

Chapter 2 Literature Review

This review covers three important aspects of solution crystallization, namely solution thermodynamics, crystal polymorphism and crystal growth kinetics.

As was pointed out in the Introduction (Chapter 1), on the one hand, solution thermodynamics can play a significant role in exploring crystal polymorphism and crystal growth kinetics; on the other hand, accurate thermodynamic activity data for supersaturated solutions are not readily available (Mohan and Myerson, 2002), mainly due to the lack of suitable experimental methods. Therefore, how to experimentally obtain the activity data in the supersaturated region will be reviewed first.

2.1 Experimental Methods for Thermodynamic Activity

Experimentally, there are several methods which may be used for measuring thermodynamic activity coefficients of solutions (Rard and Platford, 1991). These methods include diffusivity-based method, freezing-point depression, boiling-point elevation, vapor pressure measurement, isopiestic method and potentiometric method (i.e. electrochemical method), with the isopiestic method and the potentiometric method being much more commonly used (Rard and Platford, 1991). These methods have their own advantages and disadvantages in measuring either solvent or solute activity coefficient for under-saturated solutions. However, they are generally not suitable for supersaturated solutions.

The diffusivity-based method is to employ the obtained diffusion coefficients to derive the activity coefficient of a solute (Annunziata et al., 2000). An application of this method to a particular supersaturated solution was reported (Annunziata et al., 2000). But it should be noted that, the required precise diffusion coefficients may be available only for a few systems and usually only at 298.15 °C (Rard and Platford, 1991). Especially for supersaturated solutions, the data of precise diffusion coefficients are far fewer. Moreover, it seems that to obtain precise diffusion coefficients for general supersaturated solutions is challenging too (Annunziata et al., 2000; Chang and Myerson, 1986; Mohan et al., 2000).

The freezing-point depression measurements may be used to determine the solvent activity coefficient only for special temperatures at which solid-liquid equilibrium between the solution and the solvent solid (e.g. ice) can be held at a given solute concentration (Rard and Platford, 1991). This method gives the solvent activity as a function of solute concentration but at different temperatures. It is necessary to convert the solvent activity data to a common temperature, using enthalpy and heat capacity data. The solute activity coefficient data can be obtained via the Gibbs-Duhem equation once the solvent activity data are available. It is obvious that, for a solution supersaturated with a solute at a given temperature of interest, the solute may significantly nucleate already far before the freezing-point is reached. Thus this method is generally not applicable to solutions supersaturated with a solute.

The boiling-point elevation method generally would not create a supersaturation

with respect to the solute due to the increase of the solution temperature from the given one to its boiling point. Therefore, the boiling-point elevation method is not suitable for supersaturated solutions either.

The general methods for solvent activity coefficients involve a vapor-liquid equilibrium. When the solvent is the only volatile component while all other components are not volatile in a solution, the measurement of the solvent activity becomes simpler. In this particular case, for a vapor-liquid equilibrium system, the vapor pressure of the volatile solvent may be directly measured (Kuramochi et al., 1997) at a given temperature of interest, either by static or by dynamic technique. The vapor pressure is then used to calculate the solvent activity of the vapor phase. Especially when the vapor phase is an ideal gas, the calculation for solvent activity is much easier. As the vapor phase and the liquid phase (solution) is at the equilibrium, the solvent activity in the vapor phase should be equal to the solvent activity in the solution phase. When the solvent is water while the water vapor is an ideal gas, the relative humidity (RH) of the gas phase is the water activity of the solution. With the solvent activity data, the solute activity can be derived from Gibbs-Duhem equation, as was briefed in the freezing-point depression measurements.

It should be noted that, either by static or by dynamic technique, direct measurement of vapor pressure for solvent activity requires careful temperature control as vapor pressure can significantly change with temperature. According to Rard and Platford (1991), solvent activity obtained by direct measurement of vapor pressure

becomes much less accurate when the solution concentration is lower than 1 m (mole/kg solvent). Furthermore, due to the involvement of heat and mass transfer in achieving the vapor-liquid equilibrium, a means of agitation of the vapor-liquid system is needed. However, any type of agitation is very likely to trigger the solute nucleation when the solution is supersaturated with the solute, causing the failure of the measurement. Consequently, direct measurement of vapor pressure of a vapor-liquid system at equilibrium is unsuitable for a supersaturated solution.

The isopiestic method, probably the most commonly used technique for measuring solvent activity coefficients, is also based on vapor-liquid equilibrium. In this method, a reference standard, a well defined and characterized solution, is required. The solvent activities of the reference standard are known at different given concentrations. The reference standard solution and a test solution (or many test solutions) are put in separate open cups (or containers). Then these cups are placed in a sealed and temperature-controlled chamber so that the two solutions share the same vapor phase to allow the solvent to transport from one solution to the other solution. In other words, the solvent evaporates from one solution cup and condensates in the other solution cup. Eventually the thermodynamic equilibrium between the vapor phase and the solution phases should be reached, with the solvent activities in the vapor phase and in the two (or more) solution phases being the same. After the concentrations of both the reference standard and the test solution are analyzed using proper instruments, the known concentration of the standard at equilibrium yields the solvent activity of the reference

standard hence the solvent activity of the test solution, corresponding to the determined concentration of the test solution.

If the solvent is the only volatile component, analyzing the concentrations of both the reference standard and the test solution can be done simply by weighing the reference standard and the test solution after the equilibrium is reached. Since the initial amount of each component in both the standard and the test solution can be known when they are prepared, any change of the mass of the standard or the test solution is due to the volatile solvent, either by evaporation or by condensation. By mass balance, the concentrations of the equilibrated reference standard and the test solution can be determined. The solute activity data can be derived via Gibbs-Duhem equation using the obtained solvent activities and the determined concentrations of the test solutions.

Though the isopiestic method and direct measurement of vapor pressure utilize the same principle of vapor-liquid equilibrium, different quantities are measured, with the former analyzing the solution concentration while the latter directly measuring the solvent vapor pressure. Due to this, the isopiestic method is generally more accurate especially when the solution is dilute (Rard and Platford, 1991). For the isopiestic method, the lower limit of the concentration of a solution may be allowed to be as low as 0.1m (vs 1m for direct measurement of vapor pressure).

It should be noted that normally the isopiestic chamber is rocked back and forth to facilitate the heat and mass transfer so that the uniform temperature can be maintained

and the vapor-liquid phase equilibrium can be reached faster. However, even if the heat and mass transfer is enhanced, a single run of isopiestic experiments usually takes several days or even longer (Rard and Platford, 1991). As a result, a particular difficulty arises when the test solution is supersaturated. On the one hand, shaking the sample solution is required to achieve the equilibrium but it is very likely to induce an immediate nucleation and cause the measurement to fail, although a few exceptions were reported (Rard and Platford, 1991; Bui et al., 2003) when the solutes have a particularly low tendency to nucleate from their supersaturated solutions. On the other hand, without shaking, the time required to reach the equilibrium can be much longer than the induction time for spontaneous homogeneous nucleation, again rendering the measurement attempt futile.

The potentiometric method is another technique which is commonly used for the mean ionic activity coefficients of an electrolyte in solutions (Butler and Roy, 1991). As its working principle is based on the electrochemistry, this method is also termed as electrochemical method. In briefing, an electrochemical cell is filled with an electrolyte solution at a given molality m_s. Two electrodes, one reference electrode and one indicator electrode, are put in the electrolyte solution to measure the electrochemical cell potential ΔE (i.e. cell electromotive force, emf) at the given temperature. As the cell potential ΔE is related to the electrolyte molality m_S and the mean ionic activity coefficient $\gamma_{\pm}$ of the electrolyte as described by the Nernst equation, the mean ionic activity coefficient $\gamma_{\pm}$ may be calculated from the Nernst equation.

Traditionally, a AgCl/Ag electrode was often used as the reference electrode for cell potential measurement. This type of reference electrode needs filling solution which can develop liquid junction potentials and create an uncertainty in measuring cell potential. When ion selective electrodes (ISEs) for both cation and anion of a given electrolyte are available, a number of studies (Breil et al., 2001; Haghtalab and Vera, 1991; Han and Pan, 1993; Ji et al., 2001) have suggested that the liquid junctions can be eliminated by using the cation selective electrode as the indicator electrode and the anion selective electrode as the reference electrode, since both cation and anion selective electrodes do not need filling solutions.

An electrochemical cell at a given electrolyte molality (m_S) with two ion selective electrodes (ISEs) may be expressed as

cation ISE|electrolyte (m_S), H_2O|anion ISE

The Nernst equation for this cell may be generally expressed as (Bulter and Roy, 1991; Khoshkbarchi and Vera, 1996a, 1996b):

$$\Delta E = \Delta E^0 + S \ln(a) \qquad (2\text{-}1\text{-}1)$$

where ΔE^0 is the difference between the electrode standard potentials, S the slope of the Nernst equation and a the mean ionic activity of the electrolyte. For a 1:1 electrolyte (e.g. NaCl), at a given molality m_S, the Nernst equation may be given (Khoshkbarchi and Vera, 1996b):

$$\Delta E = \Delta E^0 + S \ln(m_S \gamma_\pm) \quad (2\text{-}1\text{-}2)$$

Theoretically, the slope S of the Nernst equation may be evaluated. For a 1:1 electrolyte (e.g. NaCl), we nay have:

$$S = \frac{2RT}{F} \quad (2\text{-}1\text{-}3)$$

where R is the universal gas constant (8.314 J/mol), T the absolute temperature (Kelvin) and F the Faraday constant (96497 C/mol). However, for a real cell, the actual values of the slope S and the standard potential ΔE^0 for a given pair of electrodes at a specified temperature is usually obtained from a linear graphical plot of known experimental data of ΔE vs $\ln(m_S \gamma_\pm)$ (Bates et al., 1983; Ji et al., 2001; Khoshkbarchi and Vera, 1996b), or from extrapolation of cell potentials of dilute electrolyte solutions (Bulter and Roy, 1991). With the values of the slope S and the standard potential ΔE^0, measuring the cell potential ΔE at any other given electrolyte molality m_S yields the mean ionic activity coefficient $\gamma_\pm$ of the electrolyte. As it can be seen, the potentiometric method directly measures the solute activities and therefore integrating the Gibbs-Duhem equation for the solute activity is not needed.

The correct and accurate cell potential can be obtained only when the cell reaches its steady state, i.e. when both the temperature and the concentration profiles in the cell remain unchanged. How fast the steady state of the cell can be reached depends on the rates of mass and heat transfer in the media in the cell, including the cell bulk solution, solution films on external electrode surfaces, electrode membranes and the electrode housings. To facilitate achieving a steady state of an electrochemical cell, stirring the cell solution is essential to enhance the heat and mass transfer. However, when the solution is

supersaturated at the temperature of interest, the same problem as that encountered in the isopiestic method arises: stirring the solution could cause an immediate nucleation which results in the failure of the cell potential measurement. That would explain why the potentiometric method was not used for supersaturated solution over the past decades (Roberts and Kirkwood, 1941).

In order to overcome this experimental difficulty commonly encountered in those methods just mentioned above, the electrodynamic balance (EDB) method was developed and used to measure the solvent activities for supersaturated aqueous solutions (Chan et al., 2005; Cohen et al., 1987; Knezic et al., 2004; Na et al., 1994; Peng et al., 2001).

In the EDB method, a single tiny charged aqueous solution droplet (typically 20 μm in diameter) is suspended at the centre of a direct current (dc) electric field created in the electrodynamic balance while a stream of humidity-controlled air passes over the solution droplet. The total mass of the solution droplet changes with the solvent transfer between the solution droplet and its surrounding vapor phase. The dc voltage is adjusted to maintain the suspension of the solution droplet till a steady state (i.e. an equilibrium between an under-saturated solution droplet and its surrounding vapor phase, or a quasi-equilibrium between a supersaturated solution droplet and its surrounding vapor phase) is established. At the steady state, the water activity in the solution droplet is equal to the relative humidity of the vapor phase.

The solution droplet is continuously weighed by using the dc field force to determine the steady state at a given temperature and solvent vapor pressure. In the same way, the dry mass of the solution droplet can be determined too when the humidity is zero. If water is the only volatile component in the solution droplet, the droplet concentration (mass fraction or molality) can be determined simply by the ratio $\frac{V_{DC}^{dry}}{V_{DC}^{wet}}$ of the measured dc voltages when the droplet is dry (v_{DC}^{dry}) and wet (v_{DC}^{wet}) respectively at its corresponding steady states (Mohan and Myerson, 1999), assuming that the charges of the solution droplet are kept unchanged.

With the water activities at different droplet concentrations, the thermodynamic activities of the non-volatile solute in a binary solution at different concentrations can be derived by integrating the Gibbs-Duhem equation from one reference concentration to the concentration of interest (Cohen et al., 1987; Mohan and Myerson, 2002).

The EDB method allows a very high level of supersaturation to be reached without resulting in nucleation due to the absence of nucleation sites in the suspended droplet. However, at high humidity corresponding to under-saturated solutions or solutions with a low level of supersaturation, the required time for reaching equilibrium could be prohibitively long (Cohen et al., 1987), and the droplet may become unstable (Na et al., 1995), leading to failure of experiment.

In addition, the uncertainties in controlling or determining the quantities are quite large (Chan et al., 2005; Na et al., 1995). For instance, the uncertainty of the controlled

relative humidity is up to 1% while the uncertainty of the solute mass fraction is even up to 0.03 (Chan et al., 2005). Especially when the solutes are volatile, the uncertainty in determining mass fraction may become much bigger, as the evaporation loss may be very significant (Chan et al., 2005; Na et al., 1995). Even if efforts were made, the evaporation loss of a solute was still up to 5 wt% (Chan et al., 2005), which raised the concern on the accuracy and reliability of the determined solution concentration hence the resulting solvent and solute activities. In fact, the discrepancies in the activity data obtained by different investigators using the EDB method could be significant (Chan et al., 2005; Na et al., 1995), due to the evaporation loss of the organic solutes (e.g. glyicne and alanine). It appears that it would be a hard task to address the concern of the reliability and accuracy of the data obtained by the EDB method when the solute is volatile.

In summary, the current methods except for the EDB method for activities are applicable to under-saturated solutions only. Though the EDB method is suitable for highly supersaturated solutions, it could be unreliable when the concentrations of solutions approach their saturation points or below. The evaporation loss of volatile solutes would further sabotage the applicability of the EDB method, as volatile solutes form a great spectrum of solid-liquid systems. On the other hand, due to the lack of other suitable methods, it is difficult to verify the activity data obtained by the EDB method in the supersaturated region.

One of the objectives of this study is to develop a new technique for the poteniometric method for thermodynamic activity of supersaturated solutions. To fulfill this objective, the transport phenomena occurring in an electrochemical cell used for the poteniometric method are thoroughly analyzed to reveal the rate controlling step which makes the poteniometric method fail to work for supersaturated solutions. Taking the advantages of negligible liquid expansion and relatively fast heat transfer, a unique technique termed as Steady State Shifting Technique, is proposed. The development of the new technique is elaborated in **Chapter 3**.

2.2 Crystal Polymorphism

A polymorph is generally defined as a solid crystalline phase of a given compound which has at least two different arrangements of its molecules in the solid state. Or using a safe criterion of classification, a system is classified as a polymorphic one if the crystal structures are different but lead to identical liquid and vapor states (Bernstein, 2002). A similar definition was also given by Doki, et al. (2004), stating that polymorphs are crystals with different structures while they are chemically identical. Apparently, when different polymorphs of a given crystalline substance are dissolved into a solution or become vapor, their molecules in the solution or vapor are the same. Therefore the concept of polymorphism is only meaningful to solid crystalline substances.

Crystal polymorphism is a widespread phenomenon. It can be a vital problem in solid state chemistry, material science and particularly pharmaceutical science

(Boldyreva, et al., 2003; Desiraju, 1997; Ferrari and Davey, 2004). As pointed out (Ferrari and Davey, 2004; Sun et al., 2006; Weissbuch et al., 1994a), polymorphs of a compound can have different mechanical, thermal and physical properties including solubility, melting point and crystal shape. These properties can have a great influence on the bioavailability of solid drugs in pharmacology, preparation of functional materials, filtration and tableting processes of pharmaceutical, food and other specialty materials.

Thermodynamically, polymorphs exhibit different stability. At a given condition, one of the polymorphs is the most stable while others are metastable. Consequently, polymorphs can be transformed from one to another either in a solution or in solid state (Black and Davey, 1988). In fact, polymorphs are a particularly important type of problems in pharmaceutical processing. Firstly, it is necessary to control conditions to produce the desired polymorph. Secondly, if the desired polymorph is thermodynamically metastable, it is needed to prevent the polymorphic transition from one form to another form, especially when the desired metastable form is the one approved by the regulatory agency.

Recently, Knapman (2000) well discussed the impacts of polymorphism of a drug. Failure to control polymorphs of a drug can lead to fatal consequences as the behavior of the drug can be drastically affected by its polymorphs. Alteration of polymorphs can increase or decrease the rate of uptake in human bodies, causing the biological activity to be out of the desired range. In extreme cases, a wrong polymorph can even be toxic. For example, chloramphenicol-3-palmitate (CAPP) is a broad-

spectrum antibiotic which has at least three polymorphic forms and one amorphous form. The marketed form A is the most stable one. Another form B has an eightfold higher bioactivity than form A. If the form B is unwittingly administered due to whatever reason, the danger of fatal dosages is created.

Any unknown or unexpected polymorphic form produced can have an enormous impact on a drug company. For example, the production of ritonavir (Norvir) which is an HIV protease inhibitor developed and marketed by Abbott was halted in 1998 because an unexpected polymorph was observed. Any new polymorph of a drug is not allowed to be marketed before the exact characteristics of the new form are well established, according to Food and Drug Administration (Knapman, 2000).

Another example, significantly impacting the drug company business, involves Glaxo Wellcome who sued Novopharm in 1997 for alleged patent infringement. Glaxo lost its case and Novopharm patented a different polymorphic form of Glaxo's drug, Zantac. Now Novopharm and other companies sell generic Zantac drugs with the new polymorph. This shows that different polymorphs of a drug are recognized legally as different drugs. Therefore, the ability to produce the correct polymorph and to control the polymorphic transition is critical. It rationalizes the fact that understanding and controlling polymorphs hence designing advanced materials has been a subject of broad interest and active research (Sun et al., 2006). Unfortunately, well controlling polymorphs remains challenging, though great progresses have been made (Black and Davey, 1988; Davey et al., 1997; Desiraju, 1997; Knapman, 2000).

Different polymorphs may be obtained by crystallizing a solute from its solutions at different conditions (Davey et al., 1997; Doki, et al., 2004; Towler, et al., 2004; Weissbuch et al., 1994a; Weissbuch et al., 1995). A proposed empirical working hypothesis (Weissbuch et al., 1994a) of crystal polymorphism states that, in supersaturated solutions, solute molecules may assemble to form coexisting clusters (i.e. nuclei) having different structures, with each structure resembling the structure of a particular polymorph. Only clusters exceeding the so-called critical size develop into mature crystals. Depending upon the environments (e.g. solution pH, additive, temperature etc.), the growth of those clusters with a particular structure may be favored greatly while the growth of other clusters may be inhibited extremely, eventually leading to the occurrence of only one specific polymorph from its very origin rather than from the conversion between mature polymorphs. It is also apparent that varying the environments may drastically alter the competition among different clusters and therefore the thermodynamically most stable polymorph can be directly produced too. This empirical working hypothesis is not consistent with the conventional Ostwald's Law which was once used as a guideline for the occurrence of polymorphs. According to Ostwald's Law, a metastable form appears first during crystallization from solution then it is transformed into the stable form (Davey et al., 1997; Ferrari and Davey, 2004). As pointed out by Davey et al. (1997), Ostwald's Law has no general proof, rather it is a special case of nucleation and growth in a polymorphic system.

According to the working hypothesis of crystal polymorphism, crystallization may be controlled to produce the desired polymorph via different strategies.

Traditionally, tailor-made additives were used to control polymorphs (Sun et al., 2006; Weissbuch et al., 1995). These additives are structurally similar to the host solute molecules and hence referred to as 'tailor-made'. Among the tailor-made additives, nucleation inhibitors were often designed and selected for polymorphism control, on the basis of structural information of the host solute and the corresponding crystalline forms (including crystal packing and conformation etc).

With the assistance of stereospecific nucleation inhibitors, a stereochemical approach for controlling crystal polymorphs was suggested (Shimon et al., 1986; Weissbuch et al., 1987, 1994a, 1994b; 1995). The stereochemical additives are composed of two moieties: one, the 'binder', having a similar structure (and stereochemistry) to that of the substrate molecule on the crystal surface where it adsorbs. The second moiety, referred to as the 'perturber' is modified when compared to the substrate molecule, and thus hinders the attachment of the oncoming molecular layers of the solute molecules to the crystal surface. It is understandable that, when molecules of a selected inhibitor are specifically recognized and bound at the surfaces of the particular clusters having the compatible structure, the growth of the involved clusters can be inhibited and the formed clusters may be even disintegrated while allowing other clusters to develop. In fact, designed nucleation inhibitors have been successfully applied to many polymorphic systems (Davey et al., 1997; Weissbuch et al., 1995).

Many different polymorphic systems have been used for mechanism studies, among which glycine (H_2NCH_2COOH), the simplest amino acid, was often chosen as a

model system due to its well-established solution and solid-state chemistries, physical properties and its ability to crystallize in various polymorphic forms (He et al., 2006; Towler et al. 2004; Sun et al., 2006; Weissbuch et al., 1995). In this present study, glycine was also chosen as the model polymorphic system. Therefore, glycine polymorphs are particularly reviewed as follows.

Glycine has at least three well-known polymorphs: α- , β- and γ-glycine among its other polymorphs (Dawson et al., 2005; Doki et al., 2004; Sakai, et al., 1991). The schematic structures of α-glycine and γ-glycine crystals are depicted in Figures 2-2-1 and 2-2-2, using Mercury 1.4.2.

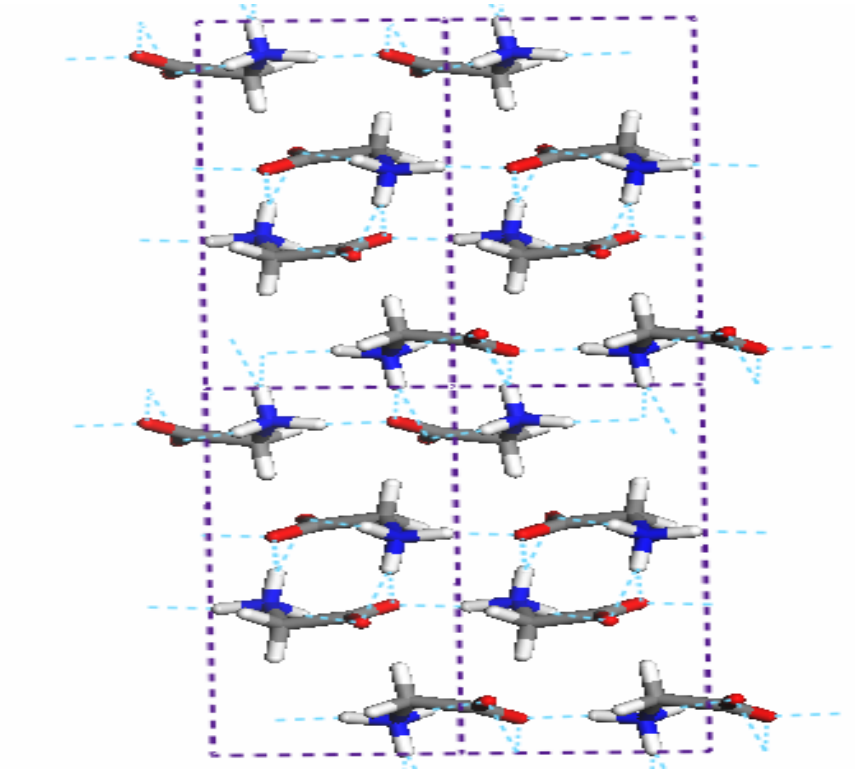

Figure 2-2-1 Schematic structure of a centrosymmetric α-glycine crystal built with elementary cyclic dimers (Towler et al., 2004)

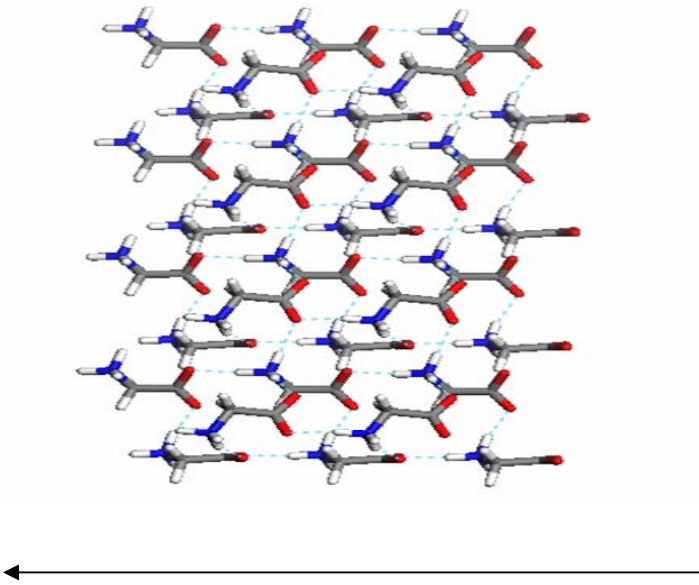

Figure 2-2-2 Schematic structure of a γ-glycine crystal with polar ends [c-axis NH_3^+ rich, slow growing end (+c) and the COO^- rich, fast growing end (-c). Towler et al., 2004]

Thermodynamically α-glycine polymorph is metastable and usually crystallizes from its aqueous solutions at natural pH, near or at its isoelectric point of 5.97, without additives being added in its solutions. As pointed out by Towler et al. (2004), as α-glycine polymorph is very often obtained under modest conditions, it was once misled to the assumption that α-glycine polymorph is thermodynamically most stable. It was only till recent years that the γ-glycine polymorph was recognized to be thermodynamically most stable at around room temperature (Boldyreva, et al., 2003; Doki et al., 2004; Towler et al., 2004). Actually, α-glycine polymorph is kinetically favored under ambient conditions (He et al., 2006). γ-glycine polymorph can be induced using various methods. Generally, tailor-made chemical additives were usually used to obtain γ-glycine (Bhat

and Dharmaprakash, 2002a and 2002b; Moolya et al., 2005; Towler et al., 2004; Weissbuch et al, 1995, 2003), while a few untraditional methods have been reported too (Aber et al., 2005; He et al., 2006; Sun et al., 2006; Zaccaro, et al., 2001). The β-glycine polymorph, formed from a mixed solvent of water and alcohol, is the least stable one at aqueous solutions at any temperature (Doki et al., 2004).

The mechanism for α-glycine polymorph nucleating from its aqueous solutions under mild conditions has been postulated (He et al., 2006; Towler et al., 2004). It suggests that, in an aqueous glycine solution, glycine molecules are transformed into dipolar ions (i.e. zwitterions, $^{+}H_3NCH2COO^{-}$); due to the opposing charges on both ends of the zwitterionic form ($^{+}H_3NCH2COO^{-}$) of a glycine molecule, the zwitterions tend to be attracted to one another via electrostatic forces and hydrogen bonds (O---H) as well. They interact particularly at their both ends. The strong hydrogen bonds make centrosymmetric cyclic dimers $\binom{OOCCH_2NH_3}{H_3NCH_2COO}$ (Chew et al., 2007; He et al., 2006; Towler et al., 2004; Weissbuch et al., 1995; Weissbuch et al., 2003). These cyclic dimers are suggested to be the elementary building units for α-glycine crystals when α-glycine nucleates or grows from neutral solutions, which was supported by atomic force microscopy (AFM) and Grazing Incident X-ray Diffraction (GID) studies where it was found that the smallest step height in the (010) face of α-glycine growing crystals approximately has the thickness of a glycine bilayer (Carter et al., 1994; Gidalevitz et al., 1997). Due to the nature of glycine cyclic dimers where the positively charged amino group ($-NH_3^{+}$) and the negatively charged carboxyl group ($-COO^{-}$) neutralize each other,

α-glycine is not polar (Towler et al., 2004). In contrast, γ-glycine is polar (refer to Figures 2-2-1 and 2-2-2).

The mechanisms for crystallization of γ-glycine polymorph from solutions vary with the methods used for making γ-glycine. Sun et al. (2006) and Zaccaro et al. (2001) reported a method, termed as nonphotochemical laser-induced nucleation (NPLIN), to produce γ-glycine from supersaturated aqueous glycine solution. It was discovered that, when aqueous glycine solutions were exposed to amplified laser impulses for about 30 minutes, crystals were found to nucleate. Upon testing, γ-glycine crystals were confirmed. A mixture of α- and γ-glycine were obtained if the solutions were left to age for a period of time before being exposed to laser impulses. As the solutions aged further, the amount of α-glycine increased.

These authors explained that glycine solutions are transparent at the wavelength of the incident nearinfrared laser pulses thus not absorbing the light, so that a photochemical mechanism for the observed laser-induced nucleation is unlikely. They postulated that the actual mechanism involves an interaction of solute molecules with the oscillating electric field associated with the laser pulses. The oscillating electric fields might be strong enough to induce the partial alignment of the dipolar glycine molecules (zwitterions) in the clusters through the optical Kerr effect in a few nano seconds. In the oscillating electric fields, anisotropically polarizable molecules experience a torque, tending to align themselves so that their most polarizable axes are parallel to the direction of polarization of the incident light. Consequently, these aligned glycine molecules help

form γ-glycine. Moreover, different polarizations can cause the induction of different types of alignments and therefore different polymorphs. Two types of polarization were used, namely linear and circular. The results they obtained showed that the type of polarization used does have a control of glycine polymorphs.

Analogous to the oscillating electric fields, static electric fields were also successfully applied to induce γ-glycine nucleation (Aber et al., 2005), via the principle of molecular polarization and alignment similar to the oscillating electric fields. It was found that when a strong direct current (dc) electric field was applied to aqueous glycine solutions, the electric field would induce the re-alignment of glycine molecules in the formed glycine clusters and the molecules would become oriented and organized, favoring γ-glycine formation.

Another interesting finding was that γ-glycine can be produced from glycine neutral aqueous solutions, by slow evaporation of water from microdroplets of aqueous glycine solutions (He et al., 2006), although it has been reported that normally α-glycine nucleates spontaneously from neutral aqueous glycine solutions (Towler et al., 2004). The evaporation rates of the solutions were varied in order to determine if they had an effect on the polymorph obtained. Results showed that, as long as the rate of evaporation was slow enough for a glycine solution to remain close to the thermodynamic equilibrium throughout the entire evaporation process, the resultant glycine crystal that nucleates from the neutral aqueous solutions would always be γ-glycine, since γ-glycine, the thermodynamically most stable polymorph, is favored under such a condition. On the

other hand, if the evaporation rates are not slow enough, the kinetically stable (but thermodynamically metastable) polymorph, α-glycine would be produced. A mixture of both α- and γ-glycine polymorphs would be formed if the rate of evaporation was intermediate between the low rate and the high rate.

Using the traditional method where a tailor-made additive is added to the glycine solution, γ-glycine could be preferentially crystallized from its aqueous solutions. Weissbuch (et al., 1994a, 1995) showed that racemic hexafluorovaline is an effective inhibitor of growth of α-glycine since it is bound to the four {011} faces of α-glycine, much more efficiently blocking growth of α-glycine, compared with other inhibitors (e.g. α-amino acid additives). Meanwhile, it does not significantly retard the nucleation and growth of γ-glycine. That is because hexafluorovaline is bound primarily at the NH_3^+ end (the slow growing end) of the polar axis of γ-glycine, thus the crystal growing unidirectionally along its polar growing c-axis at the carboxylate COO^- end (the fast growing end). The unblocked fast growing carboxylate COO^- end makes γ-glycine nuclei develop and exceed the critical size faster, thus reinforcing the competitiveness of γ-glycine over α-glycine, highlighting that the fast growing carboxylate COO^- end can play a more important role in controlling polymorphs and enhancing crystal growth. It should be noted that, depending on the solution conditions, carboxylate COO^- end of γ-glycine may grow slower than the NH_3^+ end, as demonstrated by Lahav and Leiserowitz (2001) and Weissbuch et al. (2005).

As γ-glycine polymorph can also nucleate from acidic or alkaline aqueous solutions, Towler et al. (2004) systematically investigated the impacts of pH on glycine polymorphs and therefore revealed the self-poisoning mechanism at either a low or a high pH. In their study, glycine crystallization was carried out in a glass, agitated, 50ml thermostated vessel. It was then found that in the pH range from 3.8 to 8.9, the crystals obtained from glycine supersaturated solutions were always α-glycine, while they were γ-glycine in pH values below 3.8 or above 8.9, regardless of the initial glycine relative supersaturation levels they used.

According to these authors (Towler et al., 2004), when the pH is away from the isoelectric point 5.97, the solution chemistry changes and the glycine zwitterions and/or its cyclic dimers partly become singly charged ions (i.e. charged glycine species). Under acidic conditions (at a low pH), the amino (NH_2) functionality of a glycine molecule can be protonated to form a cation ($^{+}H_3NCH2COOH$). While in alkaline solutions (at a high pH), the carboxylate functionality (COOH) can be deprotonated to form an anion ($H_2NCH_2COO^{-}$). When the polymorph switched at pH 3.8 or 8.9, the mole fraction of these charged glycine ions were estimated to be 0.03 of cations (pH 3.8) or 0.12 of anions (pH 8.9), based on total glycine, with the rest being zwitterions and dimers. It was further estimated that a relative minor change in speciation of ca. 7 wt% charged glycine species is needed to induce crystallization of γ-glycine. As the dimer pairs (i.e. growth units for α-glycine) was only decreased by a very modest amount (ca. 7 wt%), disruption of the nucleation of α-glycine due to the growth units (dimers) destroyed by pH was highly unlikely and therefore excluded.

Their further analysis of the interaction between the charged glycine species and the structure of α-glycine crystals suggested that the α-glycine inhibition at low or high pH was due to self-poisoning. At either a low or a high pH, the charged cations ($^{+}H_3NCH2COOH$) or anions ($H_2NCH_2COO^{-}$) would approach the surface of α-glycine nuclei and would be firmly bound at the surface owing to the affinity. However these charged species do not fit into α-glycine lattices, as a result these adsorbed charged glycine species on α-glycine nuclei prevent α-glycine growth units (cyclic dimers) from integration into α-glycine lattices. Consequently α-glycine nuclei could not eventually develop into critical-sized molecular clusters within a reasonable period of time before the onset of γ-glycine nucleation. These singly charged glycine species ($^{+}H_3NCH_2COOH$ and/or $H_2NCH_2COO^{-}$) would thus act as selective tailor-made additives to inhibit the crystallization of α-glycine.

As for the impact of pH on γ-glycine nucleation, Towler et al. (2004) pointed out that, at a low pH, cations ($^{+}H_3NCH2COOH$) would add to the faster growing, carboxylate rich, end (COO^{-}) of γ-glycine nuclei, while at a high pH, anions ($H_2NCH_2COO^{-}$) would approach and integrate at slower growing, amino rich, end (NH_3^{+}) of γ-glycine nuclei. Hence, it can be seen that, at either a low or a high pH, γ-glycine can nucleate as there is always one available end for γ-glycine to grow (Figure 2-2-2). This proposed 'self-poisoning' mechanism well explains the inhibition of the growth of α-glycine and relative promotion of γ-glycine at a pH away from the isoelectric point 5.97.

Bhat and Dharmaprakash (2002a and 2002b) reported another observation that γ-glycine was produced from glycine solutions when a sodium salt (sodium electrolyte) was added. The used sodium salts included NaCl, NaF, $NaNO_3$ and NH_4Ac (sodium acetate). In order to discover the mechanism, Towler et al. (2004) carried out more experiments for investigation. They crystallized glycine polymorphs from salt solutions containing one of these salts: NaCl, Na_2SO_4, Na_2CO_3, $MgSO_4$, $Mg(NO_3)_2$, $Ca(NO_3)_2$. They found γ-glycine polymorph was induced as long as sodium ions were present in the solutions while no γ-glycine was produced when sodium ions were absent. Since the ionic strength was controlled to be 5.17 for each glycine solution, the impact of nucleus surface energy change on glycine polymorphs due to adsorption of the charged electrolyte ions was not decisive. Eventually, these observations led to the postulation that sodium ions have specific interaction with α-glycine clusters and therefore retard α-glycine growth. However, subsequently, Moolya et al. (2005) obtained γ-glycine from a NH_4NO_3 solution, which apparently was not consistent with the assumed specific interaction between sodium ions and α-glycine clusters, since NH_4NO_3 does not contain any sodium ions.

It can be seen that a better understanding is required in order to interpret the role of electrolyte ions in controlling glycine polymorphs. In this research, the effects of electrolytes on glycine polymorphs are investigated to provide an in-depth insight into the mechanisms. The notable results are presented in **Chapter 5**.

2.3 Kinetics of Crystal Growth

Crystal growth is a process where tiny crystals (microscopic nuclei or macroscopic crystal seeds) grow larger (Myerson and Ginde, 2002). It may start with stable nuclei or macroscopic crystal seeds. As long as stable nuclei (i.e. particles larger than the critical size) are formed in a supersaturated or supercooled solution, they begin to grow on their surfaces, leading to mature crystals of visible size (Mullin, 1993). Similarly, when macroscopic crystal seeds are put in a supersaturated solution, the corresponding solute can deposit on the seed surface, thus crystals grow larger.

BCF theory (Burton, Cabrera and Frank, 1951) is commonly accepted for interpretation of crystal growth mechanism (Mohan and Myerson, 2002). Crystal growth proceeds on a molecular level by the sequential addition of growth units (single solute molecules, ions, or even clusters of these) to the crystal lattices. These growth units are typically solvated, i.e. a solute molecule or cluster is closely surrounded by a few or many solvent molecules. In general, three major steps are involved in the growth: transportation of solute molecules from bulk solution to the diffusion boundary layer at the interfacial region on the crystals; adsorption of solute molecules on the surface; and the eventual integration of solute molecules into the crystal lattices. Before solute molecules are integrated into the crystal lattices, the diffusion on the interface may be two-dimensional. However, when kinks are present on the crystals surfaces, three-dimensional diffusion occurs. During the surface diffusion step, the solvated solute molecules are desolvated as bonds between the solute and solvent molecules are broken.

The freed solute molecules form the bonds with the surface solute molecules on the crystals, thus completing their integration into the crystal lattices.

It should be noted that, due to the complexity of solute molecules, a single crystal may have many different faces. As pointed out (Garside et al., 2002), in general, each face will grow at a different rate and the relative growth rates of different faces determine the crystal habit or shape. Faster growing faces tend to grow out of the crystal and those faces making up the major part of the crystal surface are the slow growing faces. Many factors (e.g. pH, additives etc) can drastically alter the face growth rates (Lahav and Leiserowitz, 2001; Towler et al., 2004; Weissbuch et al., 2005).

The crystal growth rate can be defined in different ways (Hounslow et al., 2005; Garside et al., 2002; Mullin, 1993; Myerson and Ginde, 2002; Tavare, 1995). Mass growth rate (R_A) and linear growth rate (R_G) are commonly used. For a batch crystallizer, mass growth rate is defined as the increase of crystal mass per unit crystal surface per unit time, while linear growth rate is determined by the increase of the crystal characteristic dimension (e.g. diameter) per unit time.

$$R_A = \frac{1}{A}\frac{dW}{dt} \approx \frac{1}{A}\frac{\Delta W}{\Delta t} \tag{2-3-1}$$

$$R_G = \frac{dL}{dt} \approx \frac{\Delta L}{\Delta t} \tag{2-3-2}$$

where A is crystal surface area (m^2), W the crystal mass (kg), L the crystal size (meter) and t the time (second). The mass growth rate R_A and the linear growth rate R_G may be related (Hounslow et al., 2005):

$$R_A = 3\frac{k_v}{k_a}\rho_s R_G \tag{2-3-3}$$

where k_v is the volume shape factor, k_a is the surface shape factor and ρ_s is the crystal intrinsic density (kg/m^3). For detailed mechanism study, a specific linear growth rate, normal to a particular growth face, may be needed. The crystal growth rate is size-dependent in general (Mullin, 1993; Martins and Rocha, 2006), though size-independent growth may be observed (Hounslow et al., 2005).

For approximation of the crystal surface area (A) and size (L), the following equations may be used when the changes of the volume and surface shape factors k_v and k_a with crystal size are insignificant (Tavare, 1995):

$$A = \left(\frac{W}{W_0}\right)^{\frac{2}{3}} A_0 \qquad (2\text{-}3\text{-}4)$$

$$L = \left(\frac{W}{W_0}\right)^{\frac{1}{3}} L_0 \qquad (2\text{-}3\text{-}5)$$

where A_0, W_0 and L_0 are the initial crystal surface area, mass and size respectively. However, when crystal shape factors (especially the surface factor k_a) vary with crystal size significantly, they should be taken into account in determining the crystal surface area and size. Cautions should be exerted in measuring volume shape factor and surface shape factor. It should be noted that surface shape factor is more difficult to be determined and its uncertainty may lead to a considerable error (Mullin, 1993).

Experimentally, many different techniques have been developed for crystal growth measurement (Mullin, 1993). A batch crystallizer is often used to study crystal growth kinetics in a laboratory, since it is simple and suitable for small-scale operation. As pointed out by Jones et al. (1986), it would be challenging to achieve highly accurate

experimental measurements for crystal growth, and it was not unusual for an experimental error to be up to 25%. Therefore great care should be exerted.

The experimental kinetic data may be correlated empirically by power low (Mohan and Myerson, 2002; Tavare, 1995; Ottens, et al., 2004), especially when the relative supersaturation level σ is low:

$$R_G = k_g \sigma^g \tag{2-3-6}$$

where k_g is growth coefficient and g growth power. The solute relative supersaturation σ is usually defined as $\sigma = \frac{m - m^{Sat}}{m^{Sat}}$, with m and m^{Sat} being the supersaturated and saturated concentration (molality is often the concentration unit) respectively. It should be noted that the relative supersaturation σ is often replaced by solute concentration difference ($m - m^{Sat}$) in the correlation. However, the thermodynamic driving force for crystal growth should be used for better correlation when the relative supersaturation level σ is high.

The thermodynamic driving force for crystal growth is the solute thermodynamic activity difference $\ln\left(\frac{a}{a^{Sat}}\right)$ which is expressed as (Mohan and Myerson, 2002):

$$\ln\left(\frac{a}{a^{Sat}}\right) = \ln\left(\frac{\gamma m}{\gamma^{Sat} m^{Sat}}\right) \tag{2-3-7}$$

When the relative supersaturation σ is quite low ($\sigma << 1$), the solute activity coefficient γ in its supersaturated solution may be considered to be equal to that (γ^{Sat}) in its saturated solution. Therefore Eq. 2-3-7 is simplified to

$$\ln\left(\frac{a}{a^{Sat}}\right) = \ln\left(\frac{m}{m^{Sat}}\right) = \ln(1+\sigma) \tag{2-3-8}$$

By expansion, we obtain

$$\ln\left(\frac{a}{a^{Sat}}\right) = \ln(1+\sigma) \approx \sigma \qquad (\sigma << 1) \qquad (2\text{-}3\text{-}9)$$

This suggests that the relative supersaturation σ may be a good approximation of the intrinsic driving force $\ln\left(\frac{a}{a^{Sat}}\right)$ for crystal growth when the relative supersaturation σ is much smaller than 1 ($\sigma << 1$). Note that the average relative supersatuation in a time interval Δt is used for better correlation of kinetic data from a batch crystallizer (Martins et al., 2006).

Another important aspect is the impact of impurities on crystal growth. This is because, in the reality, there is no crystallization can take place from a single pure solvent. In fact, beside the crystallized solute, there are other substances commonly termed as impurities in a supersaturated solution. Impurities can have tremendous effects on crystallization. It has been well known that minor quantities (even traces) of certain impurities can extremely alter crystal habits, growth rate and polymorphs (Al-Jibbouri and Ulrich, 2001; Ottens, et al., 2004; Qu et al., 2006; Sangwal and Mielniczek-Brzoska, 2001; Scott and Black, 2005; Thompson et al., 2004; Towler et al., 2004; Weissbuch et al., 1995).

Some impurities come from the up-stream operation processes (e.g., unreacted reactants, by-products, etc.). They are unwanted impurities which generally have a negative impact on the nucleation and growth rate kinetics (Ottens et al., 2004). On the other hand, it is quite often that, selected impurities which may be better termed as additives or tailor-made additives (Kuznetsov et al., 1998; Weissbuch et al., 1995), are intentionally added into the supersaturated solutions to modify the shapes and to improve

the quality of the crystalline products in a desirable manner (Al-Jibbouri and Ulrich, 2001; Qu et al., 2006). Usually these impurities or tailor-made additives lead to a decrease rather than increase of the growth rates of crystal faces (Al-Jibbouri and Ulrich, 2001; Kuznetsov et al., 1998; Sangwal, 1999; Sangwal and Mielniczek-Brzoska, 2001).

As crystallization is a molecular recognition process, the influence of impurities (and solvents) can be rationalized in terms of molecular interactions. The molecular interactions occur in the liquid phase (solution), at the interface between liquid and the solid crystal phases and in solid phase itself. Therefore the solution chemistry (e.g. complex formation) and solid-state chemistry (e.g. crystal structure) are essential for a fundamental understanding of the effects of impurities.

Rak et al. (2005) conducted certain theoretical study on the effects of impurities. They suggested that impurities are usually considered to exert their effects via an interaction with the growing crystal surface, implying that these effects are not likely to be exerted during crystal dissolution. Impurities may thermodynamically decrease the edge free energy and may kinetically incorporate into crystal lattices of the host crystals. Impurity incorporation usually deforms the lattices in the nearest region of an impurity molecule (or ion etc), leading to lattice stress. In turn, the deformed lattices cause an increase in the local chemical potential. The authors also highlighted the geometrical importance in impurity incorporation. They suggested that, for an ionic impurity, when the ionic radii are compatible with the geometrical dimensions of the voids (or vacancies) in the host crystals, these impurity ions may be possibly placed in these vacancies. In

fact, solvent molecules as impurities may directly incorporate into the lattices of the crystallizing host too (Meena et al., 2002).

As discussed by a few researchers (Sangwal, 1996; Kuznetsov et al., 1998), both thermodynamic and kinetic effects of an impurity may simultaneously play a role in affecting the growth kinetics. But usually kinetic effect is dominant over thermodynamic one, leading to an overall inhibiting effect of an impurity on crystal growth. That may explain the fact that most of the impurities suppress (even completely stop) crystal growth while only a few impurities enhance crystal growth by exerting a catalytic effect (Kubota, 2001; Kuznetsov et al., 1998; Sangwal and Mielniczek-Brzoska, 2001).

It can be seen that impurity incorporation is an important phenomenon. Unfortunately it is often difficult to generally characterize the effects of impurities (Scott and Black, 2005). As pointed out by Mullin (1993), it would be unwise to attempt a general explanation of the phenomenon of nucleation and growth suppression by added impurities with so little quantitative evidence available, due to its diversification. Nevertheless certain patters of the effects are beginning to emerge: for example, the higher the charge on the cation the more powerful inhibiting effect. Furthermore, there often appear to be a threshold concentration of impurity above which the effect may actually diminish (Mullin, 1993). Though the effects of impurities may also be caused by changing solution structure due to complex formation, little has been done to reveal the influence of complex formation (Kuznetsov et al., 1998; Lu et al., 2001; Mullin, 1993).

A great effort has been made to characterize and model the inhibiting effects of impurities on crystal growth (Al-Jibbouri and Ulrich, 2001; Black and Davey, 1986; Kubota, 2001; Kubota and Mullin, 1995; Martins et al., 2006; Sangwal, 1999). Surface adsorption was often used for correlation and modeling. The adsorption of an impurity on the active sites on the host crystals would block or impede the growth units from integrating into the lattices, thus reducing the growth rate. The surface adsorption model may well interpret the inhibiting effect, but it is difficult to be used to characterize and model an enhancing effect of a particular impurity (additive) on crystal growth.

Kuznetsov et al. (1998) reported one of a few interesting enhancing effects. They added EDTA (0.0005 mol %) into KDP (KH_2PH_4) solution and they observed that the growth rate of KDP face {1 0 0} increased eight times. Their analysis showed that this increase of growth rate was not connected to the thermodynamic effect (i.e. decrease of edge free energy), instead they attributed this promotion effect to the formation of favorable complexes which increase the concentration of growth units. Lu et al. (2001) further studied this system using Raman spectroscopy. Their results revealed that EDTA enhanced the formation of phosphate anion dimerization which in turn favors the formation of KDP growth units, supporting the observation made by Kuznetsov et al. (1998). Unfortunately, neither Kuznetsov et al. (1998) nor Lu et al. (2001) discussed the quantitative characterization and modeling of this enhancing effect.

Different from unwanted impurities, tailor-made additives function uniquely. They selectively interact only with certain particular faces of crystalline materials.

Usually, the molecules of a tailor-made additive have chemical functional groups or moieties that mimic the solute molecules and are thus readily adsorbed at the growth sites on the crystal surfaces. Meanwhile their reverse sides which chemically or structurally differ from the solute (host) molecules are exposed outwards, thereby disrupting the subsequent growth processes at the affected faces. As a result, the growth rate is reduced and the shape of the crystals is altered (Meenan et al., 2002; Weissbuch et al., 1995). The roles of a tailor-made-additive in polymorph control and in crystal kinetics are quite similar.

It can be seen that tailor-made additives are usually designed to retard the growth from particular crystal faces. It would be very interesting to design tailor-made additives to promote the crystal growth. In this work, an effort has been made to enhance γ-glycine growth by using selected electrolytes. The details are reported in **Chapter 6**.

Chapter 3 A New Technique for Activity of Supersaturated Solutions

As was discussed in **Chapters 1 and 2**, thermodynamics of supersaturated solutions would be a very powerful tool to explore many phenomena, including molecular interaction, nucleation, crystal polymorphism and crystal growth kinetics, as long as the reliable and accurate thermodynamic activities of supersaturated solutions are available. Unfortunately, such activity data are not readily available. Consequently, the applications of the thermodynamics of supersaturated solutions are limited. The major obstacle in obtaining these activity data is the lack of suitable experimental methods for supersaturated solutions. In this chapter, the development of a new technique for reliable and accurate thermodynamic activity of supersaturated solutions is presented.

3.1 Development of A New Technique

Over past decades, **potentiometric method** (i.e. the electrochemical method) has been used for measuring thermodynamic activity of dilute electrolyte-containing solutions (Breil et al., 2001; Khoshkbarchi and Vera; 1996a, 1996b; Phang, et al., 1974; Roberts and Kirkwood, 1941; Rodriguez-Raposo et al., 1994). Its successful application to supersaturated solutions has not been reported. It can be shown that its failure is because the molecular-level transports (mass and/or heat transfer) in quiescent supersaturated solutions are too slow. Consequently the equilibration time for the experimental measurement is much longer than the induction time for homogeneous nucleation, resulting in nucleation of the supersaturated solution. On the other hand, mixing the supersaturated solutions to shorten the equilibration time can trigger an

immediate nucleation and cause the experimental measurement to fail too. The following analysis and experimental verification will show that the potentiometric method can be modified, leading to a new technique, Steady State Shifting Technique for measuring the mean ionic activity coefficient of electrolyte solutions supersaturated with a nonelectrolyte. Three ternary NaCl+nonelectrolyte+H_2O systems will be used to demonstrate the application of the Steady State Shifting Technique for a systematic study on thermodynamics of supersaturated solutions.

3.1.1 Theory of the Potentiometric Method

The theoretical basis of the potentiometric method can be found elsewhere (Breil et al., 2001; Khoshkbarchi and Vera, 1996a, 1996b). Generally, the electrochemical cell potential ΔE (i.e. cell electromotive force, emf) is measured and the Nernst equation is applied to obtain the mean ionic activity coefficient of an electrolyte in a solution at a given temperature. A number of studies (Breil et al., 2001; Haghtalab and Vera, 1991; Han and Pan, 1993; Ji et al., 2001) have suggested that good results can be obtained by using two ion selective electrodes (ISEs), with the cation ISE being the indicator electrode and the anion ISE the reference electrode. For a cell where only a single electrolyte is present, the cell with two ISEs may be expressed as

cation ISE|electrolyte (m_S), H_2O|anion ISE

where m_S is the electrolyte molality. The cell potential ΔE^I is related to the electrolyte molality m_S and the mean ionic activity coefficient $\gamma_{\pm}^I$ of the electrolyte as described by the Nernst equation. For a 1:1 electrolyte, we would have

$$\Delta E^{I} = \Delta E^{0} + S\ln(m_S\gamma_{\pm}^{I}) \tag{3-1-1}$$

For an actual cell, the value of the slope S at a given temperature is usually derived from a linear graphical plot of experimental data of ΔE^{I} vs $\ln(m_S\gamma_{\pm}^{I})$ (Bates et al., 1983; Ji et al., 2001; Khoshkbarchi and Vera, 1996b).

If another solute, e.g. a nonelectrolyte, is introduced into the cell solution with the electrolyte concentration m_S, the cell may be expressed as

cation ISE| electrolyte(m_S) + nonelectrolyte(m_A), H_2O |anion ISE

The introduction of the nonelectrolyte (m_A) can cause the mean ionic activity coefficient of the electrolyte to change from $\gamma_{\pm}^{I}$ to $\gamma_{\pm}^{II}$, even at the same electrolyte concentration m_S, due to the interactions between the electrolyte, the nonelectrolyte and water molecules. Accordingly, the cell potential changes from ΔE^{I} to ΔE^{II}. It should be noted that ΔE^{II} is related to the mean ionic activity coefficient $\gamma_{\pm}^{II}$ of the electrolyte by the same Nernst equation,

$$\Delta E^{II} = \Delta E^{0} + S\ln(m_S\gamma_{\pm}^{II}) \tag{3-1-2}$$

By subtracting Eq. 3-1-1 from Eq. 3-1-2 at the same electrolyte molality m_S, a useful relation between $\gamma_{\pm}^{II}$ and $\gamma_{\pm}^{I}$ is obtained,

$$\ln\left(\frac{\gamma_{\pm}^{II}}{\gamma_{\pm}^{I}}\right) = \frac{\Delta E^{II} - \Delta E^{I}}{S} \tag{3-1-3}$$

It should be kept in mind that each term in Eq. 3-1-3 is temperature-dependent. With the

measurements of cell potentials ΔE^{I} and ΔE^{II}, the electrolyte mean ionic activity coefficient ratio $\frac{\gamma_{\pm}^{II}}{\gamma_{\pm}^{I}}$ can be calculated using Eq.3-1-3.

Similarly, we can consider how an electrolyte affects the thermodynamic behavior of a nonelectrolyte, for example in the study of nonelectrolytes (e.g. biochemicals) crystallizing from aqueous electrolyte-containing solutions (Khoshkbarchi and Vera, 1996b). Introducing an electrolyte (molality m_S) into a binary nonelectrolyte+H_2O solution at a given nonelectrolyte molality m_A can cause the nonelectrolyte activity coefficient to change from γ_A^I to γ_A^{II}. In terms of activity coefficient ratios $\frac{\gamma_A^{II}}{\gamma_A^{I}}$ for the nonelectrolyte and $\frac{\gamma_{\pm}^{II}}{\gamma_{\pm}^{I}}$ for the electrolyte, they are thermodynamically related through the cross-differential relation (Breil et al., 2001; Kelly et al., 1961; Khoshkbarchi and Vera, 1996b; Roberts and Kirkwood, 1941; Robinson and Stokes, 1961):

$$\left(\frac{\partial \ln \gamma_A^{II}}{\partial m_S}\right)_{m_A} = \nu \left(\frac{\partial \ln \gamma_{\pm}^{II}}{\partial m_A}\right)_{m_S} \tag{3-1-4}$$

with ν being the stoichiometric number per mole of electrolyte. For a 1:1 electrolyte (e.g. NaCl), ν = 2.

Integrating both sides of Eq.3-1-4 with respect to m_S in the domain [0, m_S] yields

$$\frac{\gamma_A^{II}}{\gamma_A^{I}} = \int_0^{m_S} \nu \left(\frac{\partial \ln \gamma_{\pm}}{\partial m_A} \right)_{m_S} dm_s \qquad (3\text{-}1\text{-}5)$$

Eq. 3-1-5, expressed in terms of the nonelectrolyte molality m_A and the electrolyte molality m_S, shows how activity data $\frac{\gamma_A^{II}}{\gamma_A^{I}}$ of the nonelectrolyte can be derived from the measured activity data $\frac{\gamma_{\pm}^{II}}{\gamma_{\pm}^{I}}$ of the electrolyte in ternary electrolyte+nonelectrolyte+H_2O solutions.

Eqs. 3-1-3 and 3-1-5 are the governing equations for study of the thermodynamics of a broad spectrum of ternary electrolyte-containing solutions which are of great importance in biochemical manufacturing (Khoshkbarchi and Vera, 1996b). Particularly, activity data $\frac{\gamma_{\pm}^{II}}{\gamma_{\pm}^{I}}$ and $\frac{\gamma_A^{II}}{\gamma_A^{I}}$ directly indicate the salting effect. If the value of $\frac{\gamma_{\pm}^{II}}{\gamma_{\pm}^{I}}$ is less than unity, the nonelectrolyte has a salting-in effect on the electrolyte; if greater than unity, it has a salting-out effect. Similarly, the nonelectrolyte activity data $\frac{\gamma_A^{II}}{\gamma_A^{I}}$ can be analyzed to study the impact of the electrolyte on the nonelectrolyte. It should be noted that γ_A^{I} is the activity coefficient of the nonelectrolyte in its binary nonelectrolyte+H_2O solution (electrolyte $m_S = 0$) while γ_A^{II} is the activity coefficient of the nonelectrolyte in its ternary electrolyte+nonelectrolyte+H_2O solution (electrolyte $m_S > 0$), at the same nonelectrolyte molality m_A.

For dilute solutions, the potentiometric method is particularly preferred. The difficulties arise when the cell solution concentration increases significantly. It is especially true when the solution is supersaturated. It will be shown in **Section 3.1.2** that these difficulties are due to slow molecular diffusion in concentrated solutions.

3.1.2 Effects of Transport Phenomena and Temperature on Cell Potential

According to the electrical double layer theory (Goodisman, 1987), a double layer is developed on each electrode-solution interface to establish the cell potential. The cations are distributed in one end of the double layer while the anions are arrayed in the other end of the double layer. The correct and accurate cell potential can be obtained only when the cell reaches its steady state, i.e. when both the temperature and the concentration profiles in the cell remain unchanged. How fast the steady state of the cell can be reached depends on the rates of mass and/or heat transfer in each of the media and between media in the cell. The media in the cell include the cell bulk solution, solution films on external electrode surfaces, electrode membranes and the electrode housings.

In the conventional potentiometric method, the temperature of interest is controlled to be constant throughout the experiment. In order to facilitate achieving the steady state, stirring the cell solution is required to enhance heat and mass transfer. However, when the solution is supersaturated at the temperature of interest, stirring the solution could cause an immediate nucleation which results in the failure of the cell potential measurement. On the other hand, without stirring, the heat and mass transfer rates in the supersaturated region can be very low as the molecular diffusivity is

diminished significantly (Chang and Myerson, 1985, 1986; Ginder and Myerson, 1991). Thus the time required to achieve the steady state can be much longer than the induction time for homogeneous nucleation. As a result, the cell potential measurement would also fail.

Experimental data suggests that molecular diffusivity declines much more rapidly with increase in the solution concentration once the solution progresses into the supersaturated domain (Chang and Myerson, 1985, 1986; Mohan et al., 2000; Myerson and Lo, 1991; Myerson and Izmailov, 1997; Sorell and Myerson, 1982). The rapid drop in diffusivity with concentration in the supersaturated region has been attributed to the cluster formation (Chang and Myerson, 1985; Mohan et al., 2000), as cluster formation can significantly increase the solution viscosity (Ginder and Myerson, 1991, 1992). In contrast, heat transfer is not severely limited in high solute concentrations, as molecular-level diffusion is not involved in thermal transport processes. Therefore it is more likely that molecular diffusion rather than heat transfer is the rate-controlling step as the steady state of the cell is approached when the cell solution is concentrated, suggesting that slow molecular diffusion is the root cause of the failure of the potentiometric method for supersaturated solutions. In the following section (**Section 3.1.3**), it will be shown that the problem of slow molecular diffusion can be overcome so that the potentiometric method can be applicable to supersaturated solutions.

3.1.3 The Proposed Steady State Shifting Technique

As discussed above, the conventional technique for the potentiometric method

often fails to measure the cell potential when the solution is supersaturated. This failure is mainly caused by the slow molecular diffusion in highly concentrated solutions. An analysis of the proposed technique will be made to show that molecular diffusion can be improved drastically by exploiting the advantage of temperature effects on supersaturation, molecular diffusion and liquid expansion.

In the proposed steady state shifting technique, solid crystals are dissolved in a warm (even hot) solvent to prepare a cell solution. This cell solution is under-saturated at the high temperature when it is prepared, while it is supersaturated at the temperature of interest, T. When the experiment is conducted for the cell potential measurement, the cell solution and electrodes are maintained at a reference temperature T_R which is higher than the saturated temperature T_S of the cell solution. As the cell solution is under-saturated at the reference temperature T_R, there is no concern about the occurrence of nucleation, hence the cell solution can be stirred to facilitate the attainment of steady state for the cell system. The steady state is indicated by a stable reading of the cell potential.

When the steady state of the cell at the reference temperature T_R is reached, stirring is stopped. The cell solution and electrodes are then cooled to and maintained at the temperature of interest, T, until the new steady state of the cell at T is achieved. As long as the steady state of the cell at T is attained without nucleation or crystallization occurring, a successful cell potential measurement for the supersaturated solution can be made. This simple shift of steady states between T_R and T is a means of overcoming the diffusion limitation at high concentrations. The effects of temperature on the relevant

transport phenomena in the cell are discussed in detail here.

Firstly, the temperature affects the ion distribution in the ionic double layer and hence the cell potential. A step-change temperature disturbance, as proposed above, would cause a temporary instability in the ion distribution in the double layer. However, the new equilibrium state of ion distribution can be quickly established by ion neutralization or separation, as the double layer is very thin (Goodisman, 1987). Furthermore, it is reasonable to assume that the re-distribution of the ions in the double layer will not affect the concentrations in the diffusion layer (or film) which is located outside the ionic double layer, as the amount of ions to be re-distributed could be negligible compared with the total amount of the ions in the diffusion film.

Secondly, when the temperature gradient due to the temperature change is significant, it may cause local concentration gradients in the cell fluid. However, the concentration gradients are small, since density variations caused by liquid expansion or contraction are not significantly large. As a result, the pre-established stable concentration profile will remain practically unchanged when the temperature shift occurs.

It can be seen that the proposed steady state shifting technique relies on heat transfer processes (principally thermal conduction and natural convection) within the cell to obtain stable equilibrium measurements of cell potential for supersaturated and highly concentrated solutions. The critical period is the time required to re-establish a uniform

steady state in the cell after shifting the temperature downward from the saturated temperature T_S to the measurement temperature T. The required time depends on the magnitude of the temperature shift, the thermal conductivities of all the cell materials (e.g. electrode materials and cell solution), the volume and the geometry of the cell system, and the dynamic response of the temperature control system (e.g. the jacket and the water bath). In general, for activity measurement, the new technique enables the concentration of a quiescent supersaturated solution to be up to the nucleation onset. The successful application of the new technique to three ternary electrolyte+nonelectrolyte+H_2O systems will be demonstrated in **Sections 3.3 to 3.4**.

3.2 Materials and Instruments

A schematic diagram of the experimental setup for cell potential measurement is shown in Figure 3-2-1. Two external circulating water baths were maintained at temperature T_R and T respectively, and connected to a jacketed glass warming beaker for the measurement cell. By operation of valves 1, 2, 3 and 4, the recirculating water temperature and hence the cell temperature can be shifted quickly and effectively from T_R to T.

In this study, an ISE/pH meter Orion $920A^+$ and two ion selective electrodes, i.e. sodium ion selective electrode (glass Na-ISE, Orion 84-11) and chloride ion selective electrode (PVC Cl-ISE, Orion 94-17), were used to determine the cell potential. The meter Orion $920A^+$ has a readability of 0.1mV. The Orion DataCollect Software was

used for data collection. The water baths and the temperature probe (Orion ATC 11765) for the cell had a temperature resolution of 0.1 ^{o}C.

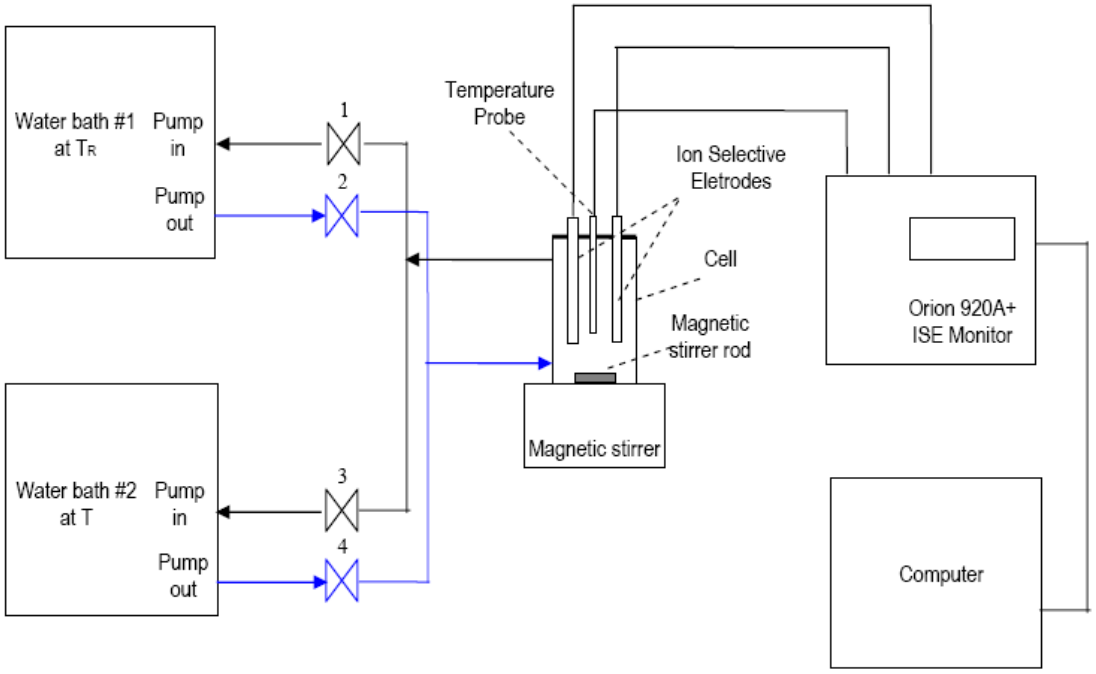

Figure 3-2-1. Schematic diagram of the experimental setup

The total mass of cell solution for each run was approximately 110 grams. In solution preparation, each mass was weighed within an accuracy of ±0.01 wt%. Ultrapure water (Millipore, resistivity 18.2 MΩcm and filtered with pore size 0.22μm) was used for sample solution preparation. NaCl (>99.5%) was from Merck. Glycine (> 99%) was from Sigma-Adrich. DL-alanine (> 99%) and DL-serine (> 99%) were from AVOCADO. NaCl was dried at 120 ^{o}C in an oven for 72 hrs then cooled in a vacuum desiccator prior to its use.

The ion selective electrodes were prepared according to instructions from their manufacturer. In accordance with previous works by Breil et al. (2001) and Haghtalab and Vera (1991), the Cl-ISE was used as the reference electrode. A stable cell potential was considered to be reached if its average value did not change by 0.1mV in 15 minutes. The cell was kept sealed throughout the experiment to avoid evaporation.

For these ternary electrolyte+nonelectrolyte+H_2O systems, in order to relate thermodynamic activity of a nonelectrolyte to its solubility for analysis of thermodynamic consistency, solubilities of these nonelectrolytes (namely glycine, DL-serine and DL-alanine) at different NaCl concnetrations were measured, using the method described by Lampreia et al. (2006) where the concentration of saturated solution (equilibrated solid-liquid solution) is determined by solution density. A solution density meter Anton-Paar DMA5000 was used here for determining saturated concentration, with high resolutions of solution density ($\pm 10^{-6}$ g/ml) and temperature (±0.001 °C), leading to accurate measurement of concentration and solubility. The uncertainty of a nonelectrolyte solubility in NaCl solutions, increasing (nearly linearly) with NaCl molality, may be only up to 0.04g/100g in a 5m NaCl solution. In fact, the excellent reproducibility and high accuracy of concentration determination using solution density have been reported (Lampreia et al., 2006; Tjahjono et al., 2005). The details of using solution density for solubility measurement via isothermal liquid-solid equilibration can be found in **Appendix A**.

It should be pointed out that glycine has several polymorphs and different polymorphs have different solubilities (Sakai, et al., 1991), with the thermodynamically stable polymorph γ-glycine having lower solubility. In this study, γ-glycine was used for its solubility measurement. Therefore there is no concern on its polymorph transition from metastable α-glycine to stable γ-glycine during the solid-liquid phase equilibration for solubility determination. Nevertheless, XRD (here either Brooker D8 Advance Diffractometer or Shimadzu X-Ray Differactometer XRD-6000, whichever was available) was performed to check the crystal polymorphs of selected nonelectrolyte crystals including glycine crystals collected after the solid-liquid equilibration for solubility measurement was completed.

3.3. Experimental Verification of the Proposed Technique

Several typical binary NaCl+water and ternary glycine+NaCl+water under-saturated solutions covering a wide range of concentrations at 25 ^{o}C were tested using both the conventional potentiometric and the new steady state shifting technique. The cell potentials (i.e. emf readings) obtained by the steady state shifting technique were then compared with those obtained by the conventional technique to check if the new technique could provide correct and reliable results. The results by the two techniques are summarized in Table 3-3-1.

From Table 3-3-1, the maximum potential deviation between the two techniques is only 0.1 mV which is actually the instrument resolution (0.1 mV). In fact, the cell potentials obtained by the two techniques are so close that no obvious difference can be

observed. Therefore the proposed steady state shifting technique has been demonstrated to work well in the under-saturated region.

Table 3-3-1 Cell potential comparison between the conventional and the proposed technique at 25 °C

Solutions	Cell potential by the conventional technique, mV	Cell potential by the proposed technique, mV	Cell potential deviation, mV
0.01 m NaCl	44.5	44.6	0.1
0.1 m NaCl	154.7	154.7	0.0
1.0 m NaCl	264.2	264.3	0.1
1.5 m NaCl	285.3	285.4	0.1
0.01 m NaCl +3.0 m glycine	28.1	28.2	0.1
0.1 m NaCl + 0.1 m glycine	154.0	153.9	– 0.1
1.0 m NaCl + 2.6 m glycine	258.8	258.7	– 0.1

The transient profiles of cell potential from the conventional (run #1) and the new (run #2) techniques are shown in Figure 3-3-1, for the cell solution consisting of 3.0 m glycine + 0.01 m NaCl (under-saturated) at 25 ^{o}C. In run #1, the ISEs were transformed from the presoak at 25 ^{o}C into the cell solution which was also maintained at 25 ^{o}C. Even with vigorous stirring, it took about 3 hours to achieve the steady cell potential of 28.1 mV, as shown in Figure 3-3-1. Since the temperature of the cell and electrodes remained 25 ^{o}C throughout, the long equilibration time reflects the relatively slow rate of molecular and ionic diffusion. It is anticipated that the equilibration time could be much

longer for highly concentrated solutions, thus resulting in spontaneous nucleation if the solution is supersaturated.

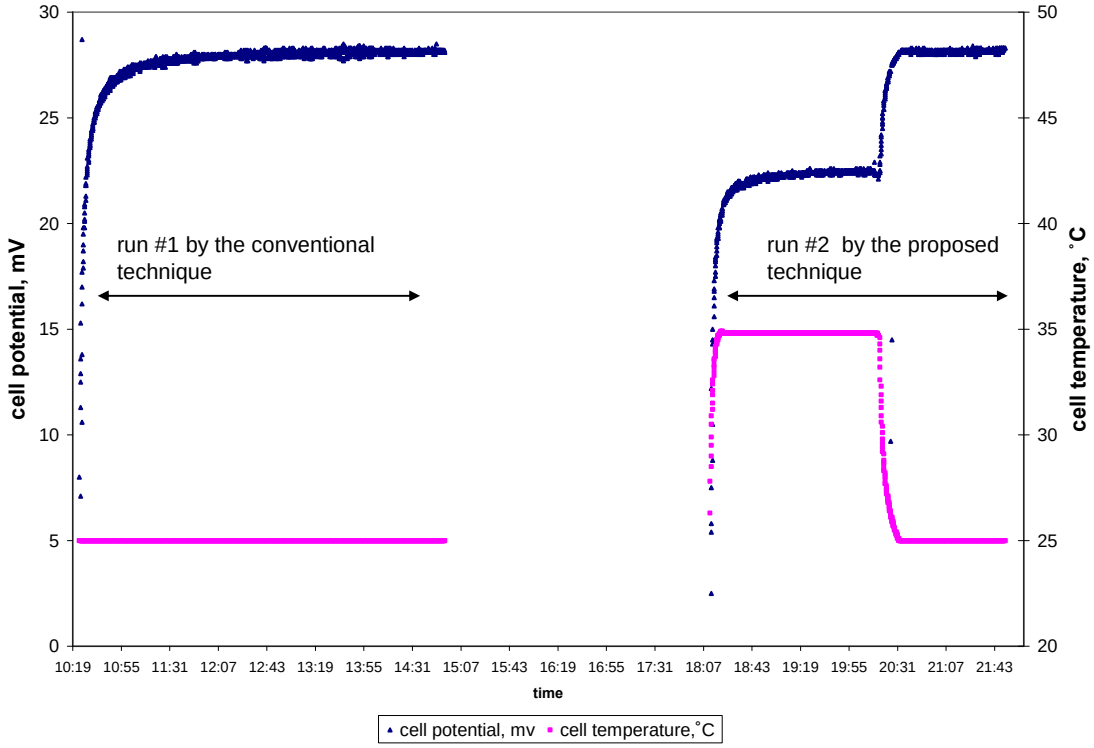

Figure 3-3-1 Cell potentials by the two techniques for the same under-saturated solution of (3.0m glycine + 0.01m NaCl)

In run #2, the cell was first equilibrated at 35 ^{o}C with stirring, then the stirring was stopped and the temperature was shifted by cooling to the measurement temperature 25 ^{o}C. The cessation of stirring is a key requirement when making measurements on supersaturated solutions. Even without stirring, the re-equilibration time at 25 ^{o}C took

only about 35 minutes, as compared with 3 hours in run #1. A steady cell potential of 28.2 mV (vs 28.1 mV in run #1) was obtained.

Comparing the equilibration times at 25 ^{o}C for runs #1 and #2, it can be inferred that the rate of heat transfer with possible free convection is significantly higher than that of molecular diffusion with forced convection (stirring) in the absence of heat transfer. These experimental results agree with our previous analysis of the heat and mass transfer rates in the cell.

Under typical laboratory conditions and over the range of the experimental conditions used, it took an average of 40 minutes to complete the shifting of the steady state of the cell for a temperature change 10 to 15 ^{o}C, without stirring. For other cells with different solutions (e.g. KCl+glycine+water, NaCl+DL-alanine+water and NaCl+DL-serine+water, supersaturated with the corresponding amino acid) and a different ion selective electrode (PVC K-ISE, Orion 93-19), it was found that the steady state of the cell can be shifted equally quickly, regardless of the cell solutions and the ISEs used. A typical cell potential measurement on a supersaturated solution using the steady state shifting technique is shown in Figure 3-3-2. It is expected that the proposed potentiometric method with steady state shifting would be applicable to supersaturated solutions in general.

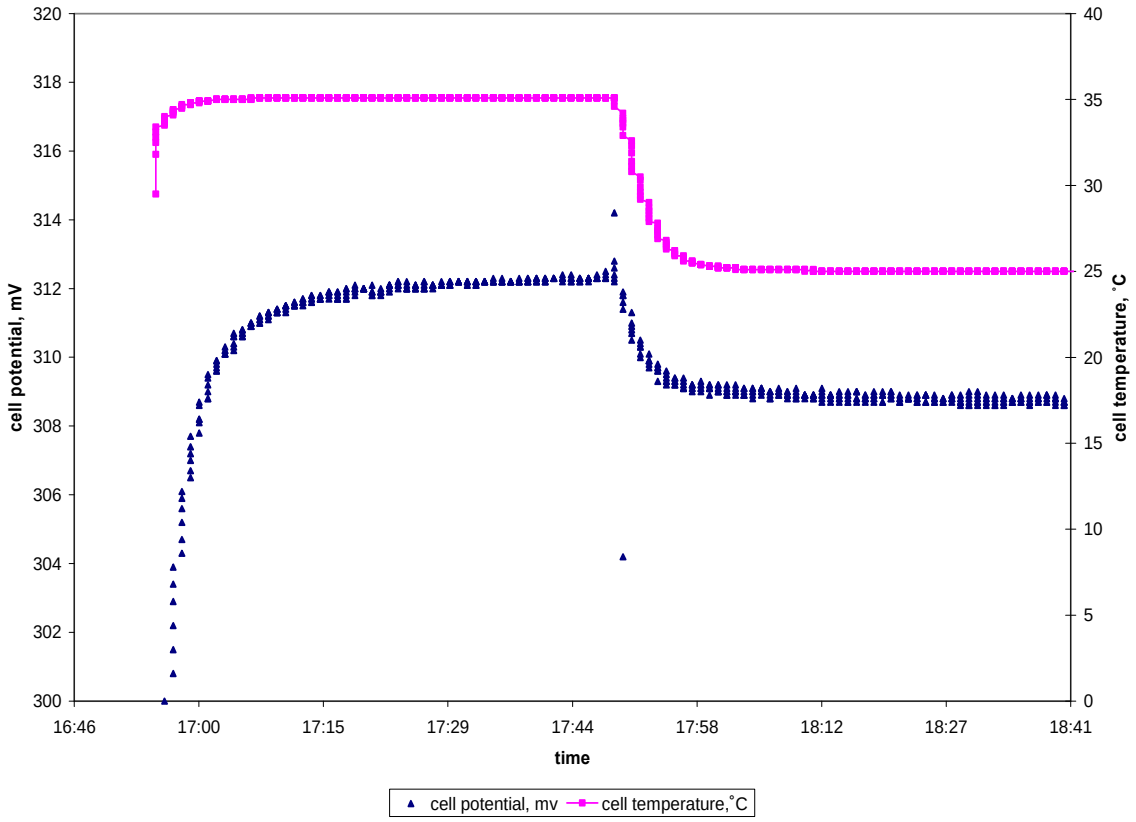

Figure 3-3-2 A typical cell potential measurement on a supersaturated solution of (4.2m glycine + 2.5m NaCl), using the steady state shifting technique

3.4 Results and Discussion

The thermodynamic activities for the three ternary NaCl+noneletrolyte+H_2O systems (namely NaCl+glycine+H_2O, NaCl+DL-serine+H_2O and NaCl+DL-alanine+H_2O) are measured in both under-saturated and supersaturated regions, using the proposed steady state shifting technique. Note that these three nonelectrolytes glycine, DL-serine and DL-alanine are amino acids. The thermodynamic consistency between activity and solubility is analyzed. Furthermore, binary supersaturated activities of a nonelectrolyte in its aqueous solutions (without electrolyte) are derived.

3.4.1 Activities for Ternary Solutions

Before carrying out the tests on the ternary solutions, the Na-ISE and Cl-ISE were calibrated using binary NaCl+water solutions in the NaCl molality range of 0.01 m – 5 m at the specified temperature 25 ^{o}C. The mean ionic activity coefficients of NaCl used for the calibration are given by Zemaitis et al. (1986). As shown in Figure 3-4-1, the calibration curve of cell potential ΔE^{I} vs $\ln(m_s \gamma_{\pm}^{I})$ is highly linear with a correlation coefficient R^2 = 0.99995 and a typical slope S = 51.35 (vs its theoretical value 51.38. Khoshbarchi and Vera, 1996b). Hence the performance of the Na-ISE and Cl-ISE closely followed the Nernst equation Eq.3-1-1.

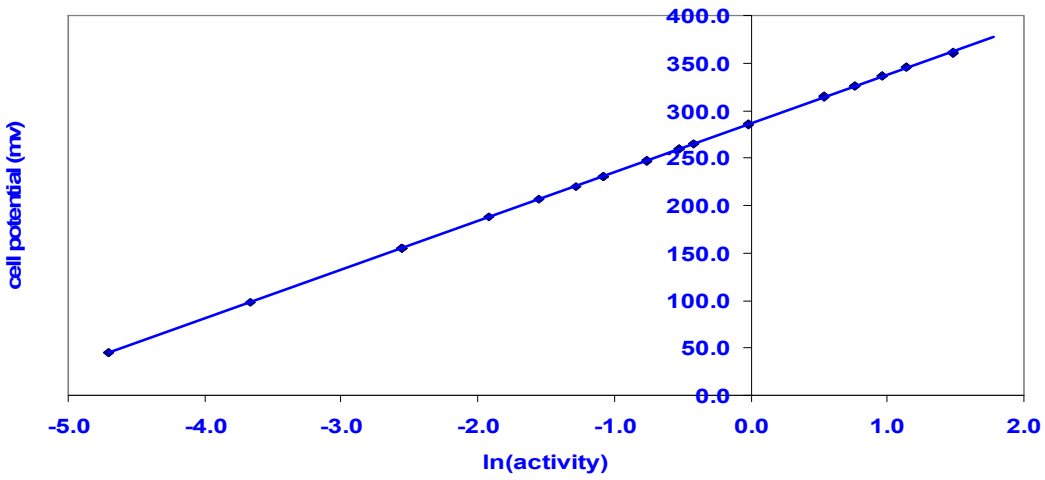

Figure 3-4-1 Calibration of Na-ISE vs Cl-ISE at 25 °C

Based on the cell potentials ΔE^{I} and ΔE^{II} measured respectively for binary NaCl+H_2O and ternary NaCl+nonelectrolyte+H_2O solutions at a given NaCl

concentration, the mean ionic activity coefficient ratios $\frac{\gamma_{\pm}^{II}}{\gamma_{\pm}^{I}}$ for NaCl were calculated for the three ternary systems, using Eq. 3-1-3 with S = 51.35. These activity data, together with the saturation curves which will be discussed later, are shown in Figures 3-4-2 to 3-4-4. As the data of activity coefficient $\gamma_{\pm}^{I}$ for NaCl in its binary aqueous solutions (i.e. without nonelectrolyte) are available (e.g. Zemaitis et al., 1986), the data of NaCl activity coefficient $\gamma_{\pm}^{II}$ in the ternary aqueous solutions can be calculated readily.

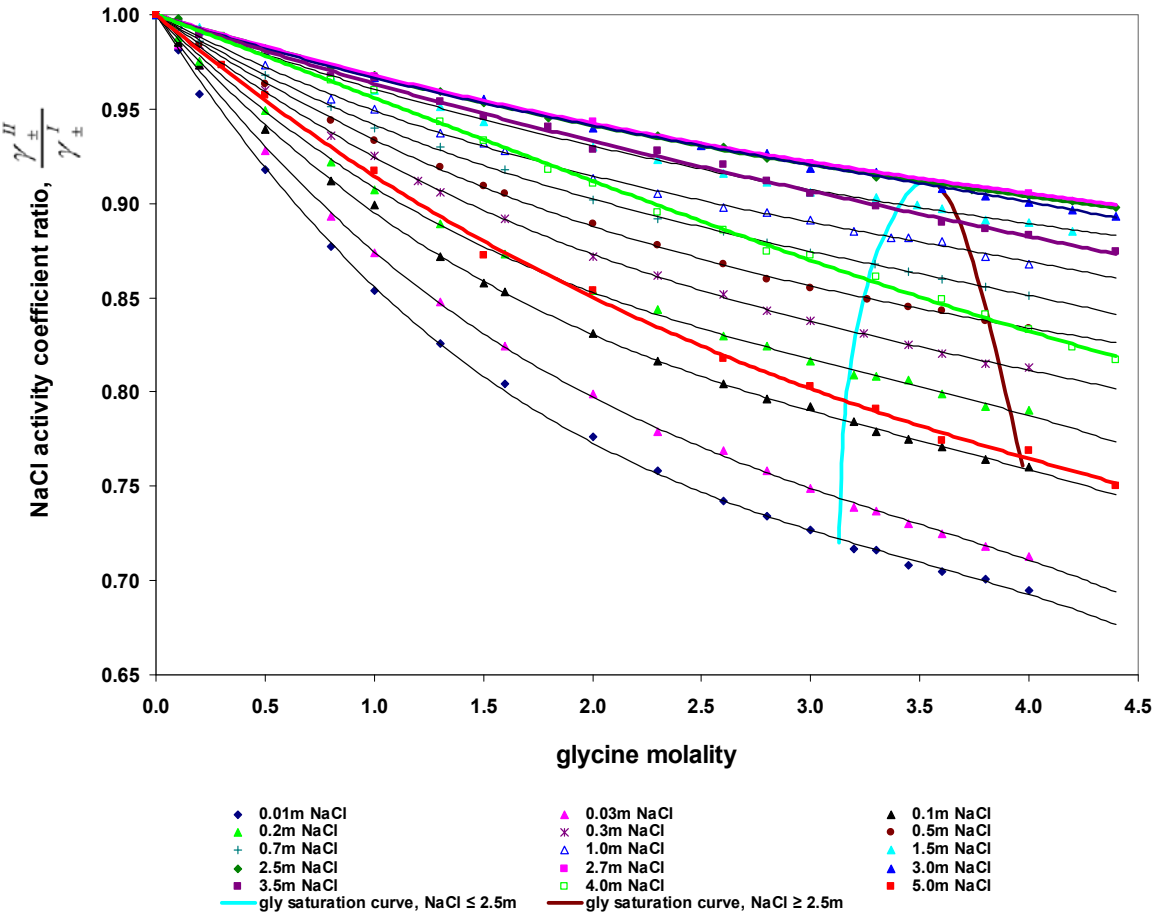

Figure 3-4-2 Effects of glycine and NaCl concentrations on NaCl mean ionic activity coefficient ratio $\frac{\gamma_{\pm}^{II}}{\gamma_{\pm}^{I}}$ at 25 °C

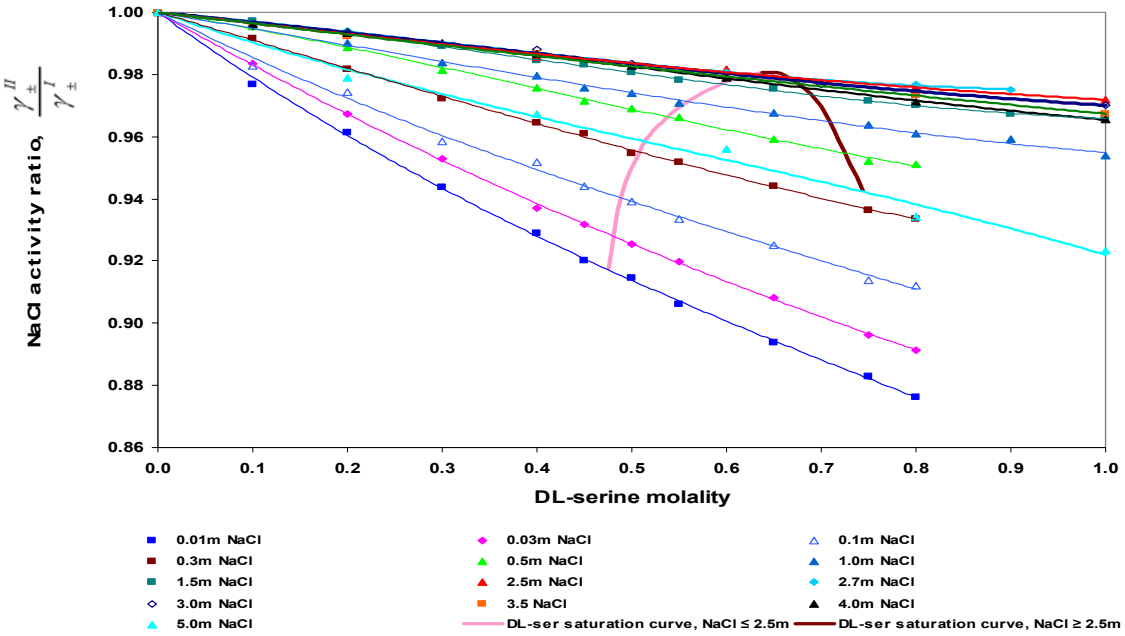

Figure 3-4-3 Effects of DL-serine and NaCl concentrations on NaCl mean ionic activity coefficient ratio $\frac{\gamma_{\pm}^{II}}{\gamma_{\pm}^{I}}$ at 25 °C

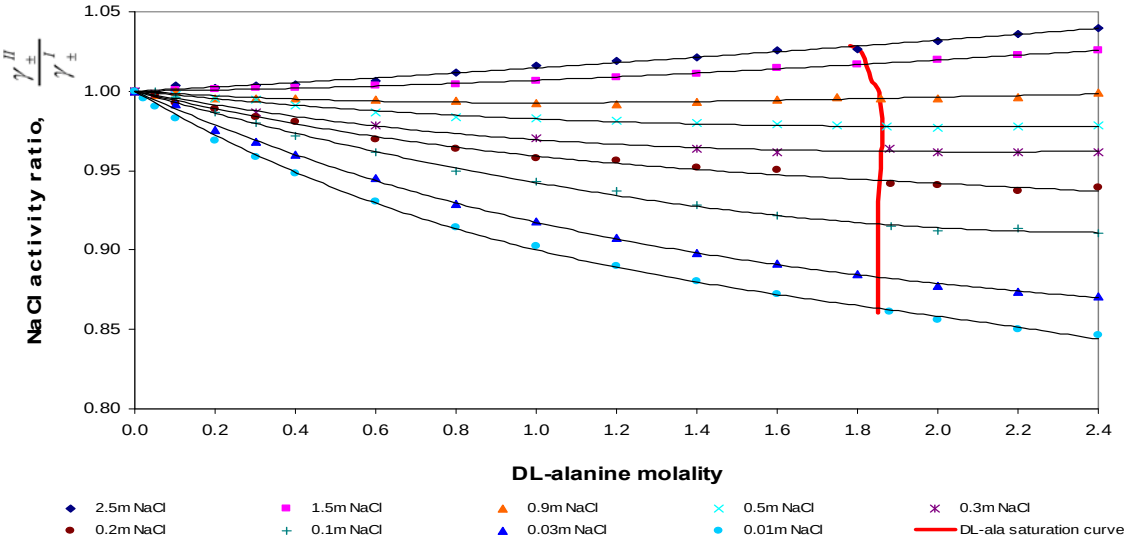

Figure 3-4-4 Effects of DL-alanine and NaCl concentrations on NaCl mean ionic activity coefficient ratio $\frac{\gamma_{\pm}^{II}}{\gamma_{\pm}^{I}}$ at 25 °C

For each ternary system in its under-saturated region, NaCl mean activity coefficient ratios $\frac{\gamma_{\pm}^{II}}{\gamma_{\pm}^{I}}$ from this study were compared with previously published data (Khoshbarchi and Vera, 1996b; Khoshkbarchi et al., 1997; Phang, et al., 1974; Rodriguez-Raposo et al., 1994; Scherier and Robison 1971). It is found that our data agree reasonably well (mean deviation < 1%) with those from earlier studies over a wide range of solution concentrations. In fact, these deviations, except the one from Khoshkbarchi and Vera (1996b) for NaCl+glycine+H_2O system are very close to the experimental uncertainty of about 0.5% in this study. The error analysis for the technique used in this study can be found in the work of Ong (2007).

For a given ternary system, NaCl mean activity coefficient ratios $\frac{\gamma_{\pm}^{II}}{\gamma_{\pm}^{I}}$ at different molalities of NaCl (m_S) and the nonelectrolyte (m_A) may be correlated based on the experimental data using the following equation,

$$\begin{aligned} \nu \ln\left(\frac{\gamma_{\pm}^{II}}{\gamma_{\pm}^{I}}\right) = {} & A \cdot m_A + B \cdot m_A^{1.5} + C \cdot m_A^{2} + D \cdot m_A^{2.5} + \\ & E \cdot m_A \cdot m_S^{0.5} + F \cdot m_A \cdot m_S + G \cdot m_A \cdot m_S^{1.5} + H \cdot m_A \cdot m_S^{2} + \\ & I \cdot m_A^{1.5} \cdot m_S^{0.5} + J \cdot m_A^{1.5} \cdot m_S + K \cdot m_A^{1.5} \cdot m_S^{1.5} + L \cdot m_A^{1.5} \cdot m_S^{2} + \\ & M \cdot m_A^{2} \cdot m_S^{0.5} + N \cdot m_A^{2} \cdot m_S + O \cdot m_A^{2} \cdot m_S^{1.5} + P \cdot m_A^{2} \cdot m_S^{2} + \\ & Q \cdot m_A^{2.5} \cdot m_S^{0.5} + R \cdot m_A^{2.5} \cdot m_S + S \cdot m_A^{2.5} \cdot m_S^{1.5} + T \cdot m_A^{2.5} \cdot m_S^{2} \end{aligned} \qquad (3\text{-}4\text{-}1)$$

where ν = 2 for NaCl. These 20 parameters (A to T in Eq. 3-4-1) are obtained by the least square method and they are tabulated in Table 3-4-1. The absolute mean relative difference (amrd) between experimental data and the data obtained from the correlation

was found to be 0.25% for NaCl+glycine+H_2O, 0.15% for NaCl+DL-serine+H_2O and 0.13% for NaCl+DL-alanine+H_2O, with amrd being defined by

$$amrd = \frac{1}{n}\sum \left[\left| \left(\frac{\gamma_{\pm}^{II}}{\gamma_{\pm}^{I}}\right)_{\exp} - \left(\frac{\gamma_{\pm}^{II}}{\gamma_{\pm}^{I}}\right)_{corr} \right| / \left(\frac{\gamma_{\pm}^{II}}{\gamma_{\pm}^{I}}\right)_{\exp} \right] \qquad (3\text{-}4\text{-}2)$$

The small values of amrd indicate that the correlation used is satisfactory.

Table 3-4-1 Values of correlation parameters (A toT in Eq. 3-4-1) for NaCl activity coefficient ratios $\frac{\gamma_{\pm}^{II}}{\gamma_{\pm}^{I}}$ in NaCl+nonelectrolyte+H_2O solutions at 25 °C

Parameter	Value of Parameter		
	NaCl+Glycine+H_2O	DL-serine+NaCl+H_2O	NaCl+DL-alanine+H_2O
A	-0.580919386093	-0.657203624594	-0.714173950667
B	0.274735020235	0.358736855661	0.826442900517
C	-0.075390670155	0.019207370378	-0.495390182910
D	0.015517377910	-0.102853739633	0.118616013834
E	1.397856841851	0.983831995792	3.444351859360
F	-1.610655725684	-0.534638075259	-6.672281788450
G	0.834019373579	0.384988678058	5.408789819456
H	-0.156655610766	-0.164451089265	-1.507081414902
I	-1.350337551286	2.018785098763	-5.907654522845
J	1.834906085162	-4.999381250045	13.066436439971
K	-0.906959055403	2.330195819652	-11.120410606385
L	0.141052417019	-0.111821292041	3.174621436461
M	0.771884722221	-5.686711576541	4.092741264214
N	-1.185692533023	11.161419131738	-9.334691515145
O	0.610102363910	-5.727285957828	8.052021043201
P	-0.096294446598	0.675162774024	-2.318828140344
Q	-0.187707173061	3.458136722673	-0.982076294139
R	0.305476731449	-6.490580358764	2.240012038750
S	-0.166275141163	3.494886911919	-1.938881975544
T	0.028369281976	-0.502421013822	0.560824925186

It should be pointed out that, more terms are required for accurate correlation (Eq. 3-4-1) because the trends of $\frac{\gamma_{\pm}^{II}}{\gamma_{\pm}^{I}}$ data are complicated (Figures 3-4-2 to 3-4-3) due to the very wide range of solution concentrations involved. Nevertheless, the increase of the number of parameters for correlation does not significantly increase the difficulty in determining these parameters, since the used correlation relationship is linear with respect to these parameters.

With the correlation equation Eq. 3-4-1 and solubility data in Table 3-4-2, NaCl activity data $\frac{\gamma_{\pm}^{II}}{\gamma_{\pm}^{I}}$ at a given NaCl solution saturated with γ-glycine, DL-serine and DL-alanine respectively were calculated and also shown in Figures 3-4-2 to 3-4-4. These particular NaCl activity data form the saturation curves and they are presented separately for the two NaCl concentration ranges 0.01m ≤ NaCl ≤ 2.5m and 2.5m ≤ NaCl ≤ 5.0m, due to the complexity. They define the under-saturated and supersaturated regions. For example, in Figure 3-4-2, for each of the two NaCl concentration ranges 0.01m ≤ NaCl ≤ 2.5m and 2.5m ≤ NaCl ≤ 5.0m, the region on the right of the corresponding saturation curve is the supersaturated region with respect to γ-glycine.

Activity data $\frac{\gamma_{A}^{II}}{\gamma_{A}^{I}}$ for a nonelectrolyte (e.g. glycine) in its ternary NaCl+nonelectrolyte+H_2O solutions may be evaluated using the following equation which is derived from Eqs.3-1-5 and 3-4-1:

$$\frac{\gamma_A^{II}}{\gamma_A^{I}} = \exp[\, A\cdot m_S + \tfrac{3}{2}B\cdot {m_A}^{0.5}\cdot {m_S}^{1.5} + 2C\cdot m_A\cdot m_S + \tfrac{5}{2}D\cdot {m_A}^{1.5}\cdot m_S +$$
$$\tfrac{2}{3}E\cdot m_S^{1.5} + \tfrac{1}{2}F\cdot {m_S}^{2} + \tfrac{2}{5}G\cdot {m_S}^{2.5} + \tfrac{1}{3}H\cdot m_S^{3} +$$
$$I\cdot {m_A}^{0..5}\cdot {m_S}^{1.5} + \tfrac{3}{4}J\cdot {m_A}^{0..5}\cdot {m_S}^{2} + \tfrac{3}{5}K\cdot {m_A}^{0.5}\cdot {m_S}^{2.5} + \tfrac{1}{2}L\cdot {m_A}^{0.5}\cdot {m_S}^{3} + \qquad (3\text{-}4\text{-}3)$$
$$\tfrac{4}{3}M\cdot m_A\cdot {m_S}^{1.5} + N\cdot m_A\cdot {m_S}^{2} + \tfrac{4}{5}O\cdot m_A\cdot {m_S}^{2.5} + \tfrac{2}{3}P\cdot m_A\cdot {m_S}^{3} +$$
$$\tfrac{5}{3}Q\cdot {m_A}^{1.5}\cdot {m_S}^{1.5} + \tfrac{5}{4}R\cdot {m_A}^{1.5}\cdot {m_S}^{2} + S\cdot {m_A}^{1.5}\cdot {m_S}^{2.5} + \tfrac{5}{6}T\cdot {m_A}^{1.5}\cdot {m_S}^{3}\,]$$

where γ_A^I is the nonelectrolyte activity coefficient at its molality m_A in water in absence of NaCl while γ_A^{II} is nonelectrolyte activity coefficient at the same molality m_A in a NaCl aqueous solution with NaCl molality m_S. The selected activity data $\frac{\gamma_A^{II}}{\gamma_A^{I}}$ of glycine, DL-serine and DL-alanine are shown in Figures 3-4-5 to 3-4-7 respectively. The saturation curves shown in Figures 3-4-5 to 3-4-7 are obtained using the correlation formula Eq. 3-4-3 and solubility data in Table 3-4-2. They define the under-saturated and supersaturated regions. For example, the area above γ-glycine saturation curve in Figure 3-4-5 is the supersaturated region.

For NaCl+glycine+H_2O, the activity data show that glycine decreases NaCl activity ($\frac{\gamma_{\pm}^{II}}{\gamma_{\pm}^{I}} < 1$, Figure 3-4-2) and NaCl reduces glycine activity ($\frac{\gamma_A^{II}}{\gamma_A^{I}} < 1$, Figure 3-4-5) in both under-saturated and supersaturated regions (with respect to γ-glycine), aptly demonstrating that NaCl and glycine have salting-in effects on each other. Similar observations can be made for NaCl+DL-serine+H_2O (Figures 3-4-3 and 3-4-6). System NaCl+DL-alanine+H_2O behaves differently. Its thermodynamic activity data (Figures 3-4-4 and 3-4-7) indicate that the salting effects are complicated. With increase of solution concentrations, salting effects change from the salting-in to salting-out. All these

observations together with many other interesting phenomena (e.g. inflection points and the trends of activity curves) will be discussed in **Chapter 4**.

For an analysis of thermodynamic consistency, solubilities of γ-glycine, DL-serine and DL-alanine in NaCl aqueous solutions at 25 °C were measured by using solution density (**Appendix A**). The solubility data obtained in this work are tabulated in Table 3-4-2. These solubility data and those obtained by Khoshkbarchi and Vera (1997) through solution desupersaturation, together with the related activity data are presented in Figures 3-4-8 to 3-4-10 for a better comparison and analysis.

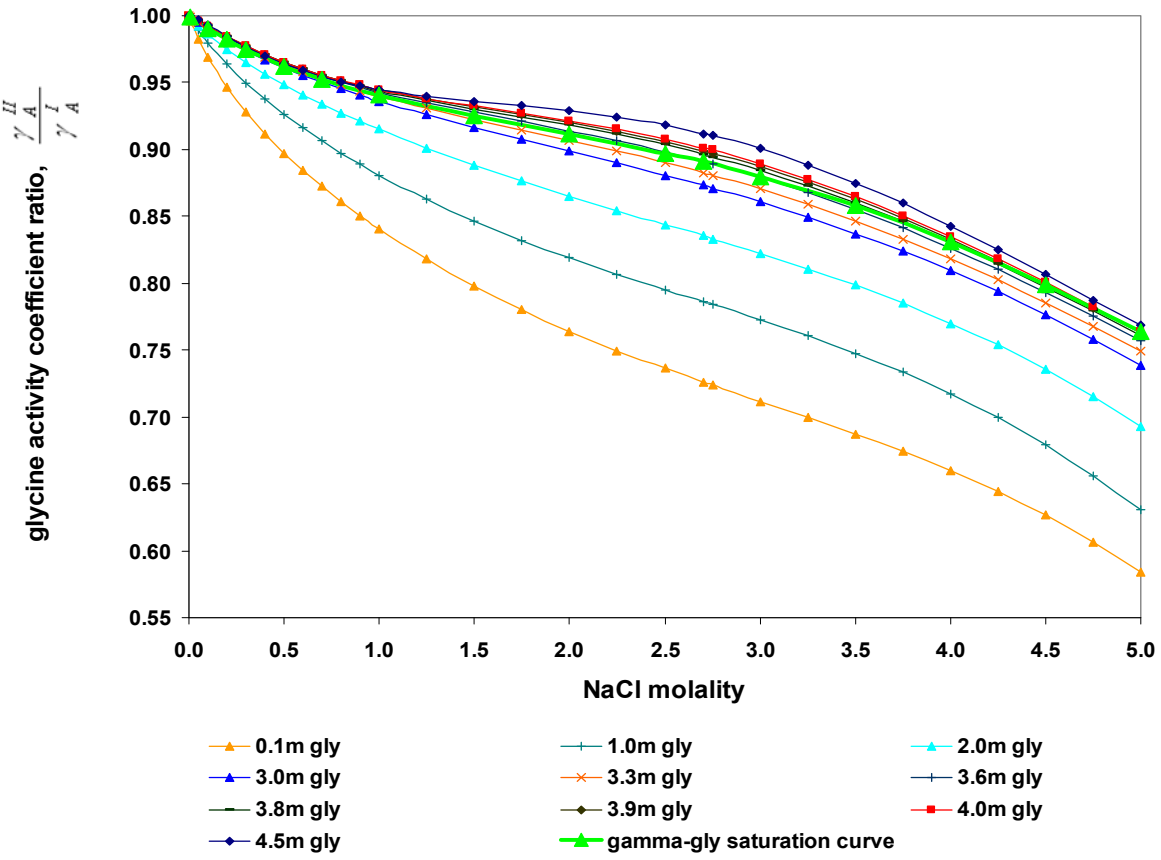

Figure 3-4-5 Effect of glycine and NaCl concentrations on glycine activity coefficient ratio $\frac{\gamma_A^{II}}{\gamma_A^{I}}$ at 25 °C

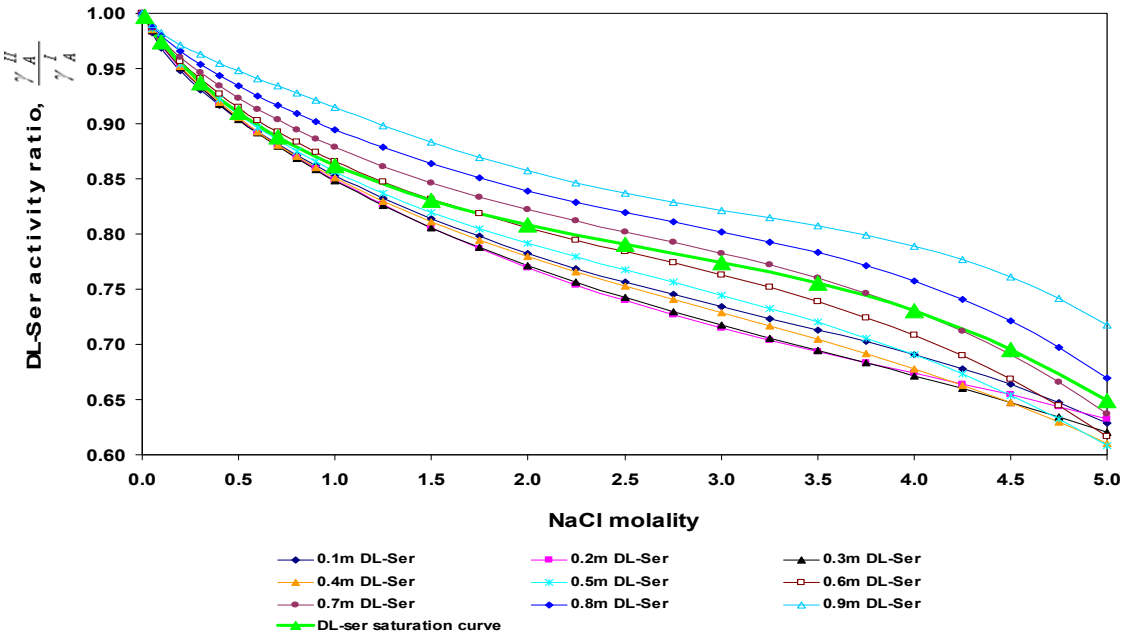

Figure 3-4-6 Effect of DL-serine and NaCl concentrations on DL-serine activity coefficient ratio $\frac{\gamma_A^{II}}{\gamma_A^{I}}$ at 25 °C

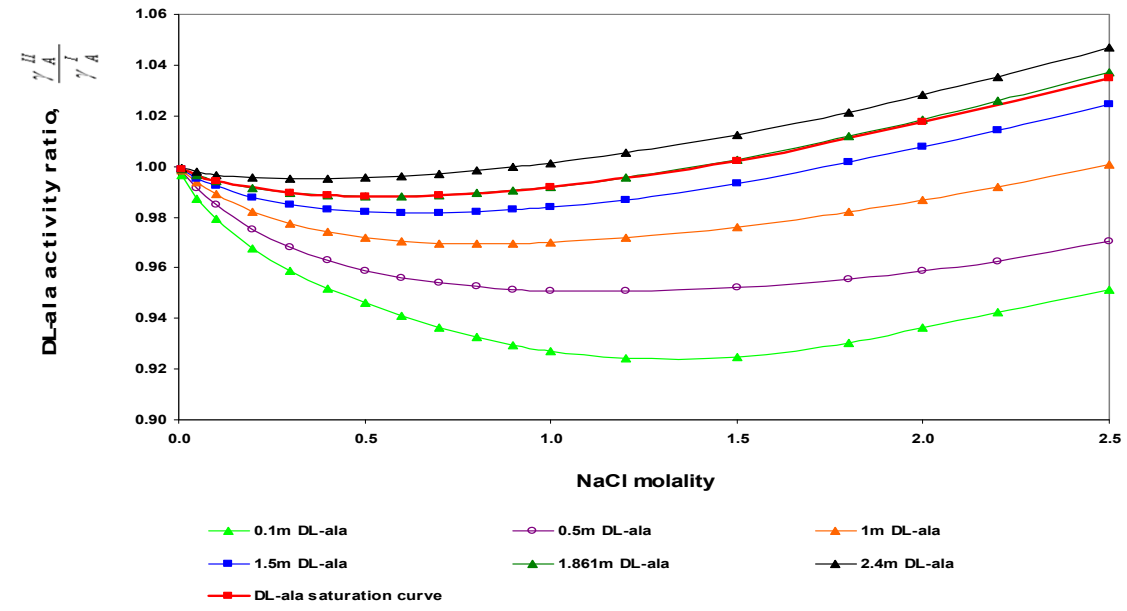

Figure 3-4-7 Effect of DL-alanine and NaCl concentrations on DL-alanine activity coefficient ratio $\frac{\gamma_A^{II}}{\gamma_A^{I}}$ of at 25 °C

Table 3-4-2 Solubilities of γ-glycine, DL-serine and DL-alanine in different NaCl solutions at 25 °C

NaCl molality	γ-glycine solubility, molality	DL-serine solubility, molality	DL-alanine solubility, molality
0.000	3.129	0.475	1.851
0.100	3.153	0.490	1.851
0.300	3.204	0.511	1.860
0.400	–	–	1.860
0.500	3.246	0.527	1.861
0.700	3.283	0.542	1.859
1.000	3.338	0.562	1.850
1.500	3.420	0.590	1.833
2.000	3.492	0.615	1.810
2.500	3.561	0.638	1.783
3.000	3.631	0.657	–
3.500	3.705	0.678	–
4.000	3.782	0.700	–
4.500	3.874	0.718	–
5.000	3.968	0.744	–

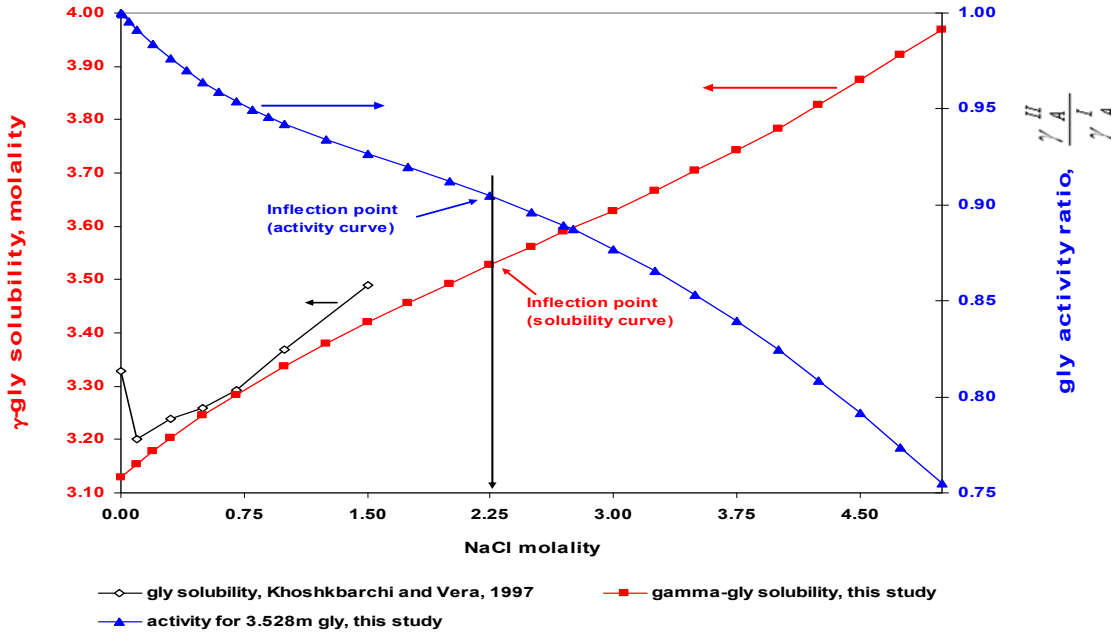

Figure 3-4-8 Solubility, activity and thermodynamic consistency for NaCl+glycine+H_2O at 25 °C

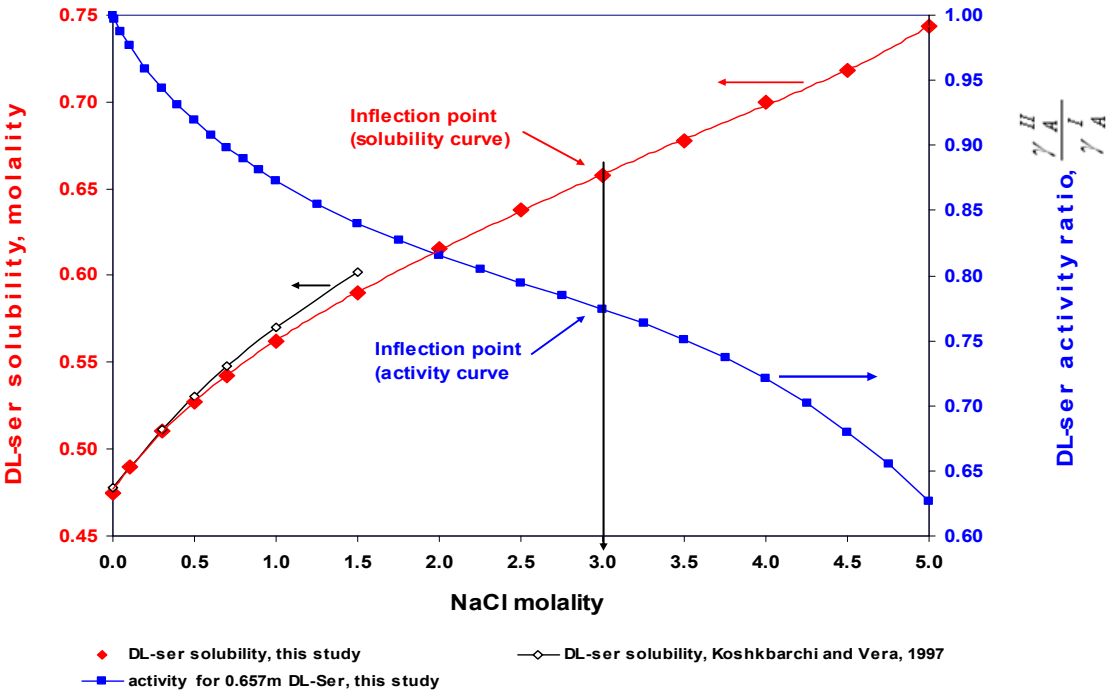

Figure 3-4-9 Solubility, activity and thermodynamic consistency for NaCl+DL-serine+H_2O at 25 °C

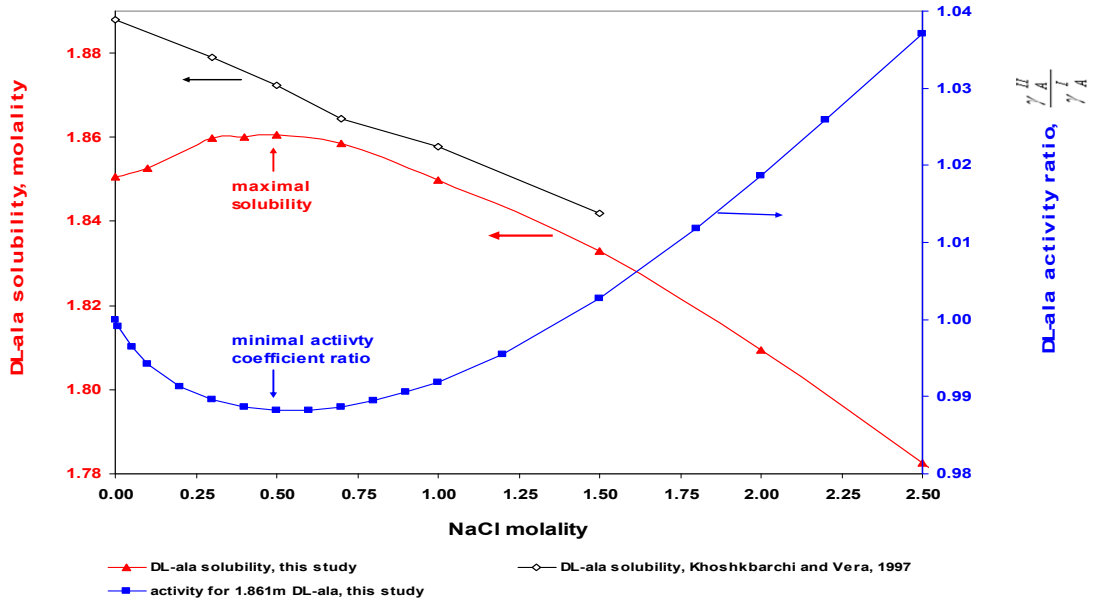

Figure 3-4-10 Solubility, activity and thermodynamic consistency for NaCl+DL-alanine+H_2O at 25 °C

Our DL-serine solubility data (Figure 3-4-9) are very close to the data reported by Khoshkbarchi and Vera (1997). But, the solubility data and data trends of γ-glycine and DL-alanine from this study are quite different from those obtained by Khoshkbarchi and Vera (1997), as shown in Figures 3-4-8 and 3-4-10. This discrepancy may be attributed to different methods for solution concentration determination. The dry-weighing method was used in the work of Khoshkbarchi and Vera (1997) while solution density was used in this study to determine solution concentrations. Compared with the commonly used dry-weighing method (Khoshkbarchi and Vera, 1997; Ferreira, et al., 2005), using solution density to determine solution concentration has obvious advantages: no concern about thermal degradation of the sample; overcoming the uncertainty due to insufficient removal of the trapped solvent among the crystals. In fact, excellent reproducibility and high accuracy of concentration measurement using solution density have been reported

(Lampreia et al., 2006; Tjahjono et al., 2005). Due to the insignificant salting effect of NaCl on DL-alanine, more precise and reliable methods for DL-alanine solubility should be used for higher accuracy.

Another possible reason for the significant discrepancy in γ-glycine solubility could partly be due to different polymorphs of the initial glycine crystals and occurrence of polymorph transition from α-glycine to γ-glycine (Sakai, et al., 1991; Doki et al., 2004). Furthermore, Khoshkbarchi and Vera (1997) employed solution desupersaturation technique for solubility test while it has been observed that γ-glycine is formed in sodium salt solutions during solution desupersaturation (Bhat and Dharmaprakash, 2002a; Towler et al., 2004). Unfortunately Khoshkbarchi and Vera did not use instruments to examine the polymorphs of the glycine crystals involved in their solubility test. It can be expected that, only if glycine polymorph is well controlled during solid-liquid equilibration, can glycine solubility data in aqueous NaCl solutions are consistent and reliable.

From the solubility curves (Figures 3-4-8 to 3-4-10), a few observations can be made. DL-alanine has a maximum solubility of 1.861m at about 0.5m NaCl (Figure 3-4-10). Thermodynamically, it can be expected that, for this particular DL-alanine molality of 1.861m, DL-alanine activity ratio $\frac{\gamma_A^{II}}{\gamma_A^{I}}$ should initially decrease and then increase with increase of NaCl, reaching its minimal value at 0.5m NaCl. Figure 3-4-10 exactly shows what is expected, with the minimal value of DL-alanine activity ratio $\frac{\gamma_A^{II}}{\gamma_A^{I}}$ being

corresponding to the maximal value of DL-alanine solubility at the same NaCl concentration of 0.5m.

γ-glycine solubility curve has an inflection point at about 2.25m NaCl, with γ-glycine having a solubility of 3.528m (Figure 3-4-8). Before and after the inflection point, NaCl exerts the salting-in effect on glycine differently. When NaCl concentration is lower than 2.25m, γ-glycine solubility increases slowly with increase of NaCl. However, when NaCl concentration is higher than 2.25m, the increase of γ-glycine solubility becomes increasingly more effective with increase of NaCl. Thermodynamically, a corresponding inflection point can be expected on the curve of glycine activity ratio $\frac{\gamma_A^{II}}{\gamma_A^{I}}$ at the particular γ-glycine molality of 3.528m to reflect the effectiveness of NaCl salting-in effect on glycine, via the decrease of glycine activity ratio $\frac{\gamma_A^{II}}{\gamma_A^{I}}$ with increase of NaCl. As it is precisely shown in Figure 3-4-8, both inflection points occur indeed at the same NaCl concentration of 2.25m. Similarly, DL-serine solubility curve shows an inflection point at about 3m NaCl, with a solubility of 0.675m (Figure 3-4-9). The two corresponding inflection points on DL-serine activity curve and solubility curve are nicely matched, as shown in Figure 3-4-9.

It can be seen that activity and solubility data for each of the three ternary systems are thermodynamically consistent. In turn, the good thermodynamic consistency supports the reliability and accuracy of both activity and solubility data obtained in this study. It

should be highlighted that only when the supersaturated activity data are available, can the thermodynamic consistency between activity and solubility be analyzed.

3.4.2 Derivation of Activities for Binary Supersaturated Nonelectrolyte Solutions

Since the steady state shifting technique relies on measurement of electrochemical cell potential, it can not be used directly for nonelectrolyte solutions, while the binary activity data γ_A^I of a nonelectrolyte in its supersaturated region are needed for crystallization studies, due to the importance of crystallization of a nonelectrolyte from its binary aqueous solutions.

A rigorous thermodynamic approach is proposed to derive the binary activity data γ_A^I of a nonelectrolyte, using cell potential data of an electrolyte added into the corresponding nonelectrolyte+H_2O solutions. In other words, an electrolyte is used as a tracer to create a measurable quantity (i.e. cell potential) for the electrochemical method. In addition, the proposed approach requires accurate solubility data of the nonelectrolyte in the electrolyte+H_2O solutions. Depending on the salting effects of the electrolyte on the nonelectrolyte, the binary activity coefficient γ_A^I for nonelectrolyte+H_2O solutions in the under-saturated and/or supersaturated regions can be derived.

The obtained activity data $\frac{\gamma_A^{II}}{\gamma_A^I}$ and the solubility data for the three ternary systems are used to extract the binary activity coefficients of the three nonelectrolytes, namely glycine, DL-serine and DL-alanine, in their own binary aqueous solutions (i.e.

glycine+H_2O, DL-serine+H_2O and DL-alanine+H_2O), especially in the supersaturated region.

3.4.2.1 Fundamental Analysis

The chemical potential μ_A of a nonelectrolyte in a solution may be generally expressed by its activity coefficient γ_A and molality m_A (Prausnitz et al., 1999):

$$\mu_A = \mu_A^0 + RT \ln(\gamma_A m_A) \tag{3-4-4}$$

When a solution (liquid phase) is at equilibrium with the nonelectrolyte crystal (solid phase), the solution is saturated with the nonelectrolyte and the nonelectrolyte concentration of the saturated solution is its solubility (m_A^{Sat}). At the solid-liquid equilibrium, the chemical potential μ_A^{Sat} of the nonelectrolyte in the liquid phase should be equal to the chemical potential μ_A^{Crys} of the nonelectrolyte crystal. For a binary saturated nonelectrolyte+H_2O solution, the following expression applies:

$$\mu_A^{I,Sat} = \mu_A^o + RT \ln(\gamma_A^{I,Sat} m_A^{I,Sat})_{m_S=0} = \mu_A^{Crys} \tag{3-4-5}$$

where $\mu_A^{I,Sat}$ is the chemical potential, $m_A^{I,Sat}$ and $\gamma_A^{I,Sat}$ are the solubility and the corresponding activity coefficient of the nonelectrolyte at the saturation point. Similarly, for a ternary electrolyte+nonelectrolyte+H_2O solution saturated with the nonelectrolute ($m_A^{II,Sat}$) at a given electrolyte molality m_S, the chemical potential $\mu_A^{II,Sat}$ of the nonelectrolyte is determined by

$$\mu_A^{II,Sat} = \mu_A^o + RT \ln(\gamma_A^{II,Sat} m_A^{II,Sat})_{m_S>0} = \mu_A^{Crys} \tag{3-4-6}$$

At the same temperature, Eq.3-4-5 and Eq. 3-4-6 are equal and it gives:

$$\mu_A^{I,Sat} = \mu_A^{II,Sat} = \mu_A^{Crys} \tag{3-4-7}$$

It should be noted that only if the chemical potentials of the nonelectrolyte crystals in the binary nonelectrolyte+H_2O solution and in the ternary electrolyte+nonelectrolyte+H_2O solution are the same, can Eq.3-4-7 be valid. In other words, to have the same chemical potentials of the nonelectrolyte crystals, the polymorphs of the nonelectrolyte crystals at equilibrium with a binary nonelectrolyte+H_2O solution and those with a ternary electrolyte+nonelectrolyte+H_2O solution should be identical and the electrolyte (as an impurity) is not incorporated into the nonelectrolyte crystal lattices. For derivation, here it is assumed that the chemical potentials of the nonelectrolyte crystals are identical. The concern of the chemical potential change of nonelectrolyte crystals due to different polymorphs and impurity incorporation will be addressed in **Section 3.4.2.2**.

Equating Eq. 3-4-5 and Eq. 3-4-6 yields:

$$(\gamma_A^{I,Sat} m_A^{I,Sat})_{m_S=0} = (\gamma_A^{II,Sat} m_A^{II,Sat})_{m_S>0} = K_{SP} \tag{3-4-8}$$

where K_{SP}, a constant at a given temperature, is the solubility product of the nonelectrolyte. Mathematical manipulation of Eq. 3-4-8 yields the following working equation to obtain the binary activity data γ_A^I of the nonelectrolyte in its binary nonelectrolyte+H_2O solution at molality $m_A = m_A^{II,Sat}$:

$$\begin{aligned} \gamma_A^I &= \frac{\gamma_A^{II,Sat}}{\left(\gamma_A^{II,Sat} / \gamma_A^I\right)} \\ &= \frac{\left(K_{SP} / m_A^{II,Sat}\right)}{\left(\gamma_A^{II,Sat} / \gamma_A^I\right)} \end{aligned} \tag{3-4-9}$$

It is evident that the nonelectrolyte solubility $m_A^{II,Sat}$ in an electrolyte+H_2O solution at a given electrolyte molality m_S can be measured experimentally. Given that m_S and $m_A^{II,Sat}$ are known, the value of activity coefficient ratio $\frac{\gamma_A^{II,Sat}}{\gamma_A^I}$ of the nonelectrolyte can be evaluated using Eq. 3-1-5 (or Eq. 3-4-3 for the three ternary systems studied here). Then applying Eq. 3-4-9, the binary activity data γ_A^I of the nonelectrolyte in its binary nonelectrolyte+H_2O solution at molality $m_A = m_A^{II,Sat}$ is readily obtained, since the solubility product K_{SP} can be available from reference resources.

Varying electrolyte molality m_S can produce a series of solubility data $m_A^{II,Sat}$ and accordingly activity coefficient ratios $\frac{\gamma_A^{II,Sat}}{\gamma_A^I}$, which results in extraction of many sets of binary activity data γ_A^I for the nonelectrolyte+H_2O solutions. It should be pointed out that, if the electrolyte has a salting-out effect on the nonelectrolyte (hence $m_A^{II,Sat} < m_A^{I,Sat}$ and $\frac{\gamma_A^{II,Sat}}{\gamma_A^I} > 1$), then the binary activity data γ_A^I for binary under-saturated nonelectrolyte+H_2O solutions are obtained; if the electrolyte has a salting-in effect on the nonelectrolyte (hence $m_A^{II,Sat} > m_A^{I,Sat}$ and $\frac{\gamma_A^{II,Sat}}{\gamma_A^I} < 1$), the binary activity data γ_A^I for binary supersaturated nonelectrolyte+H_2O solutions are obtained. The latter would be useful for the study of the nonelectrolyte crystallization from H_2O.

3.4.2.2 Activities of Binary Nonelectrolyte+H_2O Solutions

For γ-glycine, DL-serine and DL-alanine, their solubilities $m_A^{II,Sat}$ in different NaCl solutions have been obtained at 25 °C as shown in Table 3-4-2. The value of activity coefficient ratio $\frac{\gamma_A^{II,Sat}}{\gamma_A^I}$ of the nonelectrolyte at m_S and $m_A = m_A^{II,Sat}$ can be calculated using Eq. 3-4-3, with the parameters tabulated in Table 3-4-1. As the binary activity coefficients γ_A^I of each of these three amino acids in H_2O at 25 °C are available (up to saturation point) from literatures, their solubility products (K_{SP}) can be obtained by calculation. Therefore, binary activity data γ_A^I in the under-saturated and/or supersaturated region can be calculated using Eq. 3-4-9.

Ellerton et al. (1964) and Smith and Smith (1937a) used the isopeistic method to measure the activity coefficient of glycine in H_2O at 25 °C. The concentration of glycine was up to 3.114m in the experiments by Ellerton et al. (1964) and up to 3.30m in the experiments by Smith and Smith (1937a). The activity data of glycine from these two research groups are very comparable. Smith and Smith (1937b and 1940) also experimentally investigated the activity coefficients of DL-alanine (up to 1.90m) and DL-serine (up to 0.4958m) in H_2O at 25 °C, using the same isopeistic method. With the activity coefficients of glycine (Ellerton et al., 1964), DL-alanine (Smith and Smith, 1937b) and DL-serine (Smith and Smith, 1940) in H_2O at 25 °C, the solubility products K_{SP} ($= \gamma_A^{I,Sat} m_A^{I,Sat}$) were found to be 2.3087 for γ-glycine, 1.9311 for DL-alanine and 0.4332 for DL-serine. Note that $m_A^{I,Sat}$ is solubility in pure H_2O (Table 3-4-2).

Substitution of solubility $m_A^{II,Sat}$, solubility product K_{SP}, the calculated activity coefficient ratio $\frac{\gamma_A^{II,Sat}}{\gamma_A^I}$ into Eq. 3-4-9 yields the binary activity γ_A^I of each of the three amino acids in its binary aqueous solutions. These derived binary activity data γ_A^I for glycine, DL-serine and DL-alanine, together with the data obtained by other workers, are plotted in Figures 3-4-11 to 3-4-13 respectively.

Due to salting-in effect of NaCl on glycine and DL-serine, the binary activity data γ_A^I of glycine and DL-serine in their own binary supersaturated aqueous solutions are derived, as shown in Figures 3-4-11 and 3-4-12, with a relative supersaturation σ up to 0.27 for γ-glycine and 0.57 for DL-serine.

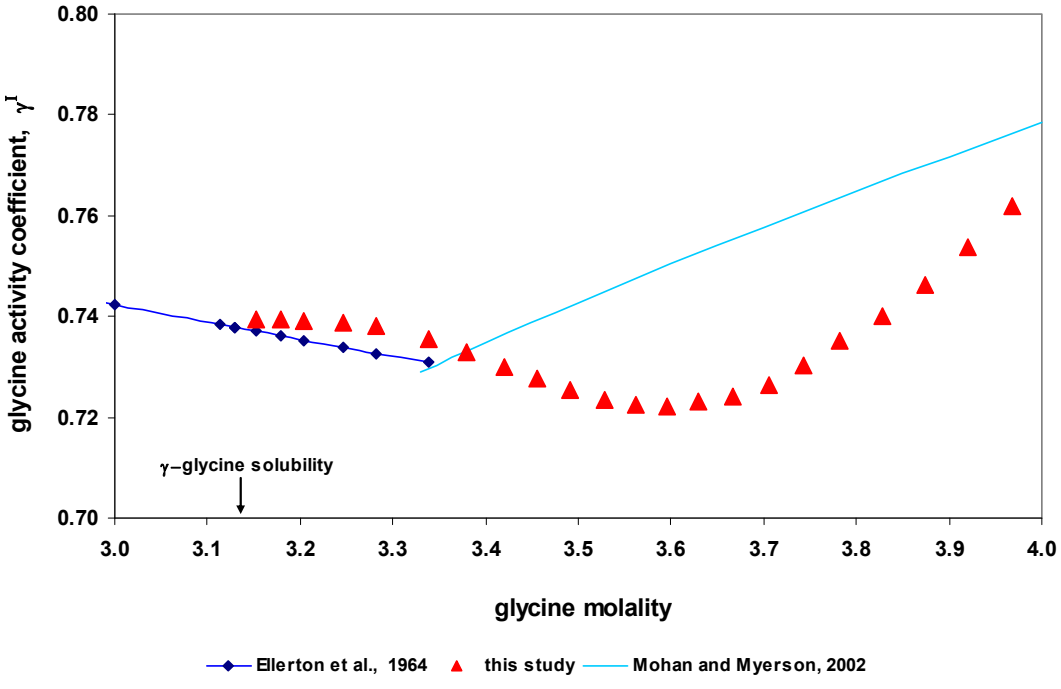

Figure 3-4-11 Binary activity data γ_A^I of glycine in its binary aqueous solutions at 25 °C

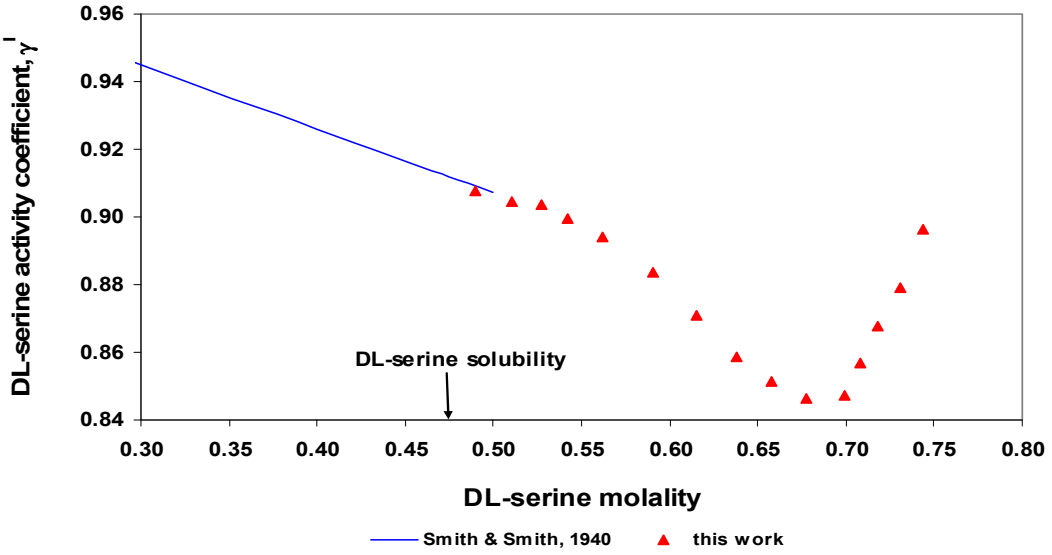

Figure 3-4-12 Binary activity data γ_A^I of DL-serine in its binary aqueous solutions at 25 °C

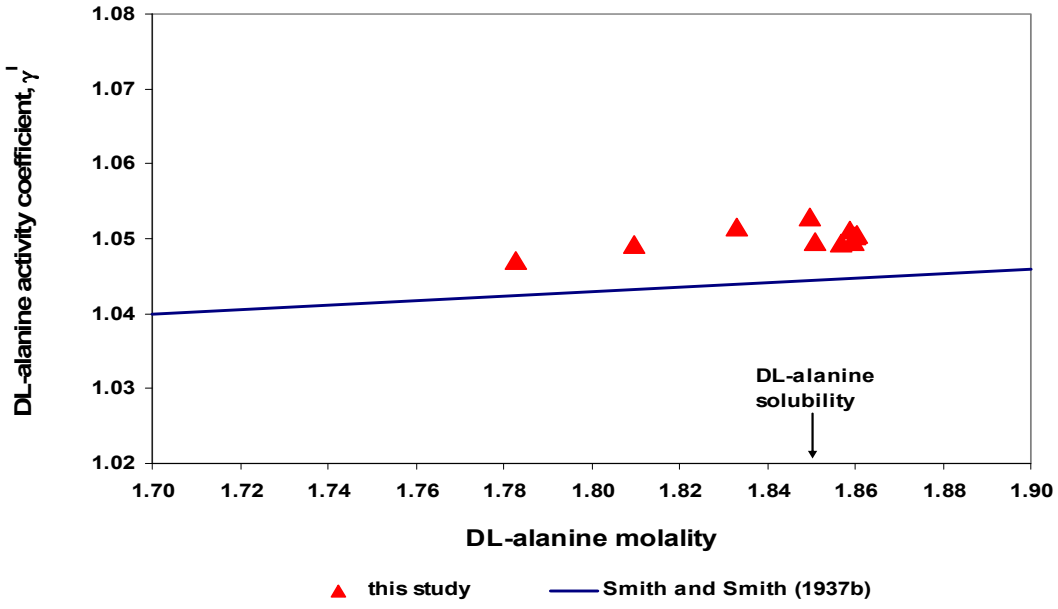

Figure 3-4-13 Binary activity data γ_A^I of DL-alanine in its binary aqueous solutions at 25 °C

For glycine, it can be seen that our binary activity data γ_A^I are well comparable with those reported by Ellerton et al. (1964) in the range of glycine 3.13 – 3.30m, as shown in Figure 3-4-11. Mohan and Myerson (2002) reported water activity data in glycine supersaturated solutions at 25 °C, using EBD method. These water activity data were used to derive glycine activity coefficients in its supersaturated solutions, via Gibbs Duhem equation. The obtained glycine activity coefficients according to the work of Mohan and Myerson are also presented in Figure 3-4-11. Our data and the data by Mohan and Myerson (2002) are not that well comparable, but both generally show a similar trend when glycine concentration is high.

For DL-serine, Figure 3-4-12 shows a good agreement between our data and the literature data in a narrow range of DL-serine concentration (around solubility). Unfortunately, there are no other reported experimental data for DL-serine in its binary highly supersaturated aqueous solutions and therefore comparison in a wide range of concentration could not be made.

Figures 3-4-11 and 3-4-12 indicate that, above certain level of supersaturation, the activity coefficients of glycine and DL-serine increase with increase of their concentrations, implying that the solute association becomes more and more significant, though salvation is still relatively dominant. This is expected, since, in the supersaturated solutions, the solute molecules should associate significantly to make microscopic clusters which eventually lead to nucleation.

For DL-alanine, NaCl has both salting-in and salting-out effects on DL-alanine (Figures 3-4-7 and 3-4-10), depending on solution concentration. The salting-in effect of NaCl (0.1 – 1.0m NaCl) leads to extracting the binary activity γ_A^I of DL-alanine in its binary very slightly supersaturated solutions in the range 1.851 – 1.859m (vs DL-alanine solubility 1.851m). In this small range, the binary activity coefficients γ_A^I are practically the same (Figure 3-4-13). In the range 1.0 – 2.5m NaCl, the salting-out effect of NaCl on DL-alanine causes DL-alanine solubility to slightly decrease from 1.850m in 1m NaCl to 1.783m in 2.5m NaCl. As a result, binary activity data γ_A^I of DL-alanine in its under-saturated aqueous solutions (from 1.783 up to solubility 1.850m) are derived, with γ_A^I slightly increasing from 1.047 at 1.783m DL-alanine to 1.053 at 1.850m DL-alanine. Comparing our data with literature data (Smith and Smith, 1937b), the deviation is very small as shown in Figure 3-4-13. As discussed earlier, NaCl+DL-alanine+H_2O system is a difficult one in activity and solubility measurements. Even for such a difficult system, very comparable binary activity data γ_A^I for DL-alanine can be obtained too, using the solubility data and activity coefficient ratio $\frac{\gamma_A^{II,Sat}}{\gamma_A^I}$ of DL-alanine.

We have demonstrated that the salting-in effect of an electrolyte on a nonelectrolyte leads to the determination of binary activity coefficients of the nonelectrolyte in its binary supersaturated aqueous solutions, while the salting-out effect of an electrolyte results in obtaining binary activity coefficients of the nonelectrolyte in its binary under-saturated aqueous solutions. The former is potentially more important as

these binary activity coefficient data would be very useful for studying nucleation and crystal growth of a nonelectrolyte from H_2O.

It should be pointed out that selecting an electrolyte which has a sating-in effect on a nonelectrolyte can be done readily by screening the nonelectrolyte solubility in the aqueous electrolyte solutions. Therefore the approach developed in this study provides a general and viable method for obtaining the activity coefficients of a noneletrolyte in its binary supersaturated solutions.

The above derivation for binary activity coefficient γ_A^I is based on the assumption that the chemical potentials of the crystals of a given nonelectrolyte (e.g. γ-glycine) are identical. This assumption actually requires that the same polymorph (if the crystals are polymorphic) of crystals should be maintained during solid-liquid equilibration for solubility test, and that impurity (here NaCl) incorporation into crystal lattices is absent or insignificant. This is understandable because different polymorphs would have different chemical potentials hence different solubilities and different solubility product Ksp. Impurity (here NaCl) incorporation which would occur more likely during crystal growth (Rak et al., 2005) would cause the chemical potential of the crystals to change.

Powder-XRD analysis has shown that there was no polymorph change in γ-glycine, DL-serine and DL-alanine before and after solubility tests. After completion of the solubility tests particularly in concentrated (4m or 5m) NaCl solutions, via both crystal dissolution and solution desupersaturation, crystals of γ-glycine, DL-serine and

DL-alanine were collected. These crystals were re-dissolved in pure H_2O to determine their NaCl contents using Ion Chromatography (Waters IC 2690, Waters 432 Conductivity Detector, IC Pak Anion HB column, injection 25µl and buffer $NaHCO_3$-Na_2CO_3 flowrate 1.0ml/min). As the impurity contents in the crystals were very low, approximately **0.0001** more fraction, it can be assumed that the effect of impurity incorporation (if any) on the chemical potential of the crystals is negligible. Therefore the validity of the assumption made for the derivation of binary activity coefficient γ_A^I is confirmed.

3.5 Summary

A new technique, namely steady state shifting technique, has been proposed for the potentiometric (electrochemical) method, so that the potentiometric method has been extended from under-saturated to supersaturated solutions. The new technique relies on relatively fast thermal phenomena to achieve a steady-state measurement, instead of slow molecular diffusion in the conventional potentiometric method. As this new technique only involves the change of the operation procedure for the cell potential measurements and additional hardware is not necessary, it is as simple and easy as the conventional potentiometric method.

The proposed technique has been experimentally verified. Its successful application to the systematic thermodynamic study of the three ternary NaCl+nonelectrolyte+H_2O systems NaCl+glycine+H_2O has been demonstrated (especially in the supersaturated region). As this new technique enables the activity

measurements to be made in a wide range of the solution concentrations, from dilute up to the onset of nucleation, new and interesting phenomena have been observed.

With the activity data of supersaturated solutions, thermodynamic consistency between activity and solubility has been analyzed. The very good thermodynamic consistency supports the claim that experimental measurements on both activity and solubility are accurate. It is expected that the new technique can be used to determine the activity coefficients for many other ternary systems, based on the experimental framework established in this study.

The obtained thermodynamic activities for three ternary systems of NaCl+nonelectrolyte+H_2O have been used to extract the binary activity coefficients of these nonelectrolytes in their own binary aqueous solutions in the supersaturated regions. Thus the proposed technique offers a convenient alternative to experimental thermodynamic studies for binary nonelectrolyte supersaturated solutions.

Furthermore, the obtained activity data confirm that the solute activity coefficients may significantly vary with solution concentration in the supersaturated regions, depending on the nature of the systems. Therefore their contributions to the driving force for crystallization may not be negligible. Particularly for binary DL-serine+H_2O system (Figure 3-4-12), using $\ln(\frac{m_A^I}{m_A^{I,Sat}})$ to approximate the intrinsic thermodynamic driving force $\ln(\frac{\gamma_A^I m_A^I}{\gamma_A^{I,Sat} m_A^{I,Sat}})$ can lead to a large error, up to 27%.

Chapter 4 Analysis of Solution Chemistry, Thermodynamics and Molecular Interaction for NaCl+Amino Acid+H_2O Solutions

It is commonly accepted that solution chemistry is one of the fundamentals for understanding polymorphism (Towler et al., 2004). That is because solution chemistry would reveal the impacts of solution change (e.g., due to pH and additives etc) on molecular interactions which are the origin of crystal polymorphism. Generally, different molecular interactions would result in formation of different structured nuclei (or clusters) which eventually develop into the corresponding macroscopic polymorphic crystals (Davey et al., 1997; Weissbuch et al., 1994a, Towler et al., 2004). In addition, molecular interactions also play an important role in crystal or nucleus growth kinetics, either inhibiting or enhancing nucleus growth, thus exerting the influence on the nucleation onset of a particular polymorph.

As nucleation, polymorphs and crystal growth can only happen in supersaturated solutions, it is of great importance to explore the solution chemistry (e.g. molecular interaction and complex formation) in the supersaturated regions of solutions so as to gain a better understanding of crystal polymorphism and kinetics. Since thermodynamic activity is related to the molecular interactions, it can be used to explore how molecules to interact especially when the solution concentration changes and/or when an additive is put in the solution. It should be emphasized that the thermodynamic activity data of supersaturated solutions are required to confidently study the impacts of molecular interaction on crystal polymorphs and kinetics.

In the previous chapter (**Chapter 3**), the thermodynamic activities for three NaCl+amino acid+H_2O systems in both under-saturated and supersaturated regions were measured and reported. In this chapter (**Chapter 4**), based on these measured thermodynamic activity data, the molecular interactions (especially ion-dipole interaction) and complex formation which change with solution concentration will be thoroughly analyzed, with the emphasis given to NaCl+glycine+H_2O to attempt the effects of a general 1:1 electrolyte on glycine polymorphs.

More importantly, the analysis would imply that a 1:1 electrolyte, whether it is a sodium salt or a non-sodium salt (e.g. NH_4Ac), would inhibit α-glycine and enhance γ-glycine. This implication indicates that it is necessary to re-look into the mechanism of γ-glycine formation from an electrolyte solution, as γ-glycine formation was once attributed to the specific interaction between sodium ions (Na^+) and α-glycine nuclei (Towler et al., 2004).

4.1 Detailed Experimental Observations

Based on the measured activity data and solubility data for the three ternary solution systems (namely NaCl+glycine+H_2O, NaCl+DL-serine+H_2O and NaCl+DL-alanine+H_2O), detailed observations may be made to facilitate revealing the general molecular interactions among the amino acid dipolar ions (e.g. glycine zwitterions) and the electrolyte ions (Na^+ and Cl^-).

Overall, as was briefed **in Chapter 3**, in both under-saturated and supersaturated regions within the experimental concentration ranges, not only NaCl and glycine but also NaCl and DL-serine have salting-in effects on each other ($\frac{\gamma_{\pm}^{II}}{\gamma_{\pm}^{I}}$ <1 and $\frac{\gamma_{A}^{II}}{\gamma_{A}^{I}}$ <1. Figures 3-4-2 to 3-4-3, 3-4-5 to 3-4-6). NaCl and DL-alanine have weak but complicated salting effects (Figures 3-4-4 and 3-4-7), exerting salting-in and salting-out effects on each other at low and high solution concentrations respectively.

In general, the salting-in effects of glycine, DL-serine and DL-alanine on NaCl are more pronounced at their low concentrations (Figures 3-4-2 to 3-4-4). However, the trends of these salting-in effects are different. For NaCl+glycine+H_2O, with increase of glycine concentration up to a moderate value, its salting-in effect on NaCl becomes less effective. When glycine concentration is very high, especially when it penetrates into its supersaturated region, its salting-in effect on NaCl tends to be more pronounced if NaCl concentration is relatively low (≤ 2.5m), suggesting an inflection point on each of these NaCl activity curves (NaCl ≤ 2.5m, Figure 3-4-2). In contrast, for NaCl+DL-serine+H_2O, no obvious inflection points are observed on NaCl activity curves (Figure 3-4-3). Nevertheless, the salting-in effects on NaCl increase monotonically with increase of glycine or DL-serine. For NaCl+DL-alanine+H_2O, with increase of DL-alanine, the transition from salting-in to salting-out effect on NaCl is observed (Figure 3-4-4).

Surprisingly, for NaCl+glycine+H_2O and NaCl+DL-serine+H_2O, it is found that the NaCl activity curve shifts, going upwards with increase of NaCl concentration (up to

approximately 2.5m NaCl) and then going downwards with further increase of NaCl (NaCl > 2.5m), as shown in Figures 3-4-2 and 3-4-3.

With respect to the activity coefficient ratios $\frac{\gamma_A^{II}}{\gamma_A^{I}}$ of glycine and DL-serine (Figures 3-4-5 and 3-4-6), it can be seen that, for a given glycine or DL-serine concentration, the salting-in effect of NaCl on either glycine or DL-serine increases monotonically with increase of NaCl. But the salting-in effect of NaCl becomes less effective with increase of NaCl up to a moderate concentration of NaCl. However, with further increase of NaCl, the effect of NaCl on glycine or DL-serine starts to be more effective, creating an inflection point on each of glycine or DL-serine activity curves. A typical inflection point and the thermodynamic consistency have been well depicted in Figures 3-4-8 and 3-4-9 for glycine and DL-serine respectively. NaCl has a different effect on DL-alanine. For a given DL-alanine, the salting-in effect of NaCl on DL-alanine is favored then deteriorated by increase of NaCl, generating a transition from salting-in to salting-out effect (Figure 3-4-7).

Glycine, DL-serine and DL-alanine activity curves shift upwards with increase of their concentrations (Figures 3-4-5 to 3-4-7), though there are a few exceptions where DL-serine activity curves intersect when DL-serine concentrations are very low (under-saturated). Particularly, some of DL-alanine activity curves shift up into the salting-out region ($\frac{\gamma_A^{II}}{\gamma_A^{I}} > 1$), as shown in Figure 3-4-7.

All these phenomena observed for the three systems NaCl+glycine+H_2O, NaCl+DL-serine+H_2O and NaCl+DL-alanine+H_2O may be interpreted based molecular interaction and complex formation (**Sections 4.2 and 4.3)**.

4.2 Solution Chemistry, Molecular Interaction and Complex Formation

Glycine, DL-serine and DL-alanine are amino acids and their molecules are dipolar ions (i.e. zwitterions). In a ternary NaCl+amino acid+H_2O solution, the important molecular interactions include dipole-dipole, ion-dipole and ion-hydrocarbon chain interactions. The resultant outcome of these interactions eventually determines the salting effect (either salting-in or salting-out) of NaCl and an amino acid on each other.

A dipolar molecule of an amino acid may be schematically expressed as $H_2NRCOOH$ (here R for a hydrocarbon chain). It has an amino group (NH_2) and a carboxyl group (COOH). In an aqueous amino acid solution, due to intra-molecular proton transfer from carboxyl group to amino group (Cohn and Edsall, 1943; Towler et al., 2004), generally an amino acid molecule is of zwitterionic form (dipolar ion, $^{+}H_3NRCOO^{-}$):

$$H_2NRCOOH \Leftrightarrow {}^{+}H_3NRCOO^{-} \qquad (4\text{-}2\text{-}1)$$

Due to the attraction between the highly polar amino group and carboxyl group, the inter-molecular dipole-dipole interaction and the hydrogen bonding can be very substantial, leading to the significant formation of cyclic dimers (Towler et al., 2004) via the following reversible reaction:

$$2\ {}^{+}H_3NRCOO^{-} \Leftrightarrow \begin{pmatrix} OOCRNH_3 \\ H_3NRCOO \end{pmatrix} \quad (4\text{-}2\text{-}2)$$

Especially for glycine zwitterions (${}^{+}H_3NCH_2COO^{-}$), glycine cyclic dimers may be formed much more readily, as glycine has much smaller steric hindrance to the formation of cyclic dimers, compared with DL-serine [${}^{+}H_3NCH(CH_2OH)COO^{-}$] and DL-alanine [${}^{+}H_3NCH(CH_3)COO^{-}$] each of which has a bigger side hydrocarbon chain. Therefore, in a glycine aqueous solution, glycine cyclic dimers $\begin{pmatrix} OOCCH2NH_3 \\ H_3NCH2COO \end{pmatrix}$ may be quite dominant over its zwitterions (${}^{+}H_3NCH_2COO^{-}$).

When an electrolyte is dissolved and dissociated (e.g. $NaCl \Rightarrow Na^{+} + Cl^{-}$) in an amino acid aqueous solution, the ion-dipole interaction between an electrolyte ion and a zwitterion ${}^{+}H_3NRCOO^{-}$ can be very significant to form different ion-zwitterion complexes, depending on solution concentration and the nature of the electrolyte. Since NaCl has been used in the thermodynamic investigation (**Chapter 3**), the discussion will focus on how NaCl to interact with an amino acid. However, the analysis of molecular interactions and complex formation should be applicable to many other electrolyte+amino acid+H_2O systems.

When NaCl molality is much lower than an amino acid molality, one ion (either Na^{+} or Cl^{-}) can physically bind one zwitterion to form two types of singly-charged ion-zwitterion complexes:

$${}^{+}H_3NRCOO^{-} + Na^{+} \Leftrightarrow {}^{+}H_3NRCOONa \quad (4\text{-}2\text{-}3)$$

$$Cl^{-} + {}^{+}H_3NRCOO^{-} \Leftrightarrow ClH_3NRCOO^{-} \quad (4\text{-}2\text{-}4)$$

With consumption of zwitterions ($^{+}H_3NRCOO^{-}$) (Eqs. 4-2-3 and 4-2-4), cyclic dimers would be destroyed or disintegrated (via Eq. 4-2-2). In fact, electrolyte ions may directly interact with a cyclic dimer $\begin{pmatrix} OOCRNH_3 \\ H_3NRCOO \end{pmatrix}$ too:

$$\begin{pmatrix} OOCRNH_3 \\ H_3NRCOO \end{pmatrix} + Na^{+} + Cl^{-} \Leftrightarrow {}^{+}H_3NRCOONa + ClH_3NRCOO^{-} \qquad (4\text{-}2\text{-}5)$$

With increase of NaCl concentration, the number of free Na^{+} and Cl^{-} ions increases. Due to electrostatic force, one free ion (either Na^{+} or Cl^{-}) can be bound onto the charged end of a singly-charged ion-zwitterion complex to form a neutral ion-zwitterion complex ($ClH_3NRCOONa$):

$$Cl^{-} + {}^{+}H_3NRCOONa \Leftrightarrow ClH_3NRCOONa \qquad (4\text{-}2\text{-}6)$$

$$ClH_3NRCOO^{-} + Na^{+} \Leftrightarrow ClH_3NRCOONa \qquad (4\text{-}2\text{-}7)$$

It should be noted that the probability of forming singly-charged ion-zwitterion complexes ($^{+}H_3NRCOONa$ and ClH_3NRCOO^{-}) may be higher than that of forming neutral ion-zwitterion complexes ($ClH_3NRCOONa$).

4.3 Interpretation of the Observed Thermodynamic Activities

These singly-charged ($^{+}H_3NRCOONa$ and ClH_3NRCOO^{-}) and neutral ($ClH_3NRCOONa$) ion-zwitterion complexes formed due to the attractive ion-dipole interaction (binding) would lower the energy of the solution hence prevent both NaCl and an amino acid from self-association (potential precipitation). Therefore these ion-zwitterion complexes would contribute to the salting-in effect on each other. On the other hand, there are repulsions including the major one between an electrolyte ion (either

Na^+ or Cl^-) and the hydrophobic hydrocarbon chain of an amino acid molecule, increasing the system energy, tending to dampen the salting-in effect and even resulting in salting-out effect.

It should be noted that, with increase of solution concentration, the distance between an ion and a hydrocarbon chain becomes shorter and the probability of their exposure to each other increases. Therefore, the repulsions between electrolyte ions and the hydrophobic hydrocarbon chains would become more pronounced in a concentrated solution.

4.3.1 Salting Effect of an Amino Acid on NaCl

As glycine has a smaller hydrocarbon chain ($^+H_3NCH_2COO^-$), its hydrophobicity is low and therefore glycine is quite hydrophilic due to its two hydrophilic polar groups (amino and carboxyl groups). For DL-serine, on the one hand, it has a side hydrophobic hydrocarbon chain (CH_2) which increases its hydrophobicity. On the other hand, the introduction of the polar group OH to the side hydrocarbon chain would overcome the hydrophobicity created by the side chain CH_2. As a result, the hydrophilicity of polar amino and carboxyl groups of a DL-serine molecule would substantially suppress the hydrophobicity. Consequently, the attractive ion-dipole interactions (bindings) between ions (Na^+ or Cl^-) and glycine and those between ions and DL-serine would override the repulsions, leading to salting-in effect on each other, as it was shown by the activity data (Figures 3-4-2, 3-4-3, 3-4-5 and 3-4-6) and the solubility data (Figures 3-4-8 and 3-4-9).

A DL-alanine molecule has a larger side hydrophobic chain (CH_3) than glycine. A bigger repulsion between an ion (Na^+ or Cl^-) and DL-alanine hydrophobic chain can be expected. The repulsion contributes to the salting-out effects at concentrated solutions (Figures 3-4-4 and 3-4-7).

For a given NaCl molality, at a relatively low amino acid concentration, binding one molecule of NaCl needs only one molecule of amino acid due to the formation of neutral complexes (Eqs. 4-2-6 and 4-2-7); while at a relatively high amino acid concentration, binding one molecule of NaCl requires two molecules of amino acid, due to the formation of singly-charged complexes (Eqs. 4-2-3 to 4-2-5); with further increase of an amino acid, the available free Na^+ and Cl^- ions to be bound would get fewer with ion-zwitterion complex formation (Eqs. 4-2-3 to 4-2-7); meanwhile, the repulsion would increase and thus retard the salting-in effect. Consequently, addition of more amino acid would make less contribution to binding Na^+ and Cl^- ions, resulting in a slower decrease of NaCl mean ionic activity coefficient ratio $\frac{\gamma_{\pm}^{II}}{\gamma_{\pm}^{I}}$ and thus weakening the salting-in effect on NaCl. Therefore the salting-in effect of an amino acid on NaCl is more pronounced in a range of low amino acid concentrations (up to the inflection points, if applicable), as it is indicated by the curve slopes in Figures 3-4-2 to 3-4-4 (especially in Figure 3-4-2).

The inflection points on NaCl activity curves for system NaCl+glycine+H_2O (Figure 3-4-2) may be interpreted based on the concept of cluster formation. Since glycine concentration can be very high due to its high solubility (about 3.1 m in pure H_2O

at 25 °C, vs DL-serine solubility about 0.5m), large glycine clusters may be formed more favorably at concentrated especially supersaturated glycine solutions. These large clusters could play a significant role in affecting the mobility of Na^+ and Cl^- ions, and hence the mean ionic activity coefficients of NaCl. As glycine clusters increase in size at high supersaturation, it is conceivable that Na^+ and Cl^- ions may be trapped within the glycine clusters thus get more stable, leading to a more effective increase in the salting-in effect of glycine on NaCl at low NaCl concentrations ($\leq$ 2.5m). This observation was also discussed by Han and Tan (2006). While at high NaCl concentrations, the amount of these trapped Na^+ and Cl^- ions may be relatively inappreciable at the same level of glycine supersaturation, the inflection gets less significant.

No obvious inflection points were found along NaCl activity curves for NaCl+DL-serine+H_2O (Figure 3-4-3). That would be because DL-serine has a very low solubility (about 0.5 m in pure H_2O at 25 °C, vs γ-glycine solubility 3.1m), thus formation of large DL-serine clusters (in terms of cluster size and number) may not be that favorable even in its supersaturated solutions. Therefore DL-serine clusters may only trap an insignificant amount of Na^+ and Cl^- ions and they would not substantially bring down NaCl activity $\frac{\gamma_{\pm}^{II}}{\gamma_{\pm}^{I}}$. DL-alanine would form large clusters especially in its supersaturated region due to high concentration (solubility 1.851m in pure H_2O at 25 °C) but the clusters would only trap an inappreciable amount of Na^+ and Cl^- ions due to significant repulsion between ions and DL-alanine hydrocarbon chains. As a result,

inflection points do not exist on curves of NaCl activities ($\frac{\gamma_{\pm}^{II}}{\gamma_{\pm}^{I}}$) in DL-alanine solutions (Figure 3-4-4).

For a given amino acid molality, the amino acid can bind a relatively bigger portion of the total NaCl when NaCl is low, hence the salting-in effect of amino acid on NaCl is more effective. While at a moderate NaCl concentration (≤ 2.5m), the same amount of amino acid can only bind a very small portion of the total NaCl, hence the salting-in effect of an amino acid is less effective. Further more, the repulsion between an ion and the hydrophobic hydrocarbon chain of an amino acid would increase when NaCl is more concentrated, retarding the salting-in effect. All these would be responsible for the trend of NaCl activity curves: at a given amino acid molality, NaCl activity curve shifts upwards with increase of NaCl in a range of low to moderate NaCl concentrations, as shown in Figures 3-4-2 to 3-4-4.

However, at a given amino acid molality, when NaCl is extremely high (≥ 2.5m), the experimental activity data for NaCl+glycine+H_2O (Figure 3-4-2) and NaCl+DL-serine+H_2O (Figure 3-4-3) show that NaCl activity curve goes downwards with increase of NaCl. This phenomenon seems unusual but it is not abnormal. In fact, when NaCl > 1.5m in pure H_2O (without amino acid), its binary activity coefficient $\gamma_{\pm}^{I}$ starts to increase with increase of NaCl concentration, indicating an increasingly greater NaCl association (clustering) in pure H_2O, as shown in Figure 4-3-1. These associated NaCl molecules in solution, tending to precipitate, can be dispersed significantly by addition of a small amount of an amino acid due to the attractive ion-dipole interaction and complex

formation, leading to a faster decrease in NaCl mean ionic activity coefficient $\gamma_{\pm}^{II}$ hence its mean ionic activity coefficient ratio $\frac{\gamma_{\pm}^{II}}{\gamma_{\pm}^{I}}$. It suggests that, when NaCl is very high (≥ 2.5m), the higher the NaCl concentration, the more pronounced the decrease of NaCl activity coefficient ratio $\frac{\gamma_{\pm}^{II}}{\gamma_{\pm}^{I}}$ by addition of the same amount of an amino acid (either glycine or DL-serine), resulting in a downward trend of NaCl activity curves with increase of NaCl at a fixed glycine or DL-serine concentration. As the experimental range for NaCl+DL-alanine+H_2O is only up to 2.5m NaCl, no observations can be made on the trend of NaCl activity coefficient ratios $\frac{\gamma_{\pm}^{II}}{\gamma_{\pm}^{I}}$ above 2.5m NaCl.

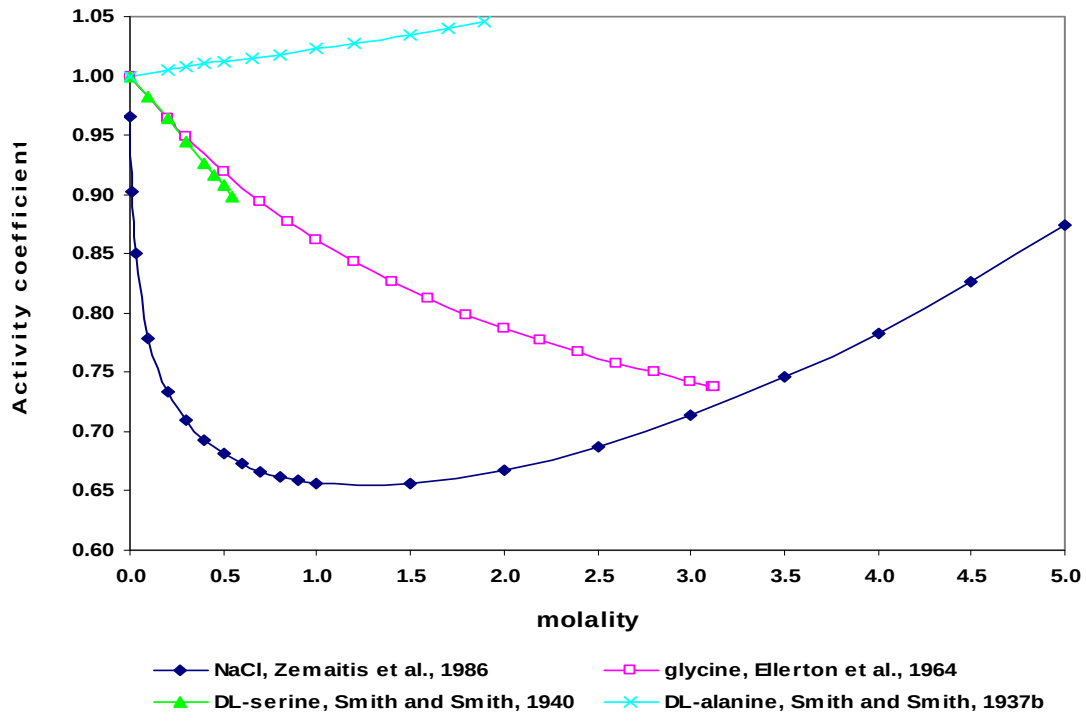

Figure 4-3-1 Activity coefficient of NaCl, glycine, DL-serine and DL-alanine in their own binary aqueous solutions at 25 °C

4.3.2 Salting Effect of NaCl on Amino Acids

A similar analysis can be applied to activities of an amino acid in NaCl solutions (Figures 3-4-5 to 3-4-7), in both under-saturated and supersaturated regions.

For a given amino acid solution, in a range of low NaCl concentrations, one mole of NaCl tends to bind **two** moles of amino acids via formation of singly-charged ion-zwitterion complexes ($^{+}H_3NRCOONa$ and ClH_3NRCOO^{-}, Eqs. 4-2-3 to 4-2-5). However, with increase of NaCl, one mole of NaCl may only bind one mole of amino acids due to formation of neutral ion-zwitterion complexes ($ClH_3NRCOONa$, Eqs. 4-2-6 to 4-2-7), accompanying the gradual depletion of amino acid molecules (either zwitterions or cyclic dimers) and the generation of more free ions (Na^{+} and Cl^{-}). Therefore, the repulsion between the free ions and the hydrocarbon chains of an amino acid would become increasingly significant with increase of NaCl. It can be seen that both the change of complex types (from singly-charged to neutral complexes) and the repulsion contribute to a slow decrease (even to an increase) of amino acid activity coefficient ratio $\frac{\gamma_A^{II}}{\gamma_A^{I}}$ with increase of NaCl (Figures 3-4-5 and 3-4-7).

It should be noted that, the addition of NaCl can cause a quicker switch from singly-charged complexes to neutral complexes in a low amino acid solution than in a high amino acid solution. In an extremely low amino acid solution where NaCl >> amino acid, this switch may not be observed as the neutral complexes may be always dominant.

The repulsion between free ions (Na^+ and Cl^-) and DL-serine hydrocarbon chains would be stronger than that between ions and glycine hydrocarbon chains, since DL-serine is less hydrophilic than glycine. Especially in a very low DL-serine solution (e.g., 0.1m), more free ions are available after the formation of ion-zwitterion complexes with increase of NaCl. As a result, one DL-serine hydrocarbon chain would be exposed to more electrolyte ions, with the repulsion getting more significant. Therefore, at low DL-serine concentrations, it may be expected that DL-serine activity $\frac{\gamma_A^{II}}{\gamma_A^{I}}$ curves may have different curvatures at the same NaCl concentration, leading to the intersection of the DL-serine activity curves, as shown in Figure 3-4-6.

However, when NaCl concentrations are very high (approximately NaCl > 2.5m), association among free ions (Na^+ and Cl^-) becomes significant and NaCl clusters can be formed too. These NaCl clusters could trap the hydrophilic amino acid molecules (e.g. glycine and DL-serine), making them more thermodynamically stable in solutions. But they may not significantly trap the less hydrophilic molecules (e.g. DL-alanine). Therefore, for glycien and DL-serine, their activity coefficient ratios ($\frac{\gamma_A^{II}}{\gamma_A^{I}}$) decrease more markedly with increase of NaCl (NaCl > 2.5m). In addition, for a solution where an amino acid is concentrated especially supersaturated, the formed amino acid clusters would be disintegrated due to being attacked by the free Na^+ and Cl^- ions, which is another factor for a faster decrease of amino acid activity $\frac{\gamma_A^{II}}{\gamma_A^{I}}$ with increase of NaCl,

leading to the occurrence of an inflection point on glycine and DL-serine activity $\frac{\gamma_A^{II}}{\gamma_A^{I}}$ curves respectively, as shown in Figures 3-4-5 and 3-4-6. No inflection points are observed on DL-alanine activity curves in NaCl solutions (Figure 3-4-7), likely due to the strong repulsion between ions (Na^+ and Cl^-) and DL-alanine molecules.

At a given NaCl concentration, with more amino acid added, the same amount of NaCl can only bind a relatively small portion of an amino acid to form ion-zwitterion complexes. In addition, the repulsion between ions and amino acid hydrocarbon chains would increase too. These two factors make the salting-in effect of NaCl on an amino acid less pronounced and they may explain the fact that the amino acid activity curves generally moves upwards with increase of the amino acid at a fixed NaCl concentration (Figures 3-4-5 to 3-4-7). It can be seen that the trends of the amino acid activity curves with increase of the amino acids are different from those of NaCl activity curves (Figures 3-4-2 and 3-4-3) with increase of NaCl, as both upward and downward shifts of NaCl activity curves are observed. That is because, compared with NaCl, the self-association of either glycine or DL-serine or DL-alanine in pure water (without NaCl) does not increase significantly with increase of its concentration, as can be seen in Figure 4-3-1.

Based on above analysis, it can be seen that the significant ion-dipole interaction, destruction of amino acid cyclic dimers, formation of different ion-zwitterion complexes and clusters are general phenomena for the hydrophilic glycine and DL-serine molecules, leading to the very similar salting-in effect of NaCl on glycine and DL-serine, especially in glycine and DL-serine supersatuared regions. The attractive ion-dipole interactions

between ions and DL-alanine molecules are less substantial and therefore destruction of DL-alanine cyclic dimers and formation of different ion-DL-alanine complexes are less significant. No obvious evidences are found to support particular or specific interaction between Na^+ ions and amino acid nuclei in the corresponding amino acid supersaturated solutions. The potential impact of these observed phenomena on glycine polymorphs and growth kinetics will be further elaborated in **Section 4.4**.

4.4 A Preliminary Insight into Glycine Polymorphs and Growth Kinetics

The commonly accepted working hypothesis of crystal polymorph control (Weissbuch et al., 1994a) suggests that in supersaturated solutions, solute molecules assemble to form coexisting nuclei (embryos) of different polymorphs, meaning that the structured nuclei are polymorphic too. Particular inhibitors would be recognized and bound on the surface of the selective polymorphic microscopic embryos, consequently preventing the particular polymorphic embryos from growth (and even disintegrating the particular polymorphic embryos). Eventually these selectively inhibited polymorphic embryos could not develop into macro crystals.

For glycine polymorphs, the metastable α-glycine nucleates from pure water. It was suggested that the glycine cyclic dimers in pure water are the assembling units for α-glycine (Carter et al., 1994; Towler et al., 2004). The thermodynamically stable γ-glycine can be obtained from sodium salt solutions (Bhat and Dharmaprakash, 2002a and 2002b; Towler et al., 2004). Based on the observation, it was once postulated that the specific interaction between sodium ions (Na^+) and α-glycine microscopic embryos

poisons α-glycine nuclei, which relatively increases the probability for γ-glycine to nucleate and subsequently grow from sodium salt solutions (Towler et al., 2004).

Though this proposed mechanism of γ-glycine nucleation from sodium salt solutions sounds agreeable with the working hypothesis of polymorphism, our activity data of glycine in NaCl solutions shows that, due to significant ion-dipole interaction, glycine cyclic dimers in glycine supersaturated solutions could be substantially destroyed by the introduction of NaCl, via Eqs. 4-2-2 to 4-2-7, at a reasonably high NaCl concentration (approximately NaCl > 1m), as illustrated in Figure 4-4-1. The lack of glycine cyclic dimers which are the elementary units assembling α-glycine cells implies that the formation of α-glycine microscopic embryos (clusters) is unlikely, leading to at least a relative promotion of γ-glycine. Therefore, it may be inferred that α-glycine is inhibited by NaCl due to the destruction of glycine cyclic dimers and not due to the specific interaction between Na^+ ions and α-glycine nuclei.

The importance of this new hypothesis is obvious. Since many other electrolytes (e.g. KCl, NH_4NO_3) similar to NaCl can play the same role in destroying the glycine cyclic dimers via ion-dipole interaction, they may induce γ-glycine too at a reasonably high electrolyte concentration. Therefore, without any other additional data or information, it could be reasonably concluded that γ-glycine nucleation from an electrolyte solution containing univalent ions would be a general phenomenon. This suggests that it is necessary to re-look into the mechanism of γ-glycine formation from an electrolyte solution.

Destroying glycine cyclic dimers hence inhibiting α-glycine does not directly means an absolute increase of γ-glycine growth. However, perusal of glycine activity data (Figure 4-4-1) and the formation of ion-glycine complexes (Eqs. 4-2-3 to 4-2-7) in glycine supersaturated region, it is found that the formation of γ-glycine in a 2.5m NaCl solution (ionic strength about 5.17, Towler et al., 2004) corresponds to the transition from glycine cyclic dimers to singly-charged and neutral ion-glycine complexes. This may suggest that these ion-glycine complexes play a significant role in promoting γ-glycine growth. Therefore, another hypothesis may be made, that is, γ-glycine growth kinetics could be generally promoted by an electrolyte containing univalent ions. It should be pointed out that, only if the thermodynamic data in the supersaturated region are available, can these two hypotheses (polymorphs and growth kinetics) be made with more confidence.

As for DL-serine, a similar change in ion-DL-serine complexes with NaCl concentration in DL-serine supersaturated solutions can be suggested, as illustrated in Figure 4-4-2. But, no DL-serine polymorphs were reported according to Cambridge Structural Database (Version 5.26). It may be due to the big side chain (CH_2OH) which would particularly determine how DL-serine molecules to pack. Since DL-alanine also has a large side chain (CH_2CH_3), DL-alanine molecules are perhaps packed uniquely therefore its polymorphs may be limited too. More investigations are required to verify this claim.

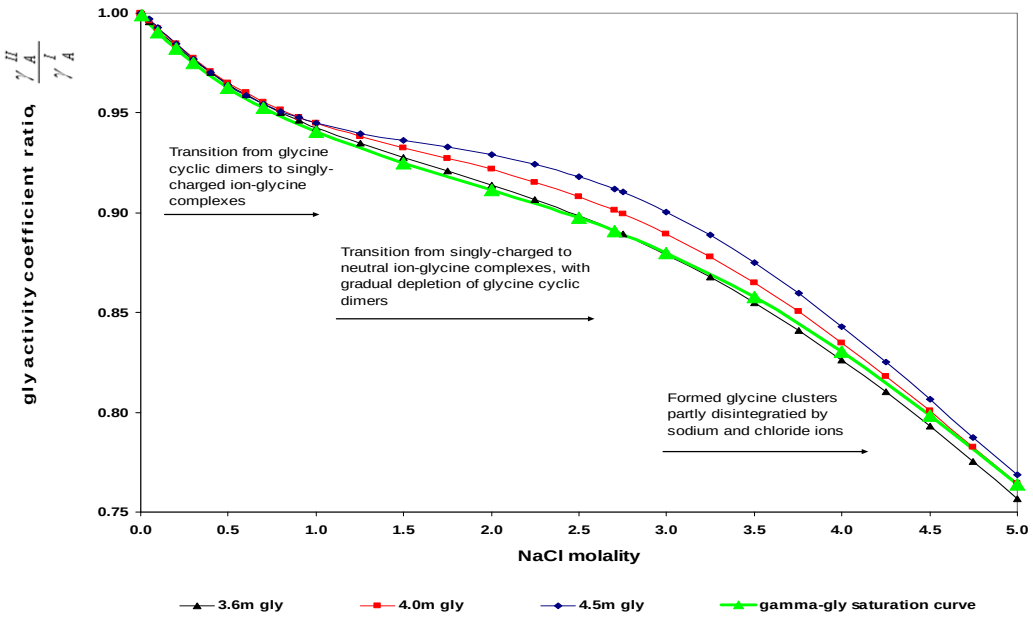

Figure 4-4-1 Solution chemistry change with NaCl concentration in glycine supersaturated region at 25 °C

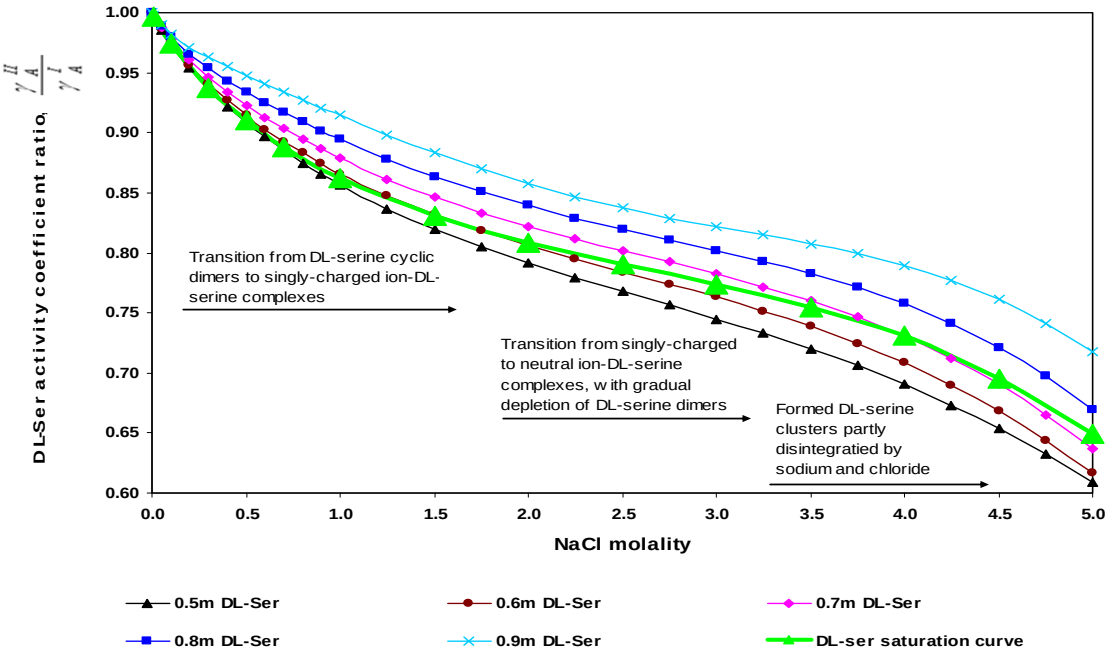

Figure 4-4-2 Solution chemistry change with NaCl concentration in DL-serine supersaturated region 25 °C

4.5 Summary

Solution chemistry, molecular interactions and formation of different complexes were analyzed for NaCl+amino acid+H_2O system. The obtained thermodynamic activities data in **Chapter 3** have been well interpreted by the proposed molecular interactions and formation of different complexes.

More importantly, the analysis made here suggests that the introduction of univalent ions from a 1:1 electrolyte would significantly disrupt the formation of glycine cyclic dimers, thus retarding the formation of α-glycine and at least relatively promoting γ-glycine. The results also imply that the singly-charged or neutral ion-glycine complexes due to the introduction of univalent ions may be the favorable building units for γ-glycine cells, thus enhancing γ-glycine nucleation, as long as the ion-dipole interaction is significant enough, regardless of the nature of these univalent ions. In order to verify these postulations, experimental investigations of the impacts of different electrolytes on glycine polymorphs and crystal growth kinetics have been done. The interesting results are presented in **Chapters 5** and **6** respectively.

Chapter 5 Impact of an Electrolyte on Glycine Polymorphs

In **Chapter 4**, the analysis of ternary NaCl+glycine+H_2O solutions supersaturated with glycine suggested that γ-glycine nucleating from an electrolyte solution containing univalent ions would be a general phenomenon, as long as the ion-dipole interaction is strong enough to destroy glycine cyclic dimers. In this chapter, the effects of different types of electrolytes on glycine polymorphs are experimentally investigated, which confirms the general phenomenon predicted in **Chapter 4**. The results of glycine polymorphs obtained from different electrolyte solutions are presented and their interpretations are given based on suggested mechanisms, with highlight of ion valences and the roles of both cations and anions.

5.1 Background of Glycine Polymorphs from Electrolyte Solutions

Bhat and Dharmaprakash (2002a and 2002b) first reported their observation that γ-glycine can nucleate from sodium salt solutions (e.g., NaCl, NaF, $NaNO_3$, NaAc). But they did not explain why γ-glycine rather than α-glycine was produced from these sodium salt (i.e. electrolyte) solutions.

Towler et al. (2004) investigated the effect of several strong electrolytes on glycine polymorphs. The electrolytes they used belong to two kinds, one being sodium salts (e.g. NaCl, Na_2CO_3, Na_2SO_4) and the other being nonsodium salts (e.g. $Ca(NO_3)_2$, $Mg(NO_3)_2$, $MgSO_4$), with an ionic strength of 5.17 for each individual electrolyte solution (approximately 2.5m for NaCl solution). They obtained glycine crystals by cooling the agitated glycine supersaturated solutions containing an electrolyte to 20 °C at

which the solutions had an initial relative supersaturation of 0.70, calculated as $(c-c_s)/c_s$) (or 0.53, calculated as $\ln(c/c_s)$) with respect to α-glycine solubility c_s (g/L). They found that the solutions not containing sodium ions (Na^+) gave pure α-glycine while those solutions containing sodium ions produced either all γ-glycine or mixtures of α-glycine and γ-glycine.

As the same ionic strength (5.17) was given for each glycine solution, it was suggested that surface energy change due to the introduction of an electrolyte and consequent double layer formation on the nuclei surface are not sufficient (likely less significant) to induce γ-glycine. Based on these findings, Towler et al. postulated that γ-glycine formation was attributed to the specific interaction between sodium ions (Na^+) and α-glycine nuclei (i.e. microscopic embryos or clusters). This specific interaction poisons (even disintegrates) α-glycine nuclei. It was also highlighted that Na^+ ions can only block the carboxylate (COO^-) rich, fast growing –c ends of γ-glycine nuclei (or crystals) while amino (NH_3^+) rich +c ends are available for the γ-glycine nuclei to grow. Eventually, γ-glycine nucleates and develops into mature crystals.

This postulation made by Towler et al. (2004) actually implies that sodium ions retard the growth rates of both α- and γ-glycine nuclei (or crystals), but α-glycine nuclei are inhibited more than γ-glycine nuclei and therefore the probability of γ-glycine nucleation is relatively increased. The role of anions (e.g. Cl^-) was neglected. Subsequently, this postulation was questioned by the result of Moolya et al. (2005),

because γ-glycine was also produced from an ammonium nitrate (NH_4NO_3) solution where no sodium ions are present.

It can be seen that the mechanism behind γ-glycine nucleation from sodium salt solutions (or from a general electrolyte solution) is still an open question. Since polymorph control is a general important problem, it is of great interest to discover the true mechanism involved in the polymorphic phenomenon. In this study, a systematic experimental investigation of the impacts of different electrolytes on glycine polymorphs has been carried out and the important results are presented.

5.2 Experimental Section

A number of electrolytes (total 15) were chosen for study of their impacts on glycine polymorphs. Based on the ratio of the valences of a cation to the valences of an anion from an electrolyte, these electrolytes fall into four types: 1:1 (e.g. NaCl, KNO_3), 1:2 (e.g. $(NH_4)_2SO_4$), 2:1 (e.g. $Ca(NO_3)_2$) and 2:2 (e.g. $MgSO_4$).

In order to have a better view of other factors which may affect glycine polymorphs, effects of different cooling modes (forced cooling and natural cooling) and solution pHs were also examined.

5.2.1 Experimental Materials

The total mass of solution for each glycine polymorph test was approximately 140 grams. In preparation of a glycine+electrolyte solution, each mass was weighed within

an accuracy of ±0.01g and ultrapure water (Millipore, resistivity 18.2 MΩcm and filtered with pore size 0.22um) was used. Glycine (>99%) and NH_4Ac (ammonium acetate, >98%) were from Sigma-Aldrich. NaCl (>99.5%), $NaNO_3$ (>99.5%), Na_2SO_4 (>99%), $NaHCO_3$ (>99%), Na2CO3 (>99.9%), KCl (>99.5%), KNO_3 (>99%), K_2SO_4 (>99%), NH_4Cl (99.8%), NH_4NO_3 (>99%), $(NH_4)_2SO_4$ (99.5%), $Ca(NO_3)_2*4H_2O$ (99%), $CaCl_2*2H_2O$ (99%) and MgSO4 (>98%) were from Merck. The particular salts NH_4Ac, $Ca(NO_3)_2*4H_2O$ and $CaCl_2*2H_2O$ were used as delivered and they were used up for solution preparation at one time to prevent moisture adsorption. All other salts were dried at 120 ^oC in an oven for 72 hrs then cooled in a vacuum desiccator prior to their use.

5.2.2 Experimental Procedure

Forced cooling and natural cooling were used to generate supersaturation. For both cooling modes, the initial supersaturation of glycine was controlled to be about 0.50 (with respect to γ-glycine, calculated as $[(m_A - m_A^{II,Sat})/m_A^{II,Sat}]$ at 25 °C. Each supersaturated solution of approximately 140g was prepared by mixing an appropriate amount of each of an electrolyte solution and glyicne crystals in a 250ml conical flask. The conical flask was then put in warm water for the solution to be heated up gradually till the glycine crystals were fully dissolved to make a homogeneous solution. To prevent water from evaporation during preparation, the conical flask was sealed with a parafilm.

For forced cooling, the prepared glycine+electrolyte solution was gently transferred into a 250ml jacketed warming beaker. Through the jacketed beaker, the temperature of glycine solution was cooled down to and maintained at 25 °C using a

refrigerating water circulator, for glycine to nucleate and grow from its stagnant solution (without mixing). The warming beaker was sealed with a parafilm, throughout glycine nucleation.

For natural cooling, the prepared glycine+electrolyte solution was gently transferred into a 250ml ordinary beaker which was also sealed using a parafilm. The homogeneous glycine solution was then left at ambient temperature (about 22 °C) for glycine to nucleate from the quiescent glycine+electrolyte solution.

For either forced cooling or natural cooling, once sufficient amount (approximately 5g) of glycine crystals was observed, the crystals were carefully collected using a spatula and/or tweezer. Clean filter papers were used to immediately absorb the solution on the surface of the collected glycine crystals before these crystals were put in a container and dried in an oven at 60 °C. This pre-absorption of solution was to assist with a quicker drying of the wet glycine crystals to prevent glycine polymorphic transformation, since metastable α-glycine (if formed) can be transformed into stable γ-glycine in a wet condition, though the transformation may take a long time to reach a significant level (Sakai et al., 1991). The dried collected glycine crystals were weighed to evaluate the supersatuartion range within which glycine nucleated and grew. A powder-XRD instrument was used to determine the polymorphs of the collected glycine crystals.

5.3 Results and Discussion

As it has been noted, the metastable α-glycine has a higher solubility than the thermodynamically stable γ-glycine, therefore α-glycine can be transformed into γ-glycine due to solution mediation when glycine concentration is lower than α-glycine solubility but higher than γ-glycine solubility (Sakai et al., 1991). The transformation from α-glycine to γ-glycine in a solution is a process where α-glycine dissolves while γ-glycine nucleates and grows. Such a polymorphic transformation creates an uncertainty when γ-glycine was obtained, because γ-glycine may not be originally formed from primary nucleation. In fact, α-glycine may be originally formed first and then it is transformed into γ-glycine via solution mediation. In order to prevent this uncertainty, it is important to ensure that the glycine concentration is higher than the solubility of the metastable α-glycine during the nucleation and growth of glycine polymorphs, so that α-glycine (if formed) is not transformed into γ-glycine. It can be seen that solubilities of both γ-glycine and α-glycine are needed for a proper study on glycine polymorph formation. Therefore, solubilities of both γ-glycine and α-glycine in an electrolyte solution were measured first.

5.3.1 Solubility

With exception of γ-glycine solubilities in different NaCl solutions which have been tested and presented in **Section 3-4**, solubilities of both α- and γ-glycine in other electrolyte solutions at 25 °C were tested using the method described in **Appendix A**. The obtained solubility data are summarized in Tables 5-3-1 to 5-3-4 and typical selected data are also presented in Figure 5-3-1.

The solubility data in Tables 5-3-1 to 5-3-4 show that the metastable α-glycine has a higher solubility than the thermodynamically stable γ-glycine, as it is expected. For any given electrolyte, the solubility difference between α- and γ-glycine at the same electrolyte concentration is approximately 1.5g/100g H_2O. These data also show that, except NH_4Ac, all other electrolytes have salting-in effects on glycine, and glycine solubility monotonically increases with increase of an electrolyte. The salting-out effect of NH_4Ac on glycine may be due to the hydrophobic chain of an acetate ion (Ac^-) which may significantly repulse the hydrophilic amino group NH_3^+ of a glycine molecule.

Table 5-3-1 α- and γ-glycine solubilities (g/100g H_2O) in NaCl, $NaNO_3$, KCl and KNO_3 solutions at 25 °C

Electrolyte	NaCl		$NaNO_3$		KCl		KNO_3	
molality	α-gly	γ-gly	α-gly	γ-gly	α-gly	γ-gly	α-gly	γ-gly
0.0000	25.03	23.49	25.03	23.49	25.03	23.49	25.03	23.49
0.1000		23.67						
0.3000		24.05		24.76		23.91		
0.5000	25.98	24.37	27.17	25.53	25.76	24.15	26.76	25.35
0.7000		24.64				24.33		
1.0000	26.64	25.06	28.97	27.29		24.55	28.13	26.47
1.5000		25.68		28.83	26.38	24.81	29.00	27.48
2.0000		26.21		30.24				
2.5000	28.46	26.73	33.34	31.59	26.76	25.17	30.83	29.02
3.0000		27.26						
3.5000		27.81					31.78	30.02
4.0000	30.12	28.39		35.15	27.02	25.42		
4.5000	30.79	29.08						
5.0000		29.79						

Table 5-3-2 α- and γ-glycine solubilities (g/100g H_2O) in NH_4Cl, NH_4NO_3, NH_4Ac and $NaHCO_3$ solutions at 25 °C

Electrolyte	NH_4Cl		NH_4NO_3		NH_4Ac		$NaHCO_3$	
molality	α-gly	γ-gly	α-gly	γ-gly	α-gly	γ-gly	α-gly	γ-gly
0.0000	25.03	23.49	25.03	23.49	25.03	23.49	25.03	23.49
0.5000			27.20	25.58	24.50	22.96		
1.0000							29.14	26.86
1.5000	27.13	25.81	30.65	28.89	23.34	21.90		
2.5000	28.91	27.51	33.57	31.70	22.19	20.83		

Table 5-3-3 α- and γ-glycine solubilities (g/100g H_2O) in Na_2SO_4, K_2SO_4 and $(NH_4)_2SO_4$ solutions at 25 °C

Electrolyte	Na_2SO_4		K_2SO_4		$(NH_4)_2SO_4$	
molality	α-gly	γ-gly	α-gly	γ-gly	α-gly	γ-gly
0.0000	25.03	23.49	25.03	23.49	25.03	23.49
0.1000	25.76	24.20	25.60	24.08		
0.5000	27.55	25.99	26.78	25.32		
1.0000	28.34	26.87			28.63	27.09
1.5000	28.81	27.29				
2.5000					29.49	27.89

Table 5-3-4 α- and γ-glycine solubilities (g/100g) in Na_2CO_3, $CaCl_2$, $MgSO_4$ and $Ca(NO_3)_2$ solutions at 25 °C

Electrolyte	Na_2CO_3		$CaCl_2$		$MgSO_4$		$Ca(NO_3)_2$	
molality	α-gly	γ-gly	α-gly	γ-gly	α-gly	γ-gly	α-gly	γ-gly
0.0000	25.03	23.49	25.03	23.49	25.03	23.49	25.03	23.49
0.5000			31.06	29.33	29.41	27.82	29.90	28.59
1.0000	34.50	33.06	36.88	34.92	32.26	30.59	35.22	33.85
1.5000			42.85	40.94	34.42	32.71	39.96	38.61
2.5000	45.91	44.40						

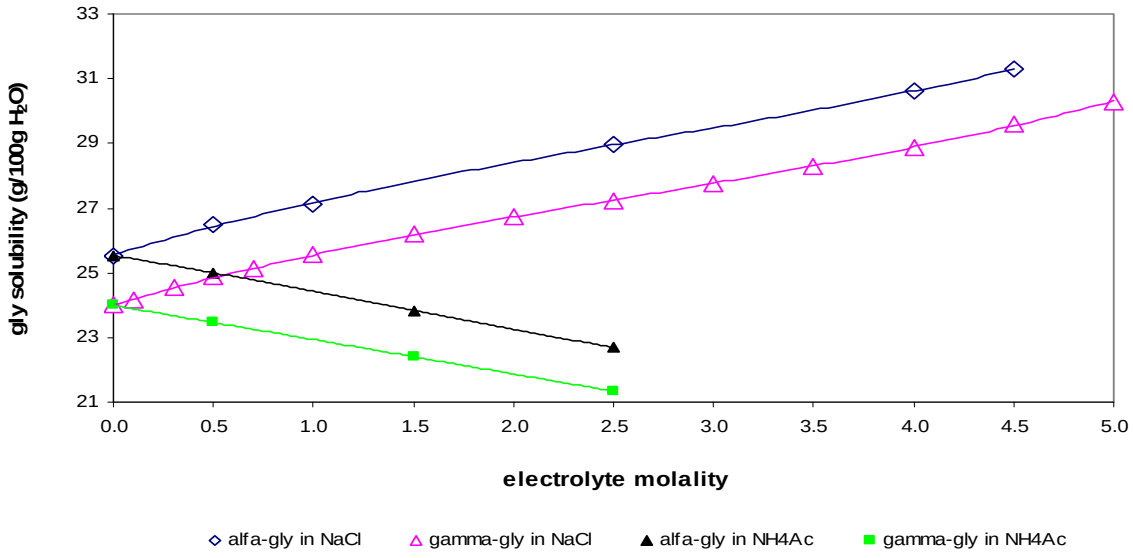

Figure 5-3-1 Solubilities of α- and γ-glycine in NaCl and NH_4Ac solutions at 25 °C

It can also be observed that these electrolytes containing ions CO_3^{2-}, Ca^{2+} and Mg^{2+} have much greater salting-in effects on glycine than other electrolytes.

Monoatomic dications (e.g. Ca^{2+} and Mg^{2+}) may be more readily to form co-valences (via coordination chemistry) with a few other polar molecules and ions (e.g. glycine, H_2O and Cl^-) to produce sophisticated complexes and to prevent glycine molecules from precipitation, thus exerting bigger sating-in effects on glycine. In fact, at a quite high concentration of Ca^{2+}, the sophisticated complexes would precipitate to form new crystals which consist of glycine and electrolyte ions (Natarajan and Rao, 1980; Rao and Natarajan, 1980; Natarajan, 1983). Monoatomic dications may be quite prone to form co-valences with other molecules because they may position and orientate themselves with less difficulty, due to their symmetry and strong electrostatic fields.

As for polyatomic dianions (e.g., SO_4^{2-} and CO_3^{2-}), atomic polarization would be significant (Piquemal et al., 2006), localizing the distribution of electrons or charges. As a result, it is difficult to form co-valence with a few other molecules, as one polyatomic dianion (as well as the involved polyatomic monoanions, e.g. NO_3^-, NH_4^+ etc) needs to take a particular position and orientation. Therefore co-valence may make less contribution to the salting-in effect. However, depending on the nature and chemistry of a polyatomic dianion, the atomic polarization may significantly reinforce the ion-dipole interaction between the dianion and a glycine zwitterion, leading to a more pronounced salting-in effect on glycine. Perhaps, atomic polarization of CO_3^{2-} would be more significant than that of SO_4^{2-}, owing to the bigger difference between carbon and oxygen atom. That would partly explain the reason why Na_2CO_3 has a bigger salting-in effect on glycine than Na_2SO_4 does, among other factors (e.g. ion salvation and size etc).

5.3.2 Glycine Polymorphs

Fifteen electrolytes were selected for study of their effects on glycine polymorphs. Based on ion valence ratio, these selected electrolytes fall into four types: 1:1 (e.g. NaCl, KNO_3), 2:2 ($MgSO_4$), 2:1 (e.g. $Ca(NO_3)_2$) and 1:2 (e.g. $(NH_4)_2SO_4$). The ions from these electrolytes include monoatomic univalent (e.g. Cl^-, K^+), monoatomic divalent ions (e.g. Ca^{2+} and Mg^{2+}), polyatomic univalent ions (e.g. NO_3^-, NH_4^+, even organic acetate ion Ac^-) and polyatomic divalent ions (e.g. SO_4^{2-} and CO_3^{2-}). Glycine polymorphs from various electrolyte solutions were investigated using the experimental procedure described in **Section 5-2-2**, with both forced cooling and natural cooling for supersaturation generation.

It was noted that forced cooling took about 30 minutes for the solution in the warming beaker to be cooled down to 25 °C using a refrigerating water circulator, while natural cooling took more than 60 minutes to cool the solution in an ordinary beaker to the room temperature (approximately 22 °C). In general, when the very first visible crystal appeared, it was estimated that the solution had been cooled to 25 °C (forced cooling) or room temperature (natural cooling).

For all the experiments, the supersatuartion level of γ-glycine in the period of nucleation and crystal growth was changed from initial 0.50 to 0.30. In other words, with respect to α-glycine, the supersatuartion level was changed from approximately 0.45 to 0.25. The low end of the supersaturation level at which the formed crystals were harvested was evaluated by weighing the collected crystals after they were dried. Since

the glycine concentration was higher than the solubility of metastable α-glycine, any originally formed metastable α-glycine would not be transformed into stable γ-glycine via solution-mediation. Therefore, metastable α-glycine, if formed, can be detected without any uncertainty. For different types of electrolytes, the obtained glycine polymorphs are reported and discussed below.

5.3.2.1 Glycine Polymorphs from 1:1 Electrolyte Solutions

Experiments for glycine polymorphs from 1:1 electrolyte solutions were carried out using procedure described in **Section 5-2-2**. A typical powder XRD result of glycine crystals formed from a 1:1 electrolyte solution is presented in Figure 5-3-2. By comparing the XRD peaks with the ones of the reference glycine polymorphs, the polymorph of the sample glycine crystals can be readily determined. Figure 5-3-2 shows that the glycine obtained from 2.5m NH_4NO_3 solution is γ-glycine.

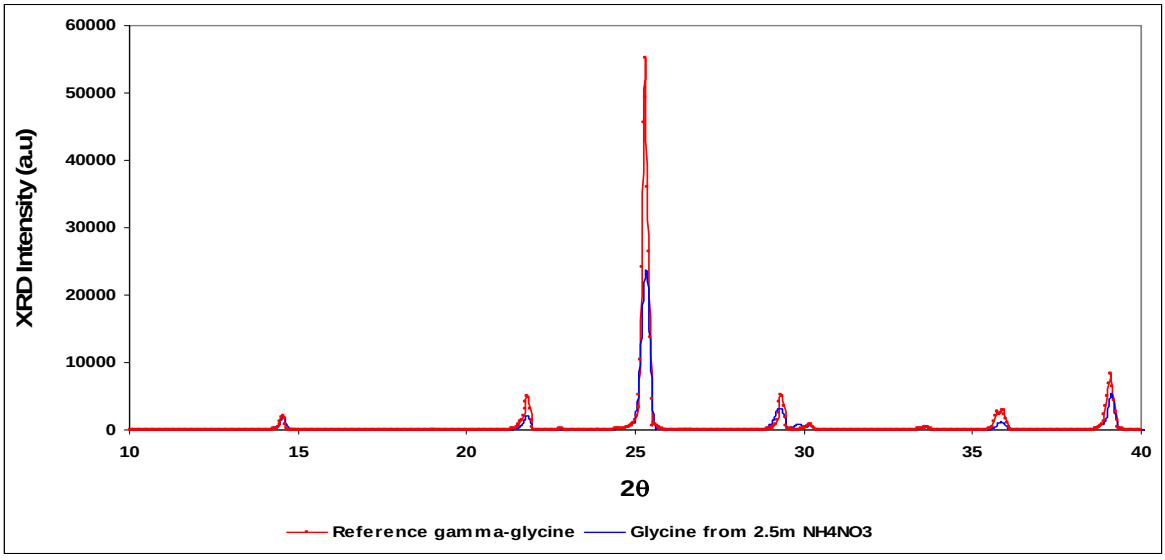

Figure 5-3-2 XRD result of glycine crystals from 2.5m NH_4NO_3 solution

The glycine polymorphs from different electrolyte solutions are summarized in Tables 5-3-5. From this table, it can be seen that the glycine crystals from various 1:1 electrolyte solutions by forced cooling are typically pure γ-glycine in a very wide range of electrolyte concentrations from dilute (e.g. 0.1m) to concentrated, despite two exceptions from low NH_4Ac solutions. These observations may be interpreted based on the molecular interactions. It will be shown that, univalent ions from a 1:1 electrolyte inhibit α-glycine nuclei (via poisoning and disintegration of glycine cyclic dimers, i.e. elementary building units for α-glycine), while they readily initiate γ-glycine nucleation and tremendously enhance the growth rate of γ-glycine nuclei, eventually leading to the formation of γ-glycine.

Table 5-3-5 Glycine polymorphs from 1:1 electrolyte solutions, by forced cooling

1:1	Electrolyte molality						
Electrolyte	0.1m	0.5m	1.0m	1.5m	2.5m	3.5m	4.0m
NaCl	γ			γ	γ		
NaCl*					γ		
KCl	γ	γ		γ	γ		γ
KNO_3	γ	γ		γ	γ	γ	
$NaNO_3$	γ	γ	γ	γ	γ		γ
NH_4Cl	γ			γ	γ		
NH_4NO_3	γ	γ			γ		
NH_4Ac	γ+α	γ+α		γ	γ		
$NaHCO_3$	γ	γ	γ				

*by Towler et al. (2004) at ionic strength of 5.17

As it was discussed in **Chapter 4**, due to significant ion-dipole interaction and consumption of glycine zwitterions ($^{+}H_3NCH_2COO^{-}$), adding a 1:1 electrolyte, for example, NaCl, would substantially destroy glycine cyclic dimers (via Eqs. 5-3-1 to 5-3-3). Glycine cyclic dimers may be directly destroyed too (Eq. 5-3-4). Meanwhile two types of singly-charged ion-glycine complexes ($^{+}H_3NCH_2COONa$ and $ClH_3NCH_2COO^{-}$) are formed.

$$^{+}H_3NCH_2COO^{-} + Na^{+} \Leftrightarrow {}^{+}H_3NCH_2COONa \qquad (5\text{-}3\text{-}1)$$

$$Cl^{-} + {}^{+}H_3NCH_2COO^{-} \Leftrightarrow ClH_3NCH_2COO^{-} \qquad (5\text{-}3\text{-}2)$$

$$\begin{pmatrix} OOCCH_2NH_3 \\ H_3NCH_2COO \end{pmatrix} \Leftrightarrow 2\ {}^{+}H_3NCH_2COO^{-} \qquad (5\text{-}3\text{-}3)$$

$$\begin{pmatrix} OOCCH_2NH_3 \\ H_3NCH_2COO \end{pmatrix} + Na^{+} + Cl^{-} \Leftrightarrow {}^{+}H_3NCH_2COONa + ClH_3NCH_2COO^{-} \qquad (5\text{-}3\text{-}4)$$

Apparently, destroying glycine cyclic dimers (which are favorable for α-glycine nucleation and growth) inhibits α-glycine nucleation. Meanwhile, due to the electrostatic force, one positively charged ion-glycine complex ($^{+}H_3NCH_2COONa$) and one negatively charged ion-glycine complex ($ClH_3NCH_2COO^{-}$) can bind each other readily in a particular orientation and alignment (**via hydrogen bonding**) to create the initial head-to-tail open dimers in ion-glycine complex form ($ClH_3NCH_2\mathbf{COOHNH_2}CH_2COONa$):

$$^{+}H_3NCH_2COONa + ClH_3NCH_2COO^{-} \Leftrightarrow ClH_3NCH_2\mathbf{COOHNH_2}CH_2COONa \qquad (5\text{-}3\text{-}5)$$

Based on the structure (Figure 5-3-3) of a γ-glycine nucleus (or a γ-glycine crystal), these initial glycine head-to-tail open dimers are very favorable for initiating γ-glycine nucleation. Actually they are served as the origins of γ-glycine nucleation.

Though Na^+ and Cl^- ions may be bound onto the ends of the open dimers due to electrostatic force, some of them may be removed due to molecule vibration, collision or thermal motion etc (Eq. 5-3-6), generating active sites for further addition of the growing units ($^+H_3NCH_2COONa$ and $ClH_3NCH_2COO^-$) as shown in Eqs. 5-3-7 to 5-3-8. Therefore larger γ-glycine nuclei can be developed when glycine concentration is high enough.

$$ClH_3NCH_2\mathbf{COOHNH_2}CH_2COONa \Leftrightarrow {}^+H_3NCH_2\mathbf{COOHNH_2}CH_2COO^- + Na^+ + Cl^- \quad (5\text{-}3\text{-}6)$$

$${}^+H_3NCH_2\mathbf{COOHNH_2}CH_2COO^- + {}^+H_3NCH_2COONa \Leftrightarrow {}^+H_3NCH_2\mathbf{COOHNH_2}CH_2\mathbf{COOHNH_2}CH_2COONa \quad (5\text{-}3\text{-}7)$$

$${}^+H_3NCH_2\mathbf{COOHNH_2}CH_2COO^- + ClH_3NCH_2COO^- \Leftrightarrow ClH_3NCH_2\mathbf{COOHNH_2}CH_2\mathbf{COOHNH_2}CH_2COO^- \quad (5\text{-}3\text{-}8)$$

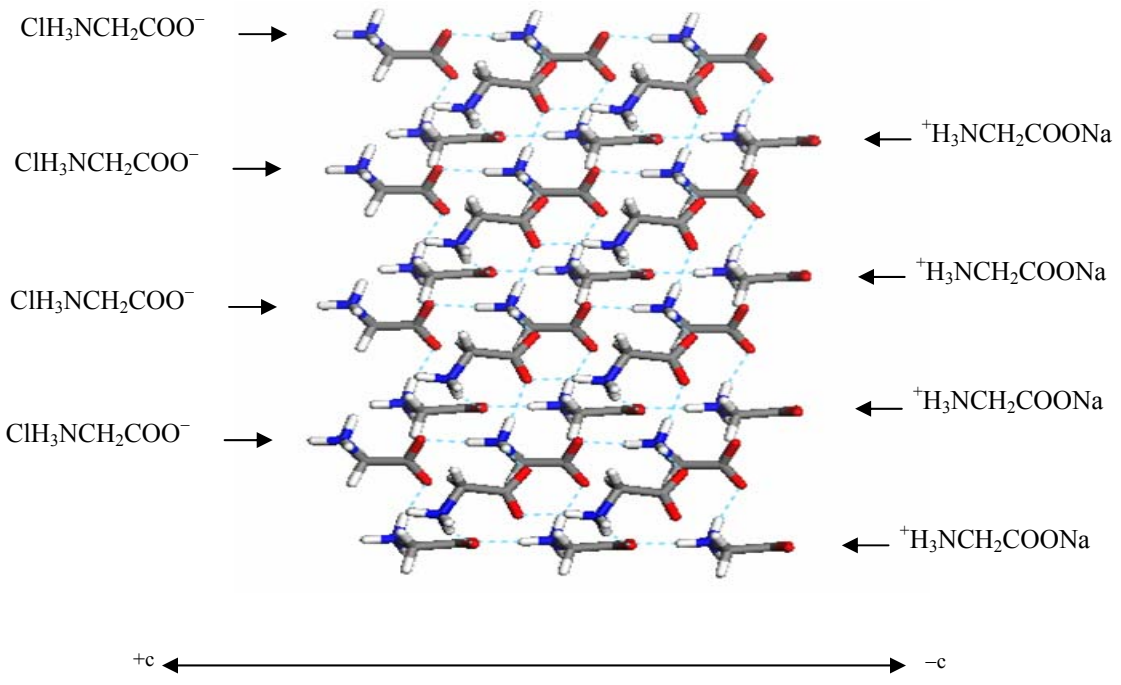

Figure 5-3-3 Effect of a 1:1 electrolyte, NaCl: The singly-charged ion-glycine complexes as the building units for a γ-glycine nucleus to grow from both polar ends [polar c-axis NH_3^+ rich, pointed, slow growing end (+c) and COO^- rich fast growing end (-c)]

After a γ-glycine nucleus is formed, its growth would be fast because the two types of singly-charged ion-glycine complexes ($^{+}H_3NCH_2COONa$ and $ClH_3NCH_2COO^{-}$), building units of γ-glycine, can favorably approach the corresponding growing end of a γ-glycine nucleus in the required head-to-tail orientation owing to the electrostatic force, as depicted in Figure 5-3-3. Once a positively charged ion-glycine complex ($^{+}H_3NCH_2COONa$) gets contacted with the COO^{-} rich –c end of a γ-glycine nucleus, the hydrogen bonding between amino group NH_3^{+} and carboxyl group COO^{-} would facilitate integrating the glycine molecules into γ-glycine lattices, thus completing the step of molecule addition. The same analysis is applicable to a negatively charged ion-glycine complex ($ClH_3NCH_2COO^{-}$) and the NH_3^{+} rich +c end. However, due to different natures and structures of –c end and +c end, NH_3^{+} rich end (+c) would be the slow growing end while COO^{-} rich end (-c) the fast growing end, as was discussed in **Section 2-2**.

After the fulfillment of the integration of the charged ion-glycine complexes into the lattices, Na^{+} ions would remain and be exposed on the outmost layer at the polar –c end of the γ-glycine nucleus while Cl^{-} ions would remain and be exposed on the outmost layer at the polar +c end. Again, these exposed Na^{+} and Cl^{-} ions, bound onto the surface lattices, can be removed due to ion vibration, collision or thermal motion etc, thus making the surface lattices (active sites) available for the oncoming singly-charged ion-glycine complexes to add into the nucleus for further growth (Figure 5-3-3). It should be noted that the ion-glycine complexes could be solvated (here hydrated), thus, as usual, desolvation is involved in the fitting process of glycine molecules into γ-glycine lattices.

As long as the γ-glycine nucleus grows bigger than the critical size, a mature γ-glycine crystal is obtained.

It should be pointed out that it is much less likely for the same type of charged ion-glycine complexes (e.g., either $^{+}H_3NCH_2COONa$ or $ClH_3NCH_2COO^{-}$) to form the head-to-tail open dimers, due to the electrostatic repulsion between the same charges. Therefore, only if both types of ions (e.g. Na^{+} and Cl^{-}) are powerful enough to open the cyclic dimers hence create the equal numbers of positively charged complexes ($^{+}H_3NCH_2COONa$) and negatively charged complexes ($ClH_3NCH_2COO^{-}$), can the initial head-to-tail open dimers (ClH_3NCH_2**COOHNH$_2$**CH_2COONa) be formed most effectively and efficiently, thus most helping initiate γ-glycine nucleation. Otherwise, if only one type of ions (e.g. Na^{+}) can readily destroy glycine cyclic dimers while the other type of ions (e.g., acetate ion, Ac^{-}) can not, the consequence is that these complexes (e.g. $^{+}H_3NCH_2COONa$ and $AcH_2NCH_2COO^{-}$) are not proportional and would not effectively produce the initial glycine head-to-tail open dimers (AcH_2NCH_2**COOHNH$_2$**CH_2COONa), thus dampening the onset of γ-glycine nucleation.

It can be expected that, with the increase of NaCl in a glycine aqueous solution, more and more glycine cyclic dimers diminish while more and more charged ion-glycine complexes hence head-to-tail open dimers occur, thus inhibiting α-glycine nucleation meanwhile promoting γ-glycine nucleation. When the concentration of NaCl is sufficiently concentrated, the cyclic dimers could deplete, then α-glycine may have no chance to form at all. This analysis is not limited to NaCl. Therefore, a 1:1 electrolyte

would generally retard α-glycine meanwhile promote γ-glycine. Consequently, regardless of the nature of a 1:1 electrolyte, as long as the ion-dipole interaction is significant enough to open glycine cyclic dimers and create singly-charged ion-glycine complexes, only γ-glycine nucleates.

It should be noted that γ-glycine can even be formed from a dilute electrolyte solution (e.g. 0.1m). This could partly be due to "self-poisoning" as suggested by Towler et al. (2004). In a dilute electrolyte solution, only a small part of glycine cyclic dimers (a few percents) are opened by the univalent ions of a 1:1 electrolyte. The remained cyclic dimers may be sufficient to form tiny α-glycine nuclei, smaller than the critical size. However, the subsequent growth of these tiny α-glycine nuclei may be significantly retarded. That is because the singly-charged ion-glycine complexes (e.g. $^{+}H_3NCH_2COONa$ and $ClH_3NCH_2COO^{-}$) are very similar to the glycine cations ($^{+}H_3NCH_2COOH$ at a low pH) and glycine anions ($H_2NCH_2COO^{-}$ at a high pH) respectively. Then they can be adsorbed onto α-glyicne surface due to affinity. But the adsorbed charged ion-glycine complexes, very different from the glycine cyclic dimers which are building units of α-glyicne, can not fit into α-glyicne lattices. Therefore these adsorbed charged ion-glycine complexes would block the way of the oncoming glycine cyclic dimers and inhibit the growth of α-glyicne nuclei substantially.

As for the two exceptions in low NH_4Ac (0.1m and 0.5m) solutions, the obtained glycine crystals are mixtures of α and γ glycine, with both α and γ-glycine being present significantly. This may be attributed to the fact that the repulsion between the

hydrophobic hydrocarbon chain of an acetate ion (Ac^-) and a hydrophilic glycine zwitterion ($^+H_3NCH_2COO^-$) is quite strong, which is supported by the salting-out effect of NH_4Ac on glycine (Figure 5-3-1). As a result, acetate ions may not effectively destroy glycine cyclic dimers which are suitable for α-glycine nucleation and it may be more difficult to form negatively charged ion-glycine complexes ($AcH_3NCH_2COO^-$) to poison α-glycine nucleation. Especially, the lack of negatively charged complexes ($AcH_3NCH_2COO^-$) makes it much less efficient to initiate γ-glycine nucleation via the formation of glycine open dimers (AcH_3NCH_2**$COOHNH_2$**CH_2COONa), even if sodium ions (Na^+) can substantially attack glycine cyclic dimers to create a plenty of positively charged ion-glycine complexes ($^+H_3NCH_2COONa$). That is because the positively charged ion-glycine complexes ($^+H_3NCH_2COONa$) themselves alone would not readily form glycine open dimers for γ-glycine nucleation. Consequently, the competition of γ-glycine nucleation against α-glycine is weakened, eventually leading to a mixture of α- and γ-glycine polymorphs.

Glycine polymorphs would also be affected by the rate of supersaturation generation. As was analyzed, close to equilibrium conditions, only those nuclei resembling the thermodynamically stable polymorph grow and exceed the critical size, developing into mature thermodynamically stable polymorph (Weissbuch et al., 1991). In other words, a low rate of supersaturation generation favors the stable polymorph while a quick rate favors the metastable (He et al., 2006). In this study, in order to evaluate the sensitivity of glycine polymorph to the rate of supersaturation generation, natural cooling was used to produce a low rate of supersaturation generation, compared

with the forced cooling which creates quick rate of supersaturation generation. The results of glycine polymorphs obtained from selected 1:1 electrolyte solutions by natural cooling, together with those by forced cooling, are tabulated in Table 5-3-6.

From Table 5-3-6, it can be seen that neither forced nor natural cooling affects glycine polymorphs. All the polymorphs formed are pure γ-glycine, with exception of the ones from a dilute NH_4Ac solution (0.1m). Even for this exception, a mixture of both α- and γ-glycine polymorphs was obtained from both forced and natural cooling. This also suggests that the modes of cooling hence the rates of supersaturation generation under the experimental conditions do not exert a significant influence on glycine polymorphs from 1:1 electrolyte solutions.

Table 5-3-6 Glycine polymorphs from 1:1 electrolyte solutions, by both modes of cooling

1:1 Electrolyte	Electrolyte molality					
	0.1m		1.0m		2.5m	
	Natural Cooling	Forced Cooling	Natural Cooling	Forced Cooling	Natural Cooling	Forced Cooling
NaCl	γ	γ			γ	γ
KCl	γ	γ			γ	γ
KNO_3	γ	γ			γ	γ
$NaNO_3$	γ	γ	γ	γ		γ
NH_4Cl	γ	γ			γ	γ
NH_4NO_3	γ	γ			γ	γ
NH_4Ac	γ+α	γ+α			γ	γ
$NaHCO_3$	γ	γ	γ	γ		

Overall, these results by both natural cooling and forced cooling reinforce the postulation that univalent ions from a 1:1 electrolyte exert a dominant effect on glycine polymorphs. Specifically, with the increase of a 1:1 electrolyte, regardless of its nature, the growth rate of α-glycine nuclei would become too slow for them to eventually develop into mature crystals, while the growth rate of γ-glycine nuclei (or crystals) would be substantially (even tremendously) promoted. Indeed, the growth rate of γ-glycine crystals is enhanced tremendously by introduction of a 1:1 electrolyte into a glycine supersaturated solution, which will be further elaborated in **Chapter 6**.

Addition of an electrolyte into a glycine solution may alter the solution pH which affects glycine polymorphs. Towler et al. (2004) showed that for glycine+H_2O solutions with absence of any electrolytes in a pH domain [4, 8], glycine zwitterions ($^+H_3NCH_2COO^-$) dominate the charged species (either $^+H_3NCH_2COOH$ or $H_2NCH_2COO^-$), greatly favoring α-glycine. Indeed, their results confirmed that glycine crystals produced from H_2O in a pH domain [3.8, 8.9] were always α-glycine. Beyond this pH range, either a low pH or a high pH promoted γ-glycine nucleation from H_2O.

In order to exclude the pH impact on glycine polymorphs from 1:1 electrolyte solutions in this study, the pHs of these 1:1 electrolyte solutions saturated with glycine at 25 °C were measured. Though the solution pHs varied with the concentration of an electrolyte, they were well within the range [6.2 to 8.5] which actually favors α-glycine according to Towler et al. (2004). Thus the pH impact on γ-glycine formation from these

1:1 electrolyte solutions can be ruled out. Therefore, it is re-ascertained that it is these univalent ions from a 1:1 electrolyte that inhibit α-glycine and promote γ-glycine.

5.3.2.2 Glycine Polymorph from 1:2 Electrolyte Solutions

Four 1:2 electrolytes, namely Na_2SO_4, K_2SO_4, $(NH_4)_2SO_4$ and Na_2CO_3, were chosen for exploring their impacts on glycine polymorphs. Using both forced cooling and natural cooling techniques, glycine polymorphs were produced from different 1:2 electrolyte solutions. The results are presented in Table 5-3-7.

Table 5-3-7 Glycine polymorphs from 1:2 electrolyte solutions, by cooling

Electrolyte	Electrolyte molality							
	0.1m		0.5m		1.5m		2.5m	
	Forced Cooling	Natural Cooling	Forced Cooling	Natural Cooling	Forced Cooling	Natural Cooling	Forced Cooling	Natural Cooling
$(NH_4)_2SO_4$	γ	γ	γ	γ	γ	γ	γ	γ
Na_2CO_3	γ	γ	γ	γ			γ	γ
Na_2CO_3*					γ			
Na_2SO_4	γ	γ	γ	γ	γ+α	γ+α		
Na_2SO_4 *					γ+α			
K_2SO_4	γ	γ	γ	γ				

*by Towler et al. (2004) at ionic strength of 5.17

From Table 5-3-7, γ-glycine formation generally highly dominates α-glycine formation from a 1:2 electrolyte solution, even though the solution pHs [from 6.2 to 8.6] favors α-glycine. Even in the mixtures of glycine polymorphs, γ-glycine is the majority.

These obtained results of glycine polymorphs from 1:2 electrolyte solutions may be well rationalized, though the solution chemistries become less straightforward. Here Na_2SO_4 is taken as a typical 1:2 electrolyte for the analysis of its impact on glycine polymorphs. Generally, the interactions between ions (Na^+ and SO_4^{2-}) and glycine zwitterions ($^+H_3NCH_2COO^-$) as well as glycine cyclic dimers $\begin{pmatrix} OOCCH_2NH_3 \\ H_3NCH_2COO \end{pmatrix}$ would produce a plenty of positive singly-charged ion-glycine complexes ($^+H_3NCH_2COONa$) and negative doubly-charged ion-glycine complexes ($^-SO_4H_3NCH_2COO^-$):

$$^+H_3NCH_2COO^- + Na^+ \Leftrightarrow {}^+H_3NCH_2COONa \qquad (5\text{-}3\text{-}1)$$

$$SO_4^{2-} + {}^+H_3NCH_2COO^- \Leftrightarrow {}^-SO_4H_3NCH_2COO^- \qquad (5\text{-}3\text{-}9)$$

$$\begin{pmatrix} OOCCH_2NH_3 \\ H_3NCH_2COO \end{pmatrix} \Leftrightarrow 2\ {}^+H_3NCH_2COO^- \qquad (5\text{-}3\text{-}3)$$

$$3\begin{pmatrix} OOCCH_2NH_3 \\ H_3NCH_2COO \end{pmatrix} + 4Na^+ + 2SO_4^{2-} \Leftrightarrow 4^+H_3NCH_2COONa + 2^-SO_4H_3NCH_2COO^- \qquad (5\text{-}3\text{-}10)$$

In a way similar to that of the impact of a 1:1 electrolyte on glycine polymorphs, a 1:2 electrolyte would destroy glycine cyclic dimers and create charged ion-glycine complexes. Both destroying glycine cyclic dimers and poisoning α-glycine nuclei due to the charged ion-glycine complexes inhibit α-glycine. Meanwhile, the created charged ion-glycine complexes would have a good chance to produce glycine head-to-tail open

dimers ($^{-}SO_4H_3NCH_2COOHH_2NCH_2COONa$) to initiate the formation of γ-glycine nuclei:

$$^{-}SO_4H_3NCH_2COO^{-} + {}^{+}H_3NCH_2COONa \Leftrightarrow {}^{-}SO_4H_3NCH_2COOHH_2NCH_2COONa \qquad (5\text{-}3\text{-}11)$$

Note that glycine head-to-tail open dimers ($^{-}SO_4H_3NCH_2COOHH_2NCH_2COONa$) may be adversely affected by possible formation of the incorrect open dimers ($NaOOCCH_2NH_3SO_4H_3NCH_2COO^{-}$), compared with those glycine head-to-tail open dimers formed in a 1:1 electrolyte solution. Nevertheless, once the tiny γ-glycine nuclei are formed, fast growth rates of these γ-glycine nuclei may be expected (Figure 5-3-4). That is because the number of Na^{+} ions is twice the number of SO_4^{2-} ions, based on the stoichiometry of Na_2SO_4. Therefore the positive singly-charged ion-glycine complexes ($^{+}H_3NCH_2COONa$) would significantly outnumber the negative doubly-charged ion-glycine complexes ($^{-}SO_4H_3NCH_2COO^{-}$). It should be highlighted that these positive singly-charged ion-glycine complexes ($^{+}H_3NCH_2COONa$), adding to the fast growing –c end (Figure 5-3-4), would primarily determine the earlier onset of γ-glycine nucleation, even if the negative doubly-charged complexes ($^{-}SO_4H_3NCH_2COO^{-}$) would adversely affect γ-glycine growth at the slow growing +c end (Figure 5-3-4) due to the incorrect orientation. As a result, γ-glycine is highly dominant, as observed.

It should be pointed out that, as concentrated Na_2CO_3 solutions have quite high pHs (8.97 for 1.5m and 9.19 for 2.5m Na_2CO_3), the high pHs may play a significant role in facilitating γ-glycine nucleation. However, the particular solution chemistry (charge separation) of CO_3^{2-} ions in aqueous solutions would promote γ-glycine nucleation

substantially, as more univalent ions are created via charge separation, thus Na_2CO_3 is quite close to an 1:1 electrolyte:

$$CO_3^{2-} + H_2O \Leftrightarrow HCO_3^- + OH^- \qquad (5\text{-}3\text{-}12)$$

Charge separation of an SO_4^{2-} ion is also possible (Gao and Lui, 2005), but it may be less likely compared with CO_3^{2-}:

$$SO_4^{2-} + H_2O \Leftrightarrow HSO_4^- + OH^- \qquad (5\text{-}3\text{-}13)$$

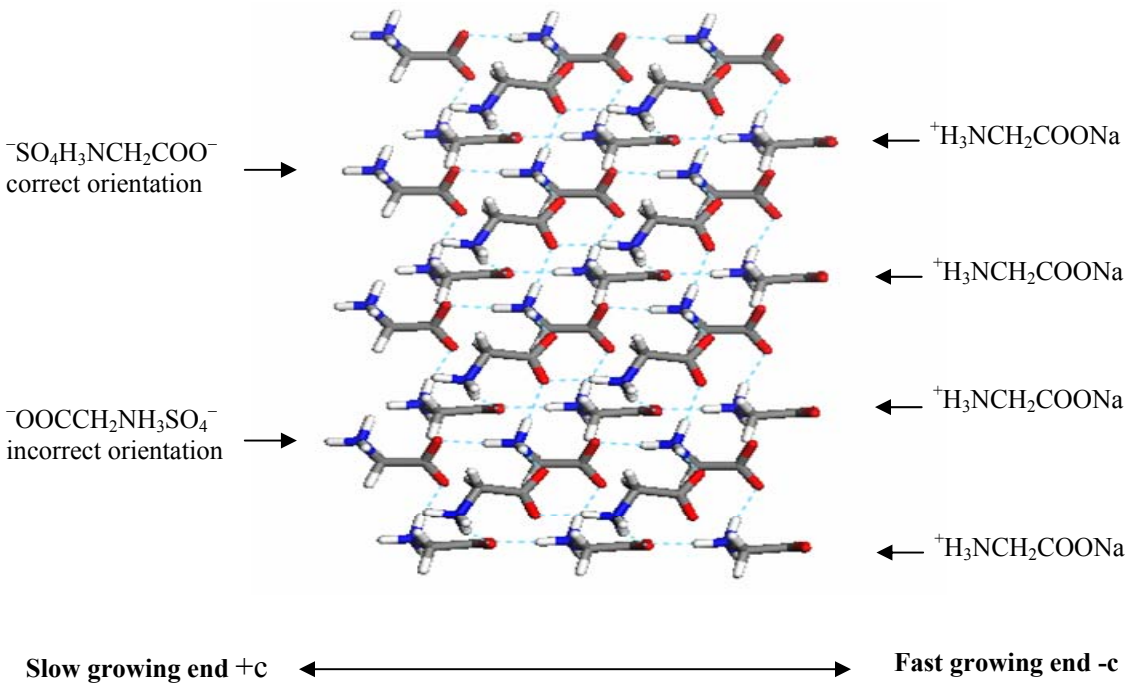

Figure 5-3-4 Effect of a 1:2 electrolyte, Na_2SO_4: The charged ion-glycine complexes as the building units for a γ-glycine nucleus to grow from both polar ends [polar *c*-axis NH_3^+ rich, pointed, end (+*c*) and COO^- rich end (-*c*)]

As for Na_2SO_4, at low concentrations of Na_2SO_4, pure γ-glycine nucleated. With Na_2SO_4 concentration increased up to 1.5m, mixtures of α- and γ-glycine polymorphs

were observed, with traces of α-glycine. Among other reasons, the appearance of α-glycine may be attributed to the formation of sophisticated complexes via coordination chemistry. It is reasonably assumed that, with significant increase of Na_2SO_4, more extra free Na^+ and SO_4^{2-} ions would be available to form sophisticated complexes in which Na^+, SO_4^{2-}, $^+H_3NCH_2COO^-$ and H_2O may be involved. Due to the lack of atomic polarization of Na^+ ions (vs polyatomic NH_4^+ ions in which atomic polarization seems much more likely) and its symmetry, there may be a relatively higher tendency for the sophisticated complexes to be formed, as Na^+ ions can position and orientate themselves relatively more readily for the coordination. Unfortunately, these sophisticated complexes are not the building units for γ-glycine. Consequently, the relative probability of γ-glycine formation is reduced while that of α-glycine increased with significant increase of Na_2SO_4.

5.3.2.3 Glycine Polymorph from 2:1 Electrolyte Solutions

Two 2:1 electrolytes (i.e. $Ca(NO_3)_2$, $CaCl_2$) were selected for investigation of their effects on glycine polymorphs. Using both forced cooling and natural cooling techniques, glycine polymorphs were formed from these 2:1 electrolyte solutions, in a natural pH. The results of glycine polymorphs from these 2:1 electrolyte solutions are tabulated in Table 5-3-8. The solution pHs range from 5.5 to 6.34.

Surprisingly, it can be seen (Table 5-3-8) that, with exception of γ-glycine from 0.1m $CaCl_2$ by natural cooling, either pure α-glycine or mixtures of α- and γ-glycine polymorphs was generally obtained from 1:2 electrolyte solutions, by either forced

cooling or natural cooling. It was also observed that, in the mixtures of the obtained glycine polymorphs, α-glycine was quite dominant though generally the amount of γ-glycine was not negligible. Therefore it was shown that, different from the observation of glycine polymorphs from a 1:2 electrolyte solution, α-glycine is generally more competitive than γ-glycine in a 2:1 electrolyte solution. In a similar analysis used for glycine polymorphs from a 1:2 electrolyte solution, the obtained results of glycine polymorphs from 2:1 electrolyte solutions may be interpreted.

Table 5-3-8 Glycine polymorphs from 2:1 electrolyte solutions, by cooling

2:1 Electrolyte	Electrolyte molality							
	0.1m		0.5m		1.0m		1.5m	
	Forced Cooling	Natural Cooling	Forced Cooling	Natural Cooling	Forced Cooling	Natural Cooling	Forced Cooling	Natural Cooling
$CaCl_2$	γ+α	γ	γ+α	γ+α	γ+α	γ+α	γ+α	γ+α
$Ca(NO_3)_2$	α	γ+α	α	γ+α			γ+α	γ+α
$Ca(NO_3)_2$*							α	
$Mg(NO_3)_2$*							α	

*by Towler et al. (2004) at ionic strength of 5.17

The interactions between ions (Ca^{2+} and Cl^-) and glycine zwitterions ($^+H_3NCH_2COO^-$) as well as glycine cyclic dimers $\begin{pmatrix} OOCCH_2NH_3 \\ H_3NCH_2COO \end{pmatrix}$ would significantly form negative singly-charged complexes ($ClH_3NCH_2COO^-$) and positive doubly-charged complexes ($^+H_3NCH_2COOCa^+$):

$$Cl^- + {}^+H_3NCH_2COO^- \Leftrightarrow ClH_3NCH_2COO^- \qquad (5\text{-}3\text{-}2)$$

$$^{+}H_3NCH_2COO^{-} + Ca^{2+} \Leftrightarrow {}^{+}H_3NCH_2COOCa^{+} \quad (5\text{-}3\text{-}14)$$

$$\begin{pmatrix} OOCCH_2NH_3 \\ H_3NCH_2COO \end{pmatrix} \Leftrightarrow 2\ {}^{+}H_3NCH_2COO^{-} \quad (5\text{-}3\text{-}3)$$

$$3\ \begin{pmatrix} OOCCH_2NH_3 \\ H_3NCH_2COO \end{pmatrix} + 4\ Cl^{-} + 2\ Ca^{2+} \Leftrightarrow 2\ {}^{+}H_3NCH_2COOCa^{+} + 4\ ClH_3NCH_2COO^{-} \quad (5\text{-}3\text{-}15)$$

It can be seen that a 2:1 electrolyte may destroy glycine cyclic dimers and create charged ion-glycine complexes. As a result, α-glycine is inhibited not only by destroying glycine cyclic dimers but also by poisoning α-glycine nuclei due to the charged ion-glycine complexes adsorbed onto the surfaces of α-glycine nuclei. Meanwhile, the created charged ion-glycine complexes would produce glycine head-to-tail open dimers ($ClH_3NCH_2COOHNH_2CH_2COOCa^{+}$) to initiate the formation of γ-glycine nuclei:

$$ClH_3NCH_2COO^{-} + {}^{+}H_3NCH_2COOCa^{+} \Leftrightarrow ClH_3NCH_2COOHNH_2CH_2COOCa^{+} \quad \text{(head-to-tail)} \quad (5\text{-}3\text{-}16)$$

After tiny γ-glycine nuclei are formed, they may grow further. However, the growth rates of γ-glycine nuclei in 2:1 electrolyte solutions may be quite slow. That is because, though the negative singly-charged complexes ($ClH_3NCH_2COO^{-}$) are very likely more than the positive doubly-charged complexes ($^{+}H_3NCH_2COOCa^{+}$) due to the fact that Cl^{-} ions are more than Ca^{2+} ions, the former ($ClH_3NCH_2COO^{-}$) can only add to the **slow growing +c end** (Figure 5-3-5)**.** Furthermore, a significant portion (maybe approximately 50%) of the positive doubly-charged complexes ($^{+}H_3NCH_2COOCa^{+}$) have an adverse interference with the fast growing –c end, due to incorrect orientation (Figure 5-3-5). Both the slow growth at the +c end and the adversely affected fast growing –c end make γ-glycine nuclei grow slow, thus γ-glycine is relatively less competitive than α-glycine.

However, it should be highlighted that, at a high concentration of Ca^{2+} ions, a dication Ca^{2+} can coordinate more readily with a few glycine molecules via co-valence to form sophisticated complexes (Natarajan and Rao,1980; Rao and Natarajan, 1980; Natarajan, 1983), as was discussed in **Section 5-3-1**. These sophisticated complexes probably deteriorate γ-glycine formation more than α-glycine formation.

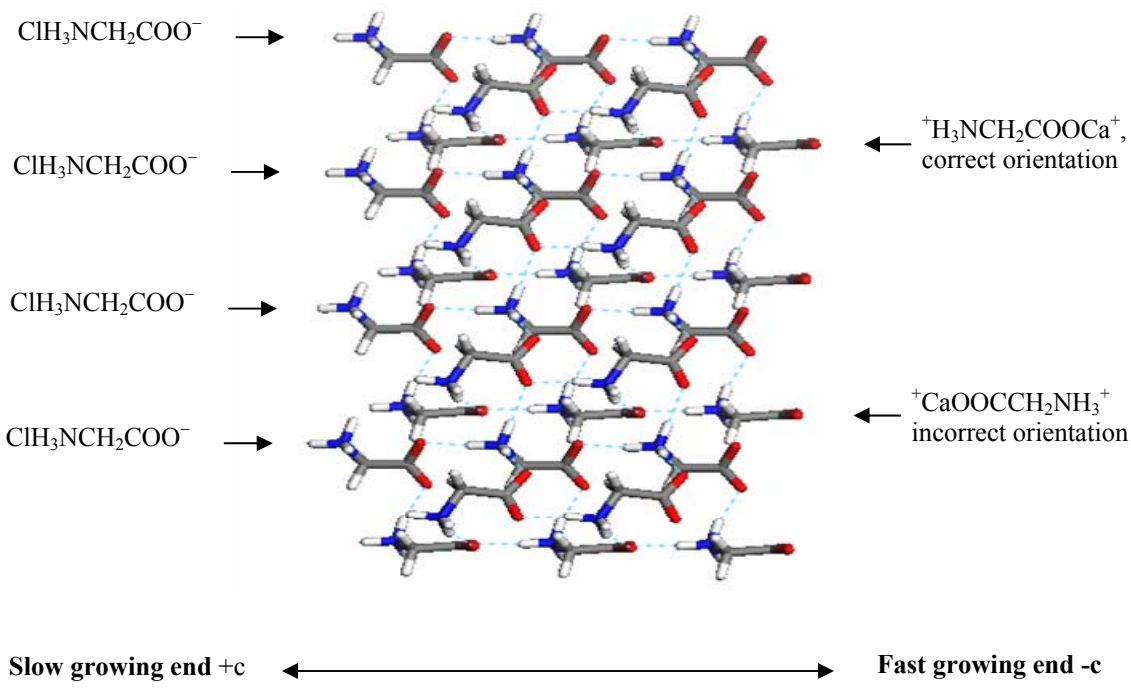

Figure 5-3-5 Effect of a 2:1 electrolyte, $CaCl_2$: The charged ion-glycine complexes as the building units for a γ-glycine nucleus to grow from both polar ends [polar c-axis NH_3^+ rich, pointed, slow growing end (+c) and COO^- rich fast growing end (-c)]

As was observed, a mixture of α- and γ-glycine polymorphs was produced from 0.1m $CaCl_2$ solution by forced cooling while pure γ-glycine was obtained by natural

cooling. Forced cooling and natural cooling also made difference in producing glycine polymorphs from 0.1m and 0.5m $Ca(NO_3)_2$ solutions, with forced cooling leading to pure α-glycine while natural cooling resulting in a mixture of α- and γ-glycine. It can be seen that natural cooling favors the thermodynamically stable γ-glycine, which can be expected as natural cooling is closer to equilibrium (He et al., 2006).

5.3.2.4 Glycine Polymorph from 2:2 Electrolyte Solutions

As a typical 2:2 electrolyte, $MgSO_4$ was selected for the study of its effect on glycine polymorphs. Four different concentrations of $MgSO_4$ ranging from 0.1m to 1.5m were used, with a pH range from 5.55 to 6.25. Results of the glycine polymorphs from these $MgSO_4$ solutions are shown in Table 5-3-9.

Table 5-3-9 Glycine polymorphs from 2:2 electrolyte solutions, by cooling

Type of Cooling	Electrolyte molality			
	0.1m	0.5m	1.0m	1.5m
Forced cooling	α	α	α	α
Forced cooling*				α
Natural cooling	α+γ	α	α	α

*by Towler et al. (2004) at ionic strength of 5.17

From Table 5-3-9, it can be seen that $MgSO_4$ solutions always produced α-glycine (either pure α-glycine or a mixture of α-glycine and γ-glycine), no matter the type of

cooling. Again, this observed phenomenon may be interpreted based on molecular interaction and complex formation.

Similar to the discussions on the effects of 1:2 and 2:1 electrolytes, the interactions between ions (Mg^{2+} and SO_4^{2-}) and glycine zwitterions ($^+H_3NCH_2COO^-$) as well as glycine cyclic dimers $\begin{pmatrix} OOCCH_2NH_3 \\ H_3NCH_2COO \end{pmatrix}$ would significantly form negative doubly-charged complexes ($^-SO_4H_3NCH_2COO^-$) and positive doubly-charged complexes ($^+H_3NCH_2COOMg^+$):

$$SO_4^{2-} + {}^+H_3NCH_2COO^- \Leftrightarrow {}^-SO_4ClH_3NCH_2COO^- \qquad (5\text{-}3\text{-}17)$$

$$^+H_3NCH_2COO^- + Mg^{2+} \Leftrightarrow {}^+H_3NCH_2COOMg^+ \qquad (5\text{-}3\text{-}18)$$

$$\begin{pmatrix} OOCCH_2NH_3 \\ H_3NCH_2COO \end{pmatrix} + Mg^{2+} + SO_4^{2-} \Leftrightarrow {}^+H_3NCH_2COOMg^+ + {}^-SO_4H_3NCH_2COO^- \qquad (5\text{-}3\text{-}19)$$

The complexes with the same charges would not approach each other for any association. Instead, due to electrostatic force, two types (type A and type B) of pseudo glycine cyclic dimers can be further formed readily:

$$^+H_3NCH_2COOMg^+ + {}^-SO_4H_3NCH_2COO^- \Leftrightarrow \begin{pmatrix} H_3NCH_2COOMg \\ SO_4H_3NCH_2COO \end{pmatrix} \quad \text{type A} \qquad (5\text{-}3\text{-}20)$$

$$^+H_3NCH_2COOMg^+ + {}^-SO_4H_3NCH_2COO^- \Leftrightarrow \begin{pmatrix} MgOOCCH_2NH_3 \\ SO_4H_3NCH_2COO \end{pmatrix} \quad \text{type B} \qquad (5\text{-}3\text{-}21)$$

Complexes of type A have a wrong structure with respect to glycine cyclic dimers $\begin{pmatrix} OOCCH_2NH_3 \\ H_3NCH_2COO \end{pmatrix}$ for α-glycine nuclei and therefore they will not fit into α-glycine lattices. Complexes of type B are likely to fit into α-glycine, since thermal vibration or molecular collision would cause them to lose ions (Mg^{2+} and SO_4^{2-}). Therefore ultimately pseudo

cyclic dimers of type B may be converted to the true glycine cyclic dimers $\binom{OOCCH_2NH_3}{H_3NCH_2COO}$, favorable for α-glycine formation. However, neither type A $\binom{H_3NCH_2COOMg}{SO_4H_3NCH_2COO}$ nor type B $\binom{MgOOCCH_2NH_3}{SO_4H_3NCH_2COO}$ is the building unit for γ-glycine nucleation due to the different structure of these pseudo cyclic dimers. Even if a small portion of negative doubly-charged complexes ($^{-}SO_4H_3NCH_2COO^{-}$) and positive doubly-charged complexes ($^{+}H_3NCH_2COOMg^{+}$) are available for γ-glycine growth, they are also very likely to adversely interfere with both polar ends (-c and +c) of a γ-glycine nucleus, due to incorrect orientation as shown in Figure 5-3-6. Therefore it can be seen that a 2:2 electrolyte retards γ-glycine much more than α-glycine, eventually resulting in α-glycine.

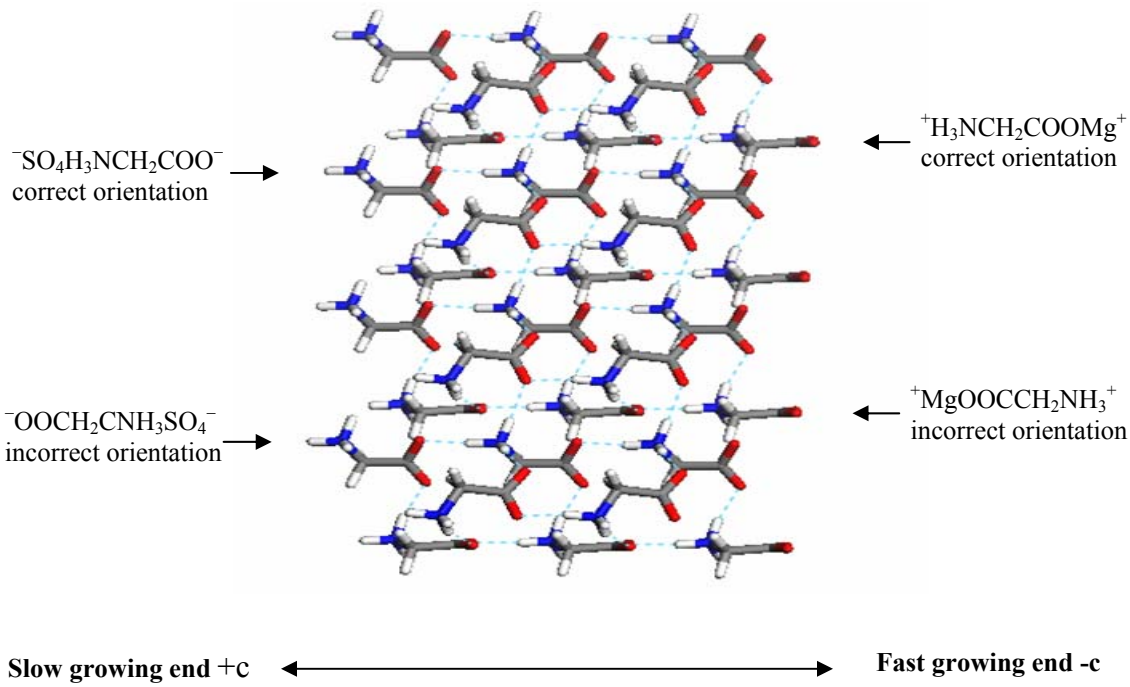

Figure 5-3-6 Effect of a 2:2 electrolyte, $MgSO_4$: The charged ion-glycine complexes as the building units for a γ-glycine nucleus to grow from both polar ends [polar c-axis NH_3^{+} rich, pointed, slow growing end (+c) and the COO^{-} rich fast growing end (-c)]

α-glycine was produced from a dilute (0.1m) $MgSO_4$ solution when forced cooling was exerted, while a mixture of α- and γ-glycine polymorphs was produced when natural cooling was used, with γ-glycine being significant. This shows that the type of cooling do have an effect on glycine polymorphs from 2:2 electrolyte solutions at a low electrolyte concentration, again reflecting the concept that the condition (here natural cooling) closer to equilibrium in the nucleation process favors the thermodynamically stable polymorph (He et al., 2006).

5.4 Summary

The effects of many different electrolytes on glycine polymorphs have been experimentally investigated. The results show that 1:1 (e.g. NaCl) and 1:2 (e.g. Na_2SO_4) electrolytes tremendously inhibit α-glycine and promote γ-glycine, while 2:1 (e.g. $CaCl_2$) and 2:2 (e.g. MgSO4) electrolytes have a higher tendency to induce α-glycine. Wherever applicable, the results of glycine polymorphs from this study are in a good agreement with the reported ones (Bhat and Dharmaprakash, 2002a and 2002b; Moolya et al., 2005; Towler et al., 2004).

The mechanisms have been proposed to interpret the observed glycine polymorphs from different electrolyte solutions. They indicate that, due to significant ion-dipole interaction, glycine cyclic dimers can be destroyed to form ion-glycine complexes. As a result, the profile of elementary building units for α-glycine and γ-glycine can be affected substantially. Moreover, the formed ion-glycine complexes can remarkably promote or inhibit (poison) nucleation initiation and nucleus growth hence

nucleation onset and outcome of glycine polymorphs. Furthermore, it has been suggested that the valence(s), rather than other properties of the ions from an electrolyte, primarily determine whether a particular glycine polymorph can be preferentially formed from the electrolyte solutions.

The roles of univalent cations (e.g. K^+, NH_4^+) and the COO^- rich fast growing –c end of γ-glycine have been particularly highlighted, as they have bigger impacts on glycine polymorphs via growth rate. Indeed, as expected, 1:1 (e.g. KCl) and 1:2 (e.g. Na_2SO_4) electrolytes that contain univalent cations tremendously enhance the growth rates of γ-glycine crystals, which will be discussed in **Chapter 6**.

The ideas presented here should be relevant for understanding and controlling crystal polymorphs of other systems. For instance, the mechanisms for γ-glycine nucleation from 1:1 and 1:2 electrolyte solutions may generally imply that these electrolytes are likely to induce polar polymorphic crystals of many other amino acids (dipolar ions).

Other factors, including ion hydration (especially for divalent ions, e.g., Ca^{2+}, Mg^{2+}, Zn^{2+} and SO_4^{2-}, as pointed out by Allen et al., 2006 and Bester-Rogac et al., 2007), ion size and steric hindrance may exert an influence on glycine polymorphs, to some extent. Quantifying the contribution of each of these factors to the formation of glycine polymorphs would form another major subject and it is beyond the scope of this current research.

Chapter 6 Effects of Electrolytes on Kinetics of γ-glycine Growth

In **Chapter 5**, the impacts of electrolytes on glycine polymorphs have been investigated. The proposed mechanisms for the observed glycine polymorphs produced from different electrolyte solutions suggest that ion-dipole interactions creating ion-glycine complexes greatly influence the profile of building units for α- and γ-glycine. A 1:1 (e.g. NaCl) and a 1:2 (e.g. Na_2SO_4) electrolyte would tremendously enhance the growth rate of γ-glycine and therefore they facilitate γ-glycine formation. In contrast, a 2:1 (e.g. $CaCl_2$) or 2:2 (e.g. $MgSO_4$) electrolyte may not sufficiently promote the growth rate of γ-glycine, leading to the fact that α-glycine is generally induced more readily than γ-glycine.

In this chapter, the growth rate of γ-glycine crystals from different electrolyte solutions is experimentally investigated to show that γ-glycine indeed grow much faster from 1:1 and 1:2 electrolyte solutions than from 2:1 and 2:2 electrolyte solutions.

6.1 Experimental Materials

A batch crystallizer was used to explore the growth kinetics of γ-glycine crystal seeds from different electrolyte solutions at 25 °C, via desupersaturation (Garside et al., 2002). The glass crystallizer was made by SG Scientific Glass Blowing Centre Pte Ltd, Singapore. It was a jacketed 500ml vessel with a round bottom, equipped with a temperature control system and an overhead stirrer. The schematic experimental rig was shown in Figure 6-1-1.

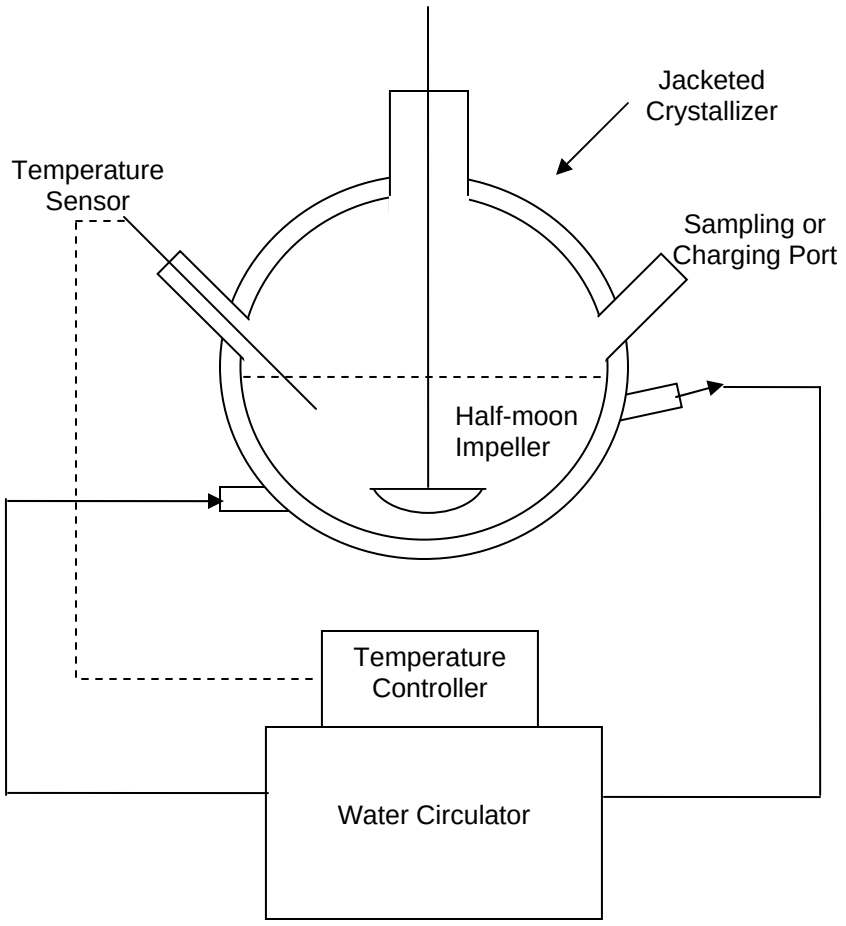

Figure 6-1-1 Schematic experimental setup for isothermal seeded crystallization

All chemicals used here were described in **Chapter 5**. The γ-glycine crystal seeds were confirmed by powder-XRD. As usual, the following assumptions are made in the present study for γ-glycine crystal growth from solutions:

Well-mixed solution in the crystallizer;

Negligible nucleation, breakage, agglomeration;

6.2 Experimental Procedure

A Teflon-coated half-moon impeller (65x18x3mm) was used for agitating the solution in the batch crystallizer. The temperature of the crystallizer was controlled at 25°C by a Julabo FP50 water circulator with a temperature resolution of ±0.01°C. The temperature sensor used for the temperature control of the solution in the batch crystallizer was Pt 100. A Heidolph Overhead Stirrer RZR 2041 was used to adjust the stirring speed to 260rpm to adequately suspend the γ-glycine crystal seeds and to facilitate achieving a uniform distribution of the seeds in the solution while the breakage of the seeds was insignificant. The γ-glycine seeds were prepared by sieving commercial γ-glycine for 355 – 425μm (average size of 390μm), using a L3P Sonic Sifter Separator. In this size range, the number of seeds was approximately 15400 per gram.

The glycine supersaturated solution was prepared by dissolving an appropriate amount of glycine in a given warm (about 45°C) electrolyte solution, with each mass weighed within an accuracy of ±0.01 wt%. A low initial relative supersaturation of σ = 0.05 with respect to γ-glycine at 25°C was strictly controlled. At this low supersaturation, the glycine concentration was lower than the solubility of α-glycine so that no α-glycine would nucleate and grow. The solubilities of both γ-glycine and α-glycine in various electrolyte solutions at 25°C have been measured and reported in **Chapter 5** (**Section 5-3-1).** The prepared warm solution was then charged into the crystallizer while minimal agitation (about 170rpm) of the solution was kept. The warm solution was then cooled to and maintained at 25°C to generate the supersaturation. Once the solution temperature was well maintained at 25°C, a solution sample was withdrawn

from the crystallizer to check if its concentration decreased so as to determine whether significant nucleation took place before 5.000±0.001g of γ-glycine crystal seeds were charged into the crystallizer. If insignificant nucleation was confirmed, the rest of the solution in the crystallizer was adjusted to contain 250.00±0.01g of H_2O and then the γ-glycine seeds were loaded into the crystallizer for crystal growth.

Using a TERUMO 5ml syringe with a Sterican fine needle (0.4mm in outer diameter and 60 mm in length), solution samples (including the sample before charging the seeds) were periodically withdrawn from the crystallizer for concentration analysis. Since the total volume of a syringe and a needle was predetermined to be 5.45±0.1ml, each solution sample was 5.45±0.1ml. A pre-test showed that the coarse seeds (355-425μm) were not sucked into the Sterican fine needle. Nevertheless, to prevent any finer crystals to grow before sample analysis, a syringe filter (Nylon 0.22μm) was used to filtrate the withdrawn sample solutions immediately.

The correlation between solution densities and glycine concentrations for a given electrolyte was established using standard solutions. This correlation, highly linear, was then applied to determine the concentration and the mass of each solution sample, by measuring the solution density using an Anton Paar density meter DMA5000 to obtain the desupersaturation data and curves. The procedures for correlation and concentration determination via solution density can be found in **Appendix A**. The seed mass (W) which changes with time can be determined by mass balance once the solution concentrations are known.

With the obtained desupersaturation data and curves (glycine concentration, g/100g H_2O, vs time t), the linear growth rate of the crystal seeds, R_G, may be evaluated over a time interval Δt, using Eqs. 2-3-2 and 2-3-5, assuming that the change of the seed volume shape factor k_v is insignificant (Tavare, 1995). The power law (Eq. 2-3-6) may be applied for data correlation between growth rate R_G and relative supersaturation σ. Note that the average relative supersaturation over a time interval Δt should be used for better correlation as suggested by Martins et al. (2006).

6.3 Evaluation of the Method for γ-glycine Kinetic Study

Before systematic investigation, the method for crystal growth study was evaluated by carrying out a few typical experiments for γ-glycine crystal growth using the experimental setup (Figure 6-1-1) and the procedure described above. The experimental conditions, including the initial seed mass and seed size, solvent (H_2O) mass, the agitation speed, the initial glycine relative supersaturation and time intervals for withdrawing samples etc, were strictly controlled to be the same for each run.

Data for two typical experiments, one for slow γ-glycine crystal growth from pure H_2O and the other for fast growth from 2.5m NaCl at 25°C, are summarized in Tables 6-3-1 and 6-3-2. The data in these tables are the average ones over two replicas. The corresponding average desupersaturation curves are shown in Figures 6-3-1 and 6-3-2. For a better view of the reproducibility, individual glycine desupersaturation curves are also presented in Figures 6-3-1 and 6-3-2.

Table 6-3-1 Experimental data of γ-glycine growth from pure H_2O at 25°C

time, minute	glycine concentration, c, g/100g H_2O	γ-glycine relative supersaturation, σ = c/c*-1	average σ over Δt	ln(average σ) over Δt	seed mass, W, g	crystal size, L, μm	growth rate R_G x10^8, m/s	ln(R_G)
0	24.66	0.050	0.049	-3.020	5.000	390.0	0.605	-0.503
10	24.61	0.048	0.047	-3.054	5.141	393.6	0.220	-1.513
20	24.59	0.047	0.046	-3.070	5.193	395.0	0.133	-2.019
30	24.57	0.046	0.046	-3.085	5.224	395.7	0.096	-2.347
50	24.56	0.045	0.045	-3.099	5.270	396.9	0.058	-2.853
70	24.54	0.045	0.045	-3.109	5.298	397.6	0.046	-3.089
90	24.53	0.044	0.044	-3.119	5.319	398.1	0.037	-3.300
120	24.52	0.044			5.346	398.8		

Table 6-3-2 Experimental data of γ-glycine growth from 2.5m NaCl solution at 25°C

time, minute	glycine concentration, c, g/100g H_2O	γ-glycine relative supersaturation, σ = c/c*-1	average σ over Δt	ln(average σ) over Δt	seed mass, W, g	crystal size, L, μm	growth rate R_G x10^8, m/s	ln(R_G)
0	28.06	0.050	0.038	-3.263	5.000	390.0	6.184	1.822
10	27.44	0.027	0.023	-3.788	6.567	427.1	1.823	0.600
20	27.23	0.019	0.016	-4.116	7.085	438.0	1.067	0.065
30	27.10	0.014	0.011	-4.499	7.400	444.4	0.581	-0.544
50	26.95	0.008	0.007	-5.006	7.754	451.4	0.336	-1.090
70	26.86	0.005	0.004	-5.496	7.963	455.4	0.184	-1.695
90	26.81	0.003	0.002	-5.997	8.079	457.6	0.088	-2.434
120	26.77	0.002			8.163	459.2		

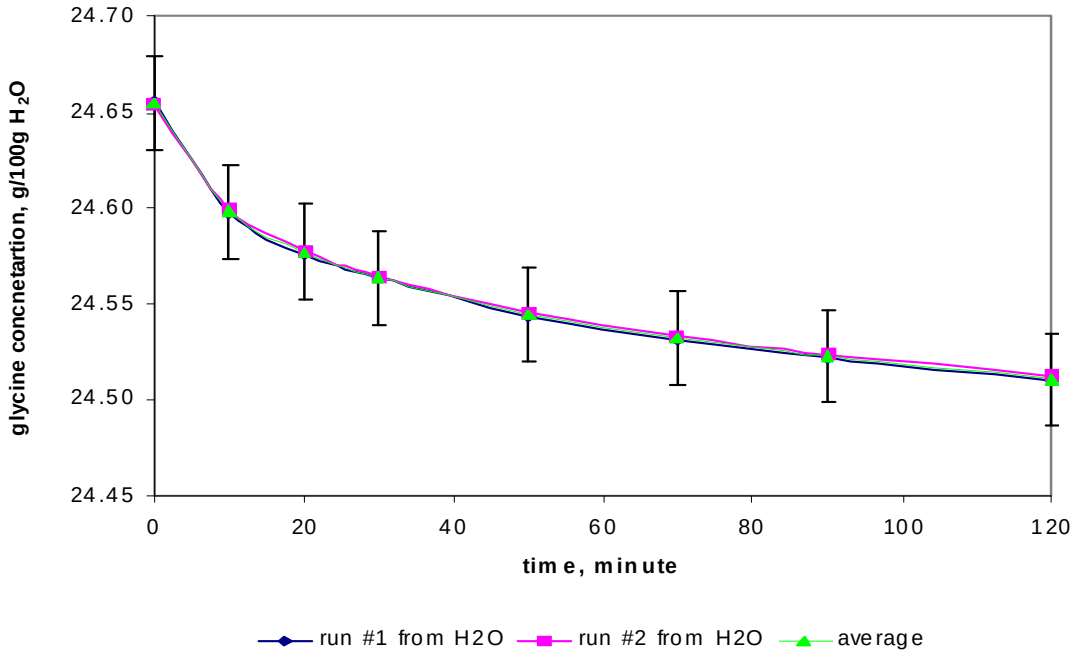

Figure 6-3-1 γ-glycine desupersaturation curve from pure H_2O at 25°C (error bar 0.5%)

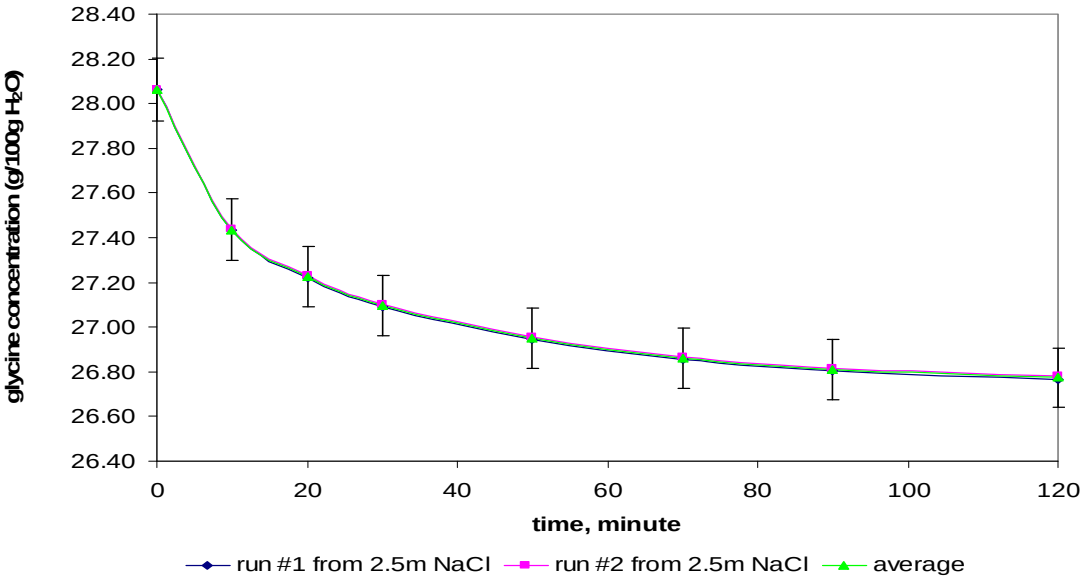

Figure 6-3-2 γ-glycine desupersaturation curve from 2.5m NaCl solution at 25 °C (error bar 0.5%)

Figures 6-3-1 and 6-3-2 show a very good reproducibility in the measurements of the desupersaturtaion curves. It can be seen that, for a given NaCl concentration (e.g. 0.0m and 2.5m), the deviations of the desuapersaturation curves of γ-glycine from different experimental runs are very small, approximately ±0.1% only (equivalent to about ±0.02g/100g H_2O). In fact, this insignificant deviation reflects the high accuracy of glycine concentrations determined by solution density, as discussed in **Appendix A**.

Using Eqs. 2-3-2 and 2-3-5, linear growth rates (R_G) of γ-glycine crystals from the two selected solutions (H_2O and 2.5m NaCl) are calculated. They are also tabulated in Tables 6-3-1 and 6-3-2 and plotted in Figures 6-3-3 and 6-3-4. From Figures 6-3-3 and 6-3-4, it can be seen that the deviations of the growth rates are reasonably small, not bigger than 5%. It is also observed that the deviations of growth rates from 2.5m NaCl solution are even much smaller than those from pure H_2O. It may be understandable. A slow growth rate results in an insignificant change of solution concentration with time (Figure 6-3-1). Therefore, even a very small error in solution concentration would lead to a relatively big error in the calculations for seed mass thus seed size and eventually the growth rate. Nevertheless, overall, the reasonably good reproducibility and small deviations suggest that this experimental method is suitable for study of γ-glycine growth kinetics.

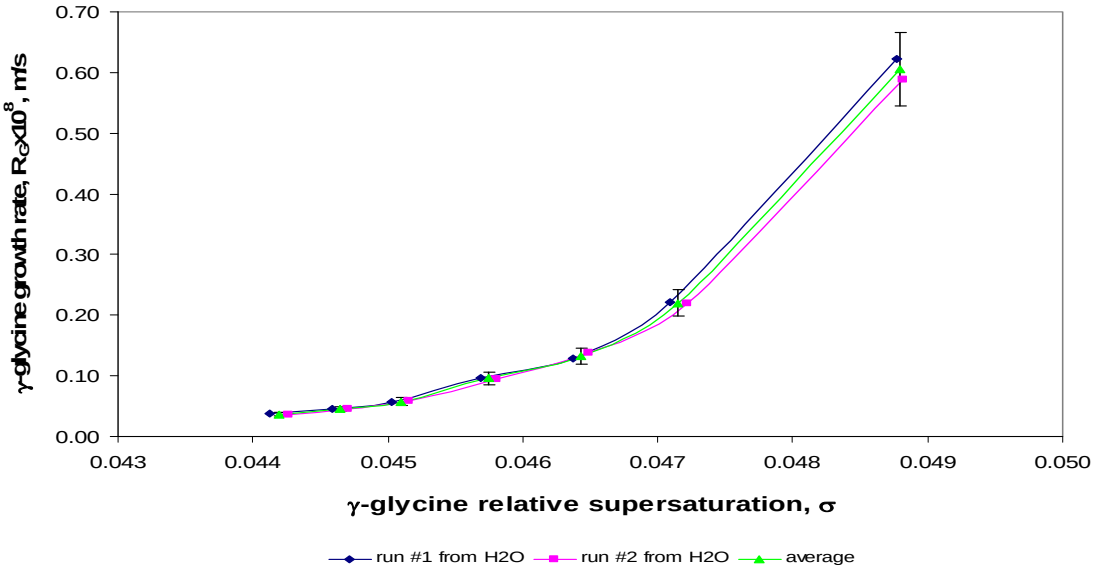

Figure 6-3-3 γ-glycine linear growth rate R_G from pure H_2O vs its relative supersaturation σ at 25 °C (error bar 10%)

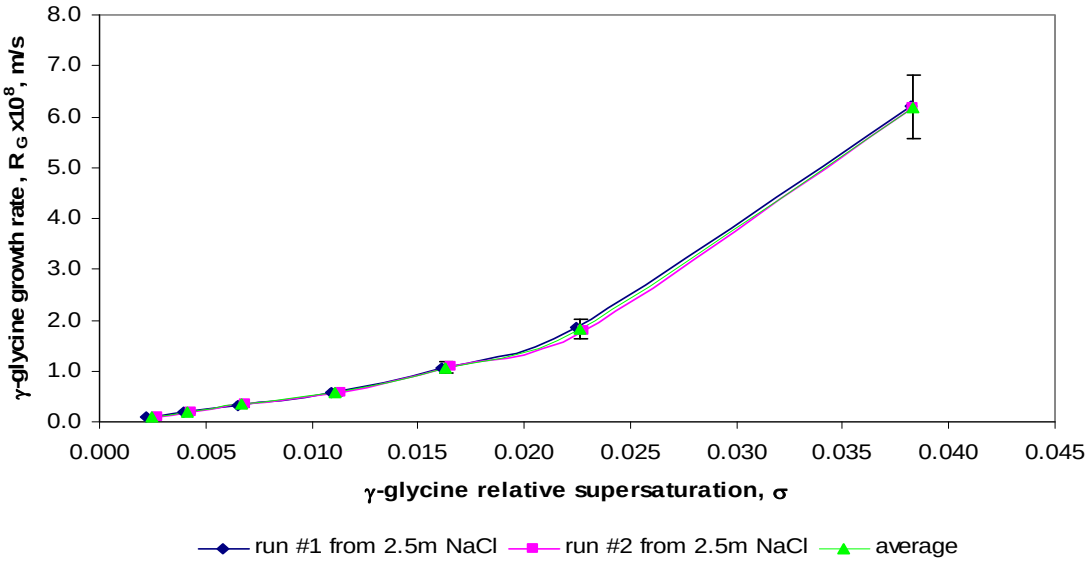

Figure 6-3-4 γ-glycine linear growth rate R_G from 2.5m NaCl vs its relative supersaturation σ at 25 °C (error bar 10%)

6.4 Effects of Different Electrolytes on γ-glycine Growth Rate

Using the experimental setup and procedure described above, the effects of different electrolytes on γ-glycine crystal growth were systematically investigated. Most of the measurements of desupersaturation curves were replicated twice. For proper comparison of the effects of these selected electrolytes on γ-glycine growth, a total ion molality of 3m was given for each electrolyte solution. As each experiment was carried out under the same conditions (e.g. initial γ-glycine relative supersaturation $\sigma = 0.050$, initial γ-glycine seed loading 5.000 g in 250.00g of H_2O, etc), the obtained experimental results would enable us to compare the impacts of electrolytes on γ-glycine growth from different aspects. In fact, the mass increment of the γ-glycine seeds in the very first time interval (here 10 minutes) of growth from a given electrolyte solution would naturally be a good indication of γ-glycine growth rate.

The mass increment of the γ-glycine seeds and the normalized mass increment are tabulated in Table 6-4-1 and plotted in Figure 6-4-1. The advantage of using seed mass increments is that the seed volume shape factor which could cause a big error is not involved in the calculations for seed masses, therefore the effects of different electrolytes on γ-glycine growth can be compared in a higher level of confidence.

The results from Table 6-4-1 and Figure 6-4-1 clearly show that, at the same total ion molality of 3m, these 1:1 and 1:2 electrolytes (NH_4Ac, KCl, KNO_3, NaCl, $NaNO_3$, NH_4Cl, NH_4NO_3, $(NH_4)_2SO_4$, Na_2SO_4 and Na_2CO_3) can tremendously enhance γ-glycine growth rate by about 7 to 11 times, compared with its growth rate from pure H_2O. These

2:1 and 2:2 electrolytes ($Ca(NO_3)_2$, $CaCl_2$ and $MgSO_4$) also have promoting effects on γ-glycine growth, but their effects are relatively less significant (generally not higher than 5 times).

Table 6-4-1 Mass increment of γ-glycine seeds in the first time interval of seed growth from various electrolyte solutions at 25°C

electrolyte solution	mass increment (g) of γ-glycine seeds in the first 10 minute interval, with an initial σ = 0.050	normalized mass increment [=mass increment/(mass increment from pure H_2O)]
H_2O	0.141	1.000
1.0m $Ca(NO_3)_2$	0.462	3.277
1.5m $MgSO_4$	0.546	3.870
1.0m $CaCl_2$	0.732	5.191
1.5m NH_4Ac	0.952	6.751
1.5m KCl	1.116	7.915
1.5m KNO_3	1.213	8.603
1.0m Na_2SO_4	1.427	10.121
1.5m NaCl	1.450	10.281
1.0m $(NH_4)_2SO_4$	1.468	10.411
1.5m $NaNO_3$	1.504	10.667
1.5m NH_4Cl	1.539	10.915
1.5m NH_4NO_3	1.550	10.992
1.0m Na_2CO_3	1.589	11.270

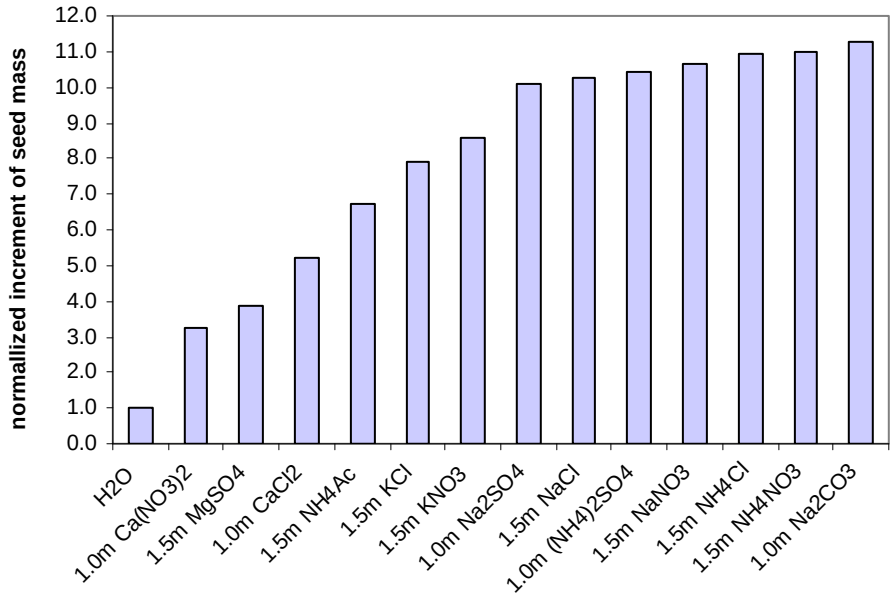

Figure 6-4-1 Normalized mass increment of γ-glycine seeds in the first 10 minute interval of seed growth at 25°C, with initial relative supersaturation σ = 0.050

As it was analyzed in **Chapter 5**, the higher the promoting effect of an electrolyte on γ-glycine growth, the more likely γ-glycine can be induced. According to this analysis and based on the obtained kinetic data, γ-glycine is supposed to be formed more readily than α-glycine from solutions with presence of a 1:1 or 1:2 electrolyte, while α-glycine formation should be more competitive than γ-glycine formation from solutions with presence of a 2:1 or 2:2 electrolyte. Therefore, γ-glycine kinetic data obtained here and the reported results of glycine polymorphs from electrolyte solutions (**Chapter 5**) are well consistent.

For gaining a better understanding of kinetics, the values of linear growth rates (R_G) would be very useful. They may be calculated, using Eqs. 2-3-2 and 2-3-5, with an assumption that crystal seed volume shape factor k_v is constant. To test whether this

assumption is valid, two runs of γ-glycine crystal growth from 1m $(NH_4)_2SO_4$ solutions were carried out. One run started with an initial γ-glycine relative supersaturation of 0.050 and the other run with 0.092. If the volume shape factor k_v is constant, then it is expected that the two curves of linear growth rates of γ-glycine crystals should be overlapped, at least very close to each other, over the same range of relative supersaturation. Unfortunately, it was found that deviations between the two kinetic curves are big, as shown in Figure 6-4-2.

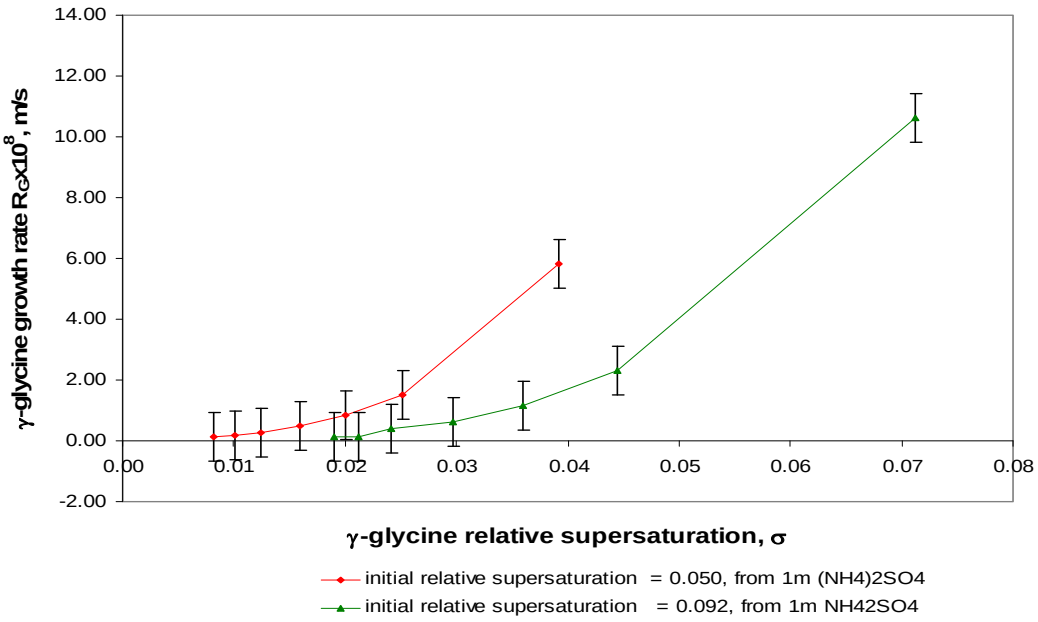

Figure 6-4-2 γ-glycine linear growth rate R_G from 1.0m $(NH_4)_2SO_4$ vs relative supersaturation σ at 25°C (error bar $0.8x10^{-8}$ m/s)

Such big growth rate deviations (up to about $5x10^{-8}$ m/s at relative supersaturation σ = 0.04) are not likely due to measurement errors, as the estimated error in growth rate R_G is about $0.8x10^{-8}$ m/s while the error in relative supersaturation σ is about 0.002 units

only. Instead, it is more likely due to the significant change in shape factor. In fact, for a polar γ-glycine crystal, it grows mainly along the c-axis, from both carboxyl rich –c and amino rich +c end (Figure 5-3-4). Therefore, due to the anisotropic growth, the shape of a γ-glycine crystal hence shape factor may change significantly with the growth of the polar crystal.

In order to reduce the adverse influence of the shape factor on the calculations for growth rates, the data obtained in the first two time intervals are used for the correlation between γ-glycine growth rate R_G and the corresponding average relative supersaturation σ to obtain the growth coefficient $\ln(k_g)$ and the power g as expressed in Eq. 2-3-6, by plotting $\ln(R_G)$ against $\ln(\sigma)$. These obtained growth coefficient $\ln(k_g)$ and the power g are tabulated in Table 6-4-2. Using the values of $\ln(k_g)$ and g, the growth rates of γ-glycine from different electrolyte solutions at the same γ-glycine relative supersaturation σ=0.050 are calculated and shown in Table 6-4-3, together with the normalized growth rates. For easier comparison of electrolyte effects at the same γ-glycine relative supersaturation σ=0.050, the normalized γ-glycine growth rates are presented in Figure 6-4-3. As expected, Figures 6-4-1 and 6-4-3 match each other quite well.

Without presence of any electrolyte in the solution, γ-glycine crystals grows extremely slow from pure H_2O, as was shown by its very slow desupersaturation (Figure 6-3-1). This is not surprised, because in pure H_2O, the glycine cyclic dimers are likely the dominant species but they do not fit into γ-glycine crystal lattices. As a result, γ-glycine can not grow fast.

Table 6-4-2 Values of parameters of power law $\ln(R_G) = g*\ln(\sigma) + \ln(k_g)$ for γ-glycine growth from different electrolyte solutions

electrolyte solution	value of power g	value of $\ln(k_g)$
H_2O	29.518	88.645
1.5m NaCl	2.750	10.650
1.5m NH4Cl	2.782	10.896
1.5m KNO3	4.172	14.895
1.5m KCl	3.911	13.998
1.5m NaNO3	2.947	11.303
1.5m NH4NO3	2.945	11.337
1.5m NH4Ac	3.888	13.750
1.0m (NH4)2SO$	3.042	11.622
1.0m Na2SO4	3.217	12.137
1.0m Na2CO3	3.267	12.319
1.0m CaCl2	8.096	26.071
1.0m Ca(NO3)2	9.762	30.374
1.5m MgSO4	9.969	31.373

Table 6-4-3 γ-glycine growth rate R_G from various electrolyte solutions at 25°C

electrolyte solution	growth rate $R_G x 10^8$ (m/s) of γ-glycine seeds at relative supersaturation σ =0.050	normalized growth rate $R_{G,N}$ [=R_G/(R_G from pure H_2O)]
H_2O	1.236	1.000
1.0m $Ca(NO_3)_2$	3.092	2.502
1.5m $MgSO_4$	4.521	3.658
1.0m $CaCl_2$	6.152	4.978
1.5m NH_4Ac	8.168	6.609
1.5m KCl	9.805	7.933
1.5m KNO_3	10.996	8.897
1.5m NaCl	11.530	9.329
1.5m $NaNO_3$	11.878	9.611
1.0m Na_2SO_4	12.184	9.858
1.0m $(NH_4)_2SO_4$	12.261	9.921
1.5m NH_4NO_3	12.349	9.992
1.0m Na_2CO_3	12.572	10.172
1.5m NH_4Cl	12.958	10.484

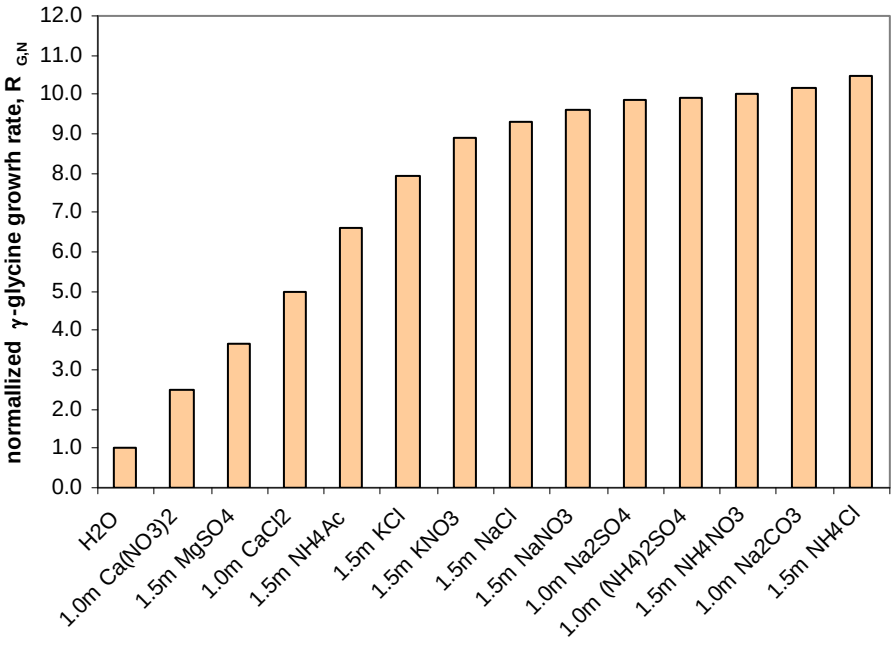

Figure 6-4-3 Normalized γ-glycine growth rate $R_{G,N}$ from various electrolyte solutions at 25°C at relative supersaturation σ = 0.050

Addition of an electrolyte into a glycine supersaturated solution makes a difference. As observed, 1:1 and 1:2 electrolytes promote γ-glycine crystal growth much more than 2:1 and 2:2 electrolytes do. Though the suggested mechanisms were presented in **Chapter 5**, the interpretation for the observed kinetic data is briefed below for convenience.

As was discussed in **Chapter 5**, for a 1:1 electrolyte, the ion-dipole interactions between the univalent ions and glycine molecules would significantly create positive singly-charged (e.g. $^{+}H_3NCH_2COONa$) and negative singly-charged (e.g. $ClH_3NCH_2COO^{-}$) ion-glycine complexes which are favorable growing units for γ-glycine crystals, with positive singly-charged ion-glycine complexes adding to the fast growing

carboxyl rich –c end while negative singly-charged ion-glycine complexes adding to the slow growing amino rich +c end of γ-glycine crystals (Figure 5-3-3). As it can be expected, these 1:1 electrolytes greatly promote the crystal growth of γ-glycine, though they do not exert an equal impact on γ-glycine growth.

As for the particular electrolyte NH_4Ac, its effect on promoting γ-glycine crystal growth is relatively smaller than those of other 1:1 electrolytes. That is because acetate ions (Ac^-) have weak interactions with glycine zwitterions or glycine cyclic dimers due to relatively high hydrophobicity of acetate ions. As a result, they do not create many negative singly-charged ion-glycine complexes ($AcH_3NCH_2COO^-$) which add to the slow growing amino rich +c end of γ-glycine, slowing down the growth rate. This particular case suggests that the roles of anions and the slow growing amino rich +c end of γ-glycine may not be negligible, though cations (e.g. Na^+) and the fast growing carboxyl rich –c end of γ-glycine play more significant roles.

For a 1:2 electrolyte (e.g. Na_2SO_4) which contains more cations than anions would create more positive singly-charged ion-glycine complexes (e.g. $^+H_3NCH_2COONa$) than negative doubly-charged ion-glycine complexes (e.g. $^-SO_4H_3NCH_2COO^-$). Fortunately, these positive singly-charged ion-glycine complexes add to the fast growing carboxyl rich –c end (Figure 5-3-4). As a result, these cations which form positive singly-charged ion-glycine complexes and the fast growing carboxyl rich –c end substantially promote γ-glycine growth, though the negative doubly-charged

ion-glycine complexes probably adversely interfere with the slow growing amino rich +c end.

In contrast, for a 2:1 electrolyte (e.g. $CaCl_2$), more anions (e.g. Cl^-) are created and therefore more negative singly-charged ion-glycine complexes (e.g. $ClH_3NCH_2COO^-$) are formed. However, these negative singly-charged ion-glycine complexes can only add to the slow growing amino rich +c ends of γ-glycine nuclei. Furthermore, the fast growing carboxyl rich –c ends of γ-glycine nuclei may be partially blocked by positive doubly-charged ion-glycine complexes (e.g. $^+H_3NCH_2COOCa^+$), thus retarding γ-glycine growth (Figure 5-3-5). Consequently, the promotion of γ-glycine growth from a 2:1 electrolyte solution is limited.

For a 2:2 electrolyte (e.g. $MgSO_4$), the ion-dipole interactions would generate positive doubly-charged ion-glycine complexes (e.g. $^+H_3NCH_2COOMg^+$) and negative doubly-charged ion-glycine complexes (e.g. $^-SO_4H_3NCH_2COO^-$). Unfortunately, a great part of these doubly-charged ion-glycine complexes would exert an adverse impact on both growing ends of γ-glycine (Figure 5-3-6). In addition, due to strong electrostatic force, these doubly-charged ion-glycine complexes subsequently form pseudo glycine cyclic dimers (Eqs. 5-3-20 and 5-3-21) which are not building units for γ-glycine. All these adverse effects impede γ-glycine growth, as it was shown by the kinetic data (Figures 6-4-1 and 6-4-3).

Mass transfer from bulk solution to the crystal surface may be a concern as it may be the growth rate controlling step. However, an experimental test showed that increasing agitation speed from 260rpm to 300rpm did not affect glycine desupersaturation curves from a concentrated 2.5m NaCl solution (Figure 6-4-4) while γ-glycine growth from the solution was fast. Therefore, the observed slow growth rates of γ-glycine crystals from some of the electrolyte solutions could not be attributed to the limitation of mass transfer.

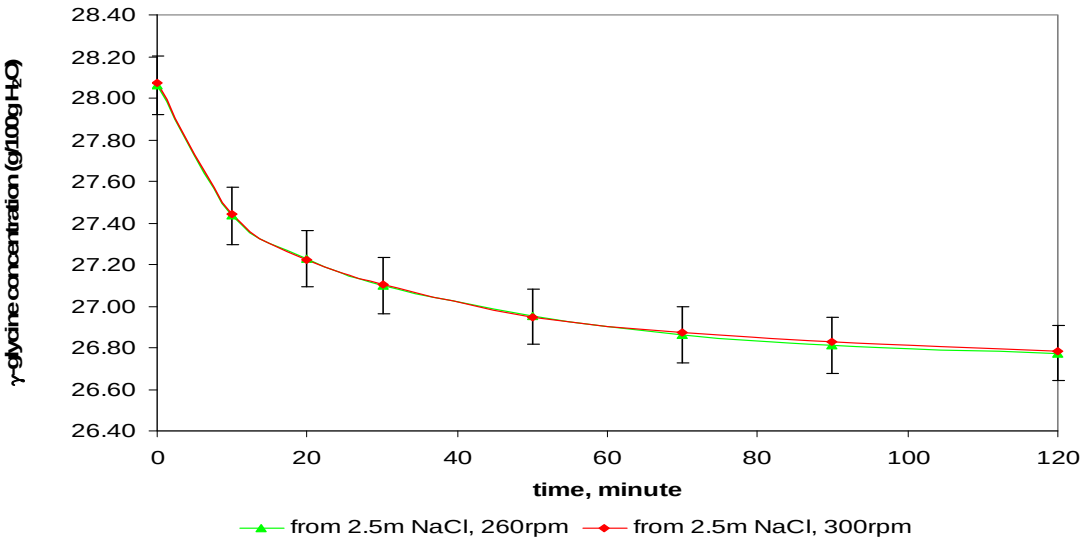

Figure 6-4-4 Agitation effect on γ-glycine desupersaturation curves from 2.5m NaCl solution at 25 °C (error bar 0.5%)

6.5 Effects of Electrolyte Concentration

In order to investigate the influence of the concentration of a 1:1 electrolyte on γ-glycine crystal growth, systematic experimental measurements were made for γ-glycine crystal growth from various NaCl solutions ranging from 0.0m to 5.0m. In a way similar to that used in the previous section, for better comparison, the mass increment of γ-glycine seeds in the first time interval (10 minutes) of seed growth, values of parameters

for power law and the linear growth rate R_G at γ-glycine relative supersaturation σ = 0.050 are calculated. They are tabulated in Tables 6-5-1 to 6-5-3 and shown in Figure 6-5-1.

Table 6-5-1 Mass increment of γ-glycine seeds in the first time interval of seed growth from various NaCl solutions at 25 °C

NaCl molality	mass increment (g) of γ-glycine seeds in the first 10 minute interval, with an initial σ = 0.050	normalized mass increment [=mass increment/(mass increment from pure H_2O)]
0.000	0.141	1.000
0.500	0.855	6.064
1.500	1.450	10.281
2.500	1.567	11.113
3.500	1.603	11.367
5.000	1.501	10.645

Table 6-5-2 Values of parameters of power law $\ln(R_G) = g*\ln(\sigma) + \ln(k_g)$ for γ-glycine growth from various NaCl solutions

NaCl molality	value of power g	value of $\ln(k_g)$
0.000	29.518	88.645
0.500	5.202	17.700
1.500	2.750	10.650
2.500	2.327	9.414
3.500	2.013	8.403
5.000	2.362	9.392

Table 6-5-3 γ-glycine growth rate R_G from various NaCl solutions at 25 °C

NaCl molality	growth rate R_G ($x10^8$ m/s) of γ-glycine seeds at relative supersaturation σ =0.050	normalized growth rate $R_{G,N}$ [=R_G/(R_G from pure H_2O)]
0.000	1.236	1.000
0.500	8.292	6.709
1.500	11.530	9.329
2.500	11.513	9.316
3.500	10.703	8.660
5.000	10.113	8.183

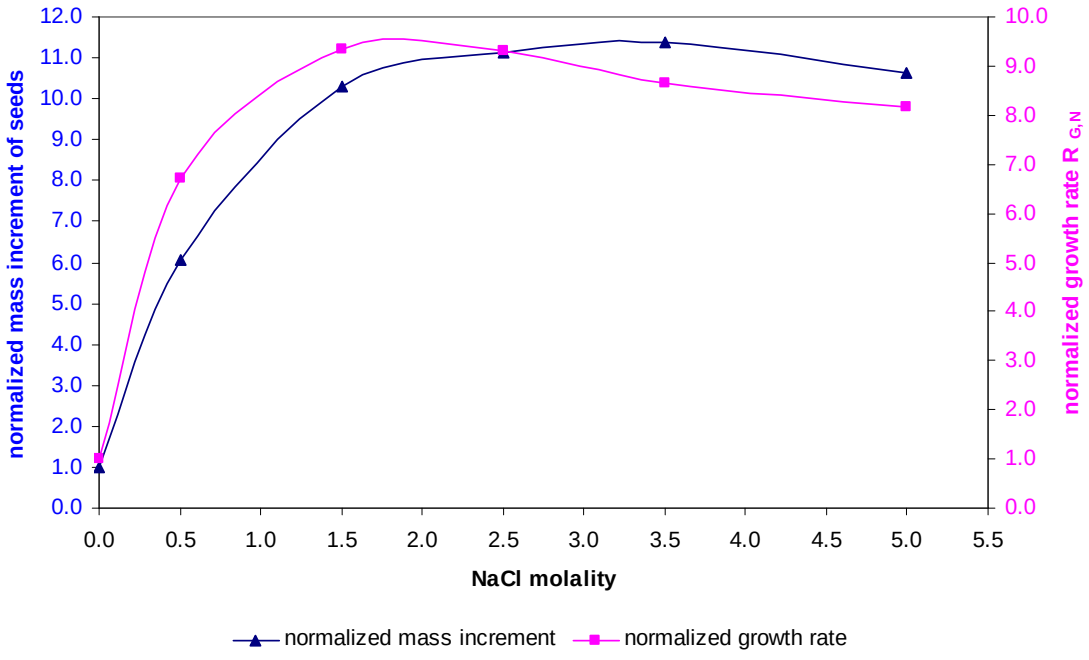

Figure 6-5-1 Normalized mass increment of γ-glycine seeds and normalized growth rate $R_{G,N}$ from various NaCl solutions at 25°C

The two curves in Figure 6-5-1, represented by normalized mass increment of γ-glycine seeds and normalized growth rate respectively, are reasonably close (though not overlapped), showing very similar trends. From both curves, it can be seen that γ-glycine crystals can grow much faster from NaCl solutions than from pure H_2O, in a wide range of NaCl concentrations.

More interestingly, γ-glycine growth rate initially increases with increase of NaCl concentration up to approximately 1.5m. With further increase of NaCl (>1.5m), γ-glycine growth rate reaches a plateau. When NaCl is very high (>2.5m), the growth rate tends to decrease with increase of NaCl concentration. These observations may be explained readily. On the one hand, with the addition of NaCl, the univalent ions from NaCl would create singly-charged ion-glycine complexes ($^{+}H_3NCH_2COONa$ and $ClH_3NCH_2COO^{-}$) which are building units for γ-glycine, thus promoting γ-glycine growth, as was analyzed in **Chapter 5**:

$$\begin{pmatrix} OOCCH_2NH_3 \\ H_3NCH_2COO \end{pmatrix} + Na^{+} + Cl^{-} \Leftrightarrow {}^{+}H_3NCH_2COONa + ClH_3NCH_2COO^{-} \qquad (5\text{-}3\text{-}4)$$

On the other hand, when NaCl concentration is very high, especially when it is much higher than that required for depletion of glycine molecules (zwitterions or cyclic dimers) in a solution via the formation of singly-charged ion-glycine complexes, some of the free ions (Na^{+} and Cl^{-}) can neutralize the singly-charged ion-glycine complexes to generate neutral complexes (ClH_3NCH_2COONa) which are not building units for γ-glycine and thus they may retard γ-glycine growth due to the decrease of building units:

$$Cl^{-} + {}^{+}H_3NCH_2COONa \Leftrightarrow ClH_3NCH_2COONa \qquad (6\text{-}5\text{-}1)$$

$$ClH_3NCH_2COO^- + Na^+ \Leftrightarrow ClH_3NCH_2COONa \quad (6\text{-}5\text{-}2)$$

Furthermore, adsorption of the extra free ions (Na^+ and Cl^-) onto the polar ends of γ-glycine crystals may become increasingly significant with Na^+ ions onto the carboxyl rich –c ends and Cl^- ions onto the amino rich +c ends, thus blocking the active growing facets of γ-glycine crystals and impeding γ-glycine growth. As a result, both the neutralization of singly-charged ion-glycine complexes (hence the decrease of building units for γ-glycine) and the blockage of the active growing facets of γ-glycine crystals would decrease the growth rate with increase of NaCl when the level of NaCl is very high.

Therefore, the promoting factors and inhibiting factors for γ-glycine growth compete with each other. At low NaCl, the promoting factors which facilitate creating building units for γ-glycine growth dominate the inhibiting factors. With increase of NaCl, the inhibiting factors start to be significant and tend to override the promoting factor. As a result, the trend of γ-glycine growth shows an initial increase, a plateau and a decrease, with increase of NaCl, as observed from Figure 6-5-1.

It should be pointed out that, with increase of NaCl, the solution viscosity would increase and it may play a part in inhibiting γ-glycine growth due to slow mass transfer. However, a study under similar conditions showed that the role of mass transfer was insignificant, since the effect of the agitating speed on γ-glycine growth from 5.0m NaCl

solution was practically negligible when it was increased from 260 rpm to 300 rpm (Tian, 2006).

6.6 Summary

The experimental results of γ-glycine crystal growth from different electrolyte solutions show that, generally 1:1 and 1:2 electrolytes have a much greater promoting effect on γ-glycine growth while 2:1 and 2:2 electrolytes have a much weaker influence on the enhancement of γ-glycine growth. Though different ions affect the growing faces of γ-glycine crystals differently, the results from the present study lend additional support to the mechanisms proposed in **Chapter 5**.

It was also revealed that, if an electrolyte in a solution is too high, it would start to impede γ-glycine growth. Therefore an optimization may be needed to determine the best dosage of an electrolyte for the fastest γ-glycine growth when the situation comes.

Chapter 7 Conclusions and Recommendations

Conclusions are drawn and recommendations are made as follows.

7-1 Conclusions

1) For measuring solution thermodynamic activity coefficients, a new and simple technique, namely steady state shifting technique, was developed to extend the application of the potentiometric (electrochemical) method from under-saturated solutions to supersaturated solutions. The new technique has been experimentally verified by comparing our results with literature data for under-saturated solutions. Its successful application to supersaturated solutions of three systems (NaCl+glycine+H_2O, NaCl+DL-serine+H_2O and NaCl+DL-analine+H_2O) has been demonstrated. New and interesting phenomena observed particularly for supersaturated solutions have been reported and discussed.

2) The very good thermodynamic consistency between activity and solubility for each of the three systems (NaCl+glycine+H_2O, NaCl+DL-serine+H_2O and NaCl+DL-analine+H_2O) would suggest that experimental measurements on both activity and solubility are accurate. It should be highlighted that, without supersaturated activity data, it is difficult to analyze thermodynamic consistency.

3) Via a rigorous thermodynamic approach, a further extension of the proposed steady state shifting technique was made so that it can be applicable to binary

nonelectrolyte solutions in the supersaturated region. Though obtaining binary activities in supersaturated region is the objective as the supersaturated binary activity data would be useful for crystallization study of a nonelctrolyte from H_2O, the obtained binary activity data for under-saturated solutions (DL-alanine+H_2O) reinforced the general validity of the proposed thermodynamic approach to extraction of binary nonelecetrolyte activity. Thus the proposed technique offers a convenient alternative to experimental thermodynamic studies for binary nonelectrolyte supersaturated solutions.

4) Based on the obtained activity data (especially the supersaturated activity data), an analysis of molecular interactions and the formation of different complexes was made, suggesting that γ-glycine polymorph produced from its aqueous solution with presence of a 1:1 electrolyte would be a general phenomenon. This analysis naturally guided the research to the systematic investigation of the effects of different electrolytes on glycine polymorphs.

5) The effects of electrolytes on glycine polymorphs were experimentally investigated. The results showed that 1:1 (e.g. KCl) and 1:2 (e.g. $(NH_4)_2SO_4$) electrolytes substantially induce γ-glycine, while 2:1 (e.g. $CaCl_2$) and 2:2 (e.g. MgSO4) electrolytes have a higher tendency to induce α-glycine. These results of glycine polymorphs are in good agreement with the reported ones (Bhat and Dharmaprakash, 2002a and 2002b; Moolya et al., 2005; Towler et al., 2004).

The mechanisms for these observed phenomena of glycine polymorphs were proposed based on molecular interactions (particularly ion-dipole interaction) and the chemistries of glycine polymorphs. As was suggested by the mechanisms, the valence(s) rather than other properties of the ions from an electrolyte primarily determine whether a particular glycine polymorph (among α- and γ-glyicne) can be preferentially formed from the electrolyte solutions, due to the significant effects of the electrolyte ions on building units and on the growing facets of glycine polymorphs. Eventually, the growth kinetics controls the nucleation onset of glycine polymorphs, which led to the quantitative evaluation of γ-glyicne growth rates from different electrolyte solutions.

6) Many experiments for γ-glycine crystal growth from different electrolyte solutions were carried out. As it is expected, generally, 1:1 and 1:2 electrolytes tremendously promote γ-glycine growth while 2:1 and 2:2 electrolytes have a much weaker influence on the enhancement of γ-glycine growth. Though different ions from electrolytes affect the growing faces of γ-glycine crystals differently, the kinetic data from this study suggest that the valence(s) of the ions from an electrolyte primarily determines the growth rate of γ-glycine, thus supporting the mechanisms proposed for glycine polymorphs from electrolyte solutions.

The kinetic study also revealed that an electrolyte at very high concentration would start to impede γ-glycine growth. Therefore the best dosage of an electrolyte exists for the fastest γ-glycine growth and it may be determined by optimization when it is needed.

7-2 Recommendations

1) Further generalization of the new technique

It is expected that the steady state shifting technique can be used for thermodynamic study for many other ternary electrolyte+nonelectrolyte+H_2O and binary nonelectrolyte+H_2O systems in their supersaturated regions, based on the framework established in this study. It is necessary to further generalize the technique, by using different ion selective electrodes (e.g. NO_3^-, K^+ and NH_4^+).

2) Effects of solvents

Solvents (or mixed solvents) can exert a big influence on thermodynamic behavior of supersaturated solutions (and polymorphs). It would be interesting and possible to look into the effects of different solvents on supersaturated solutions, using the proposed technique.

3) Thermodynamic modeling of supersaturated solutions

It is of practical importance to thermodynamically model supersaturated solutions. Literature data by UNIFAC model (Peng et al., 2001) and our preliminary study using NRTL model showed that generally these standard thermodynamic models are difficult to be applicable to supersaturated solutions. It seems necessary to develop new thermodynamic models for supersaturated solutions.

4) Investigation of other crystal systems

The mechanisms proposed for the effects of electrolytes on glycine polymorphs and γ-glycine kinetics should be relevant for understanding and controlling crystal polymorphs of other systems, as it may be generally implied that 1:1 electrolytes are likely to induce polar polymorphic crystals consisting of dipolar molecules. Therefore, investigation of the effects of 1:1 electrolytes on polymorphs and growth kinetics of other crystal systems is worthwhile.

References

Aber, J. E., Arnold, S., Garetz, B. A., Myerson, A. S., (2005). Strong dc Electric Field Applied to Supersaturated Aqueous Glycine Solution Induces Nucleation of the γ Polymorph. Physical Review Letters, **94**, 145503-1 - 145503-4.

Albright, J. G., Annunziata, O., Miller, D. G., Paduano, L., Pearlstein, A. J., (1999). Precision Measurements of Binary and Multicomponent Diffusion Coefficients in Protein Solutions Relevant to Crystal Growth: Lysozyme Chloride in Water and Aqueous NaCl at pH 4.5 and 25 °C. Journal of American Chemical Society, **121**, 3256-3266.

Al-Jibbouri, S. and Ulrich, J., (2001). The influence of impurities on crystallization kinetics of sodium chloride. Crystal Research and Technology, 36, 1365-1375.

Allen, R. N., Shukla, M. K., Burda, J. V., Leszczynski, J., (2006). Theoretical study of interaction of urate with Li^+, Na^+, K^+, Be^{2+}, Mg^{2+}, and Ca^{2+} metal cations. Journal of Physical Chemistry A, **110**, 6139-6144.

Annunziata, O., Paduano, L., Pearlstein, A. J., Miller, D. G., Albright, J. G., (2000). Extraction of Thermodynamic Data from Ternary Diffusion Coefficients. Use of Precision Diffusion Measurements for Aqueous Lysozyme Chloride-NaCl at 25°C To Determine the Change of Lysozyme Chloride Chemical Potential with Increasing NaCl Concentration Well into the Supersaturated Region. Journal of American Chemical Society, **122**, 5916-5928.

Bates, R. G., Dickson, A. G., Gratzl, M., Hrabeczy-Pall, A., Lindner, E., Pungor, E., (1983). Determination of mean activity coefficients with ion-selective electrodes. Analytical Chemistry, **55**, 1275-1280.

Bernstein, J., (2002). Polymorphism in Molecular Crystals. New York: Oxford University Press**.**

Bester-Rogac, M., Hauptman, N., Barthel, J., (2007). Conductometric study of ion association of divalent symmetric electrolytes: II. $MgSO_4$ in water plus 1,4-dioxane mixtures. Journal of Molecular Liquids, **131**, 29-35.

Bhat, N. M. and Dharmaprakash, S. M., (2002a). Growth of nonlinear optical γ-glycine crystals. Journal of Crystal Growth, **236**, 376-380.

Bhat, N. M. and Dharmaprakash, S. M., (2002b). Effects of solvents on the growth morphology and physical characteristics of nonlinear optical γ-glycine crystals. Journal of Crystal Growth, **242**, 245-252.

Black, S. N., Davey, R. J., Halcrow, M., (1986). The kinetics of crystal growth in the presence of tailor-made additives. Journal of Crystal Growth, **79**, 765-774.

Black, S. N. and Davey, R. J., (1988). Crystallisation of amino acids. Journal of Crystal Growth, **90**, 136-144.

Boldyreva, E. V.; Drebushchak, V. A.; Drebushchak, T. N.; Paukov, I. E.; Kovalevskaya, Y. A.; Shutova, E. S., (2003). Polymorphism of Glycine Thermodynamic aspects. Part I Relative stability of the polymorphs. Journal of Thermal Analysis and Calorimetry, **73**, 409-418.

Breil, M. P., Mollerup, J. M., Rudolph, E. S., Ottens, M., van der Wielen, L. A. M., (2001). Determination of the activity coefficients of glycylglycine and glycyl-L-alanine in sodium choloride solutions by an electrochemical cell with ion-selective electrodes: experimental measurements and thermodynamic theory. Fluid Phase Equilibria, **191**, 127-140.

Bui, A. V., Nguyen, H. M., Joachim, M., (2003). Prediction of water activity of glucose and calcium chloride solutions. Journal of Food Engineering, **57**, 243-248.

Burton, W. K., Cabrera, N., Frank, F. C., (1951). The Growth of Crystals and the Equilibrium Structure of their Surfaces**.** Philosophical Transactions of the Royal Society of London. Series A, Mathematical and Physical Sciences, **243**, 299-358.

Butler, J. N. and Roy, R. N., (1991). Experimental methods: Potentiometric. In Activity Coefficients In Electrolyte Solutions (2nd ed). CRC Press, Int. edited by K S Pitzer.

Carter, P. W., Hillier, A. C., Ward, M. D., (1994). Nanoscale Surface Topography and Growth of Molecular Crystals: The Role of Anisotropic Intermolecular Bonding. Journal of American Chemical Society, **116**, 944-953.

Chan, M. N., Choi, M. Y., Ng, N. L., Chan, C. K., (2005). Hygroscopicity of water-soluble organic compounds in atmospheric aerosols: amino acids and biomass burning derived organic species. Environmental Science & Technology, **39**, 1555-1562.

Chang, Y. C. and Myerson, A. S., (1985). The diffusivity of potassium chloride and sodium chloride in concentrated, saturated and supersaturated aqueous solutions. American Institute of Chemical Engineers Journal, **31**, 890-894.

Chang, Y. C. and Myerson, A. S., (1986). Diffusivity of glycine in concentrated saturated and supersaturated aqueous solutions. American Institute of Chemical Engineers Journal, **32**, 1567-1569.

Chew, J. W., Black, S. N., Chow, P. S., Tan, R. B. H., Carpenter, K. J., (2007). Stable polymorphs: difficult to make and difficult to predict. CrystEngComm, **9**, 128–130.

Cohen, M. D., Flagan, R. C., Seinfeld, J. H., (1987). Studies of concentrated electrolyte solutions using the electrodynamic balance. 1. water activities for single-electrolyte solutions. The Journal of Physical Chemistry, **91**, 4563-4574.

Cohn, E. J. and Edsall, T. J., (1943). Proteins, Amino Acids and Peptides as Ions and Dipolar Ions. Hafner, New York.

Dawson, A., Allan, D. R., Belmonte, S. A., Clark, S. J., David, W. I. F., McGregor, P. A., Parsons, S., Pulham, C. R.; Sawyer, L., (2005). Effect of High Pressure on the Crystal Structures of Polymorphs of Glycine. Crystal Growth and Design, **5**, 1415-1427.

Davey, R. J., Blagden, N., Potts, G. D., Docherty, R., (1997). Polymorphism in Molecular Crystals: Stabilization of a Metastable Form by Conformational Mimicry. Journal of American Chemical Society, **119**, 1767-1772.

Desiraju, G. R., (1997). Crystal gazing: Structure prediction and polymorphism. SCIENCE, **278**, 404-405.

Doki, N., Yokota, M., Kido, K., Sasaki, S., Kubota, N. (2004). Reliable and selective crystallization of the metastable α-form glycine by seeding. Crystal Growth & Design, **4** 103-107.

Ellerton, H. D., Reinfelds, G., Mulcahy, D. E., Dunlop, P. J., (1964). Activity, density, and relative viscosity data for several amino acids, lactamide, and raffinose in aqueous solution at 25 °C. The Journal of Physical Chemistry, **68**, 398-402.

Ferrari, E. S. and Davey, R. J., (2004). Solution-Mediated Transformation of α to β L-Glutamic Acid: Rate Enhancement Due to Secondary Nucleation. Crystal Growth & Design, **4**, 1061-1068.

Ferreira, L. A., Macedo, E. A., Pinho, S. P., (2005). Effect of KCl and Na2SO4 on the solubility of glycine and DL-alanine in water at 298.15 K. Industrial & Engineering Chemistry Research**, 44**, 8892-8898.

Garside, J., Mersmann, A., Nyvlt, J., (2002). Measurement of crystal growth and nucleation rates (2nd ed.). Rugby : Institution of Chemical Engineers.

Gidalevitz, D., Feidenhans, R., Matlis, S., Smilgies, D., Christensen, M. J., Leiserowitz, L., (1997)**.** Monitoring In Situ Growth and Dissolution of Molecular Crystals: Towards Determination of the Growth Units. Angewandte Chemie International Edition in English, **36**, 955-959.

Ginde, R. M. and Myerson, A. S., (1991). Viscosity and diffusivity in metastable solutions. AIChE Symposium Series, **284**. Particle Design via Crystallization, **87**, 124-129.

Ginde, R. M. and Myerson, A. S., (1992). Cluster size estimation in binary supersaturated solutions. Journal of Crystal Growth, **116**, 41-47.

Goodisman, J., (1987). Electrochemistry: theoretical foundations. John Wiley & Sons, Inc.

Granberg, R. A., Ducreux, C., Gracin, S., Rasmuson, A. C., (2001). Primary nucleation of paracetamol in acetone-water mixtures. Chemical Engineering Science, **56**, 2305-2313.

Grant, M. L., (2000). Effects of thermodynamic nonideality in protein crystal growth. Journal of Crystal Growth, **209**, 130-137.

Haghtalab, A. and Vera, J. H., (1991). Mean activity coefficients in the ternary NaCl-$NaNO_3$-H_2O and NaBr-$NaNO_3$-H_2O systems at 298.15K. Journal of Chemical and Engineering Data, **36**, 332-340.

Han, S. and Pan, H., (1993). Thermodynamics of the sodium bromide-methanol-water and sodium bromide-ethanol-water two ternary systems by the measurements of electromotive force at 298. 15K. Fluid Phase Equilibria, **83**, 261-270.

Han, G. and Tan, R. B. H. (2006). A steady state shifting technique for the potentiometric method: application to supersaturated solutions**.** Chemical Engineering Science, **61**, 6530-6539.

He, G., Bhamidi, V., Wilson, S. R., Tan, R. B. H., Kenis, P. J. A., Zukoski, C. F., (2006). Direct Growth of γ-Glycine from Neutral Solutions by Slow Evaporation-Driven Crystallization. Crystal Growth and Design, **6**, 1746-1749**.**

Hounslow, M. J., Lewis, A. E., Sanders, S. J., Bondy, R., (2005). Generic Crystallizer Model: I. A Model Framework for a Well-Mixed Compartment. American Institute of Chemical Engineers Journal, **51**, 2942-2955.

Izmailov, A. F. and Myerson, A. S., (1999). Thermodynamic and statistical studies of supersaturated ternary solutions. PHYSICAL REVIEW E, **60**, 3211-3218.

Ji, X., Lu, X., Lin, W., Zhang, L., Wang, Y., Shi, J., Lu, B., (2001). Mean activity coefficients of NaCl in (sodium chloride + sodium bicarbonate + water) from T = (293.15 to 308.15) K. The Journal of Chemical Thermodynamics, **33**, 1107-1119.

Jones, A. G., Budz, J., Mullin, J. W., (1986). Crystallization kinetics of potassium-sulfate in an msmpr agitated vessel. American Institute of Chemical Engineers Journal, **32**, 2002-2009.

Kelly, F. J., Robinson, R. S., Stokes, R. H., (1961). The thermodynamics of the ternary system maknitolsodiuam chloride-water at 25 °C from solubility and vapor pressure measurements. J . Phys. Chem., **66**, 1958-1960.

Khoshkbarchi, M. K. and Vera, J. H., (1996a). Measurement and modeling of activities of amino acids in aqueous salt systems. American Institute of Chemical Engineers Journal, **42**, 2354-2364.

Khoshkbarchi, M. K. and Vera, J. H., (1996b). Measurement of activity coefficients of amino acids in aqueous electrolyte solutions: experimental data for the systems H_2O+NaCl+Glycine and H_2O+NaCl+DL-Alanine at 25^oC. Industrial & Engineering Chemistry Research, **35**, 2735-2742.

Khoshkbarchi, M. K. and Vera, J. H., (1997). Effect of NaCl and KCl on the solubility of amino acids in aqueous solutions at 298.2K: measurements and modeling. Industrial & Engineering Chemistry Research, **36**, 2445-2451.

Khoshkbarchi, M. K., Soto-Campos, A. M., Vera, J. H., (1997) . Interactions of DL-serine and L-serine with NaCl and KCl in aqueous solutions. Journal of Solution Chemistry, **26**, 941-955.

Knapman, K., (2000). Polymorphic predictions - Understanding the nature of crystalline compounds can be critical in drug development and manufacture. Modern Drug Discovery, **3**, 53-54.

Knezic, D., Zaccaro, J., Myerson, A. S., (2004). Thermodynamic properties of supersaturated protein solutions. Crystal Growth & Design, **4**, 199-208.

Koop, T., Luo, B., Tsias, A., Peter T., (2000). Water activity as the determinant for homogeneous ice nucleation in aqueous solutions. Nature, **406**, 611-614.

Kubota, N. and Mullin, J. W., (1995). A kinetic model for crystal growth from aqueous solution in the presence of impurity. Journal of Crystal Growth, **152**, 203-208.

Kubota, N., (2001). Effect of impurities on the growth kinetics of crystals. Cryst. Res. Technol., 36, 749-769.

Kuramochi, H., Noritomi, H., Hoshino, D., Nagahama, K., (1997). Measurements of Vapor Pressures of Aqueous Amino Acid Solutions and Determination of Activity Coefficients of Amino Acids. J. Chem. Eng. Data, **42**, 470-474.

Kuznetsov, V. A., Okhrimenko, T. M., Rak, M., (1998). Growth promoting effect of organic impurities on growth kinetics of KAP and KDP crystals. Journal of Crystal Growth, **164**, 164-173.

Lahav, M. and Leiserowitz, L., (2001). The effect of solvent on crystal growth and morphology. Chemical Engineering Science, **56**, 2245-2253.

Lampreia, I. M. S., Magalhaes, Rodrigues, S. I. M., Mendoca, A. F. S. S., (2006). Solubility of proline-leucine dipeptide in water and in aqueous sodium chloride solutions from T = (288.15 to 313.15) K. Journal of Chemical Thermodynamics, **38**, 240-244.

Larson, M. A. and Garside, J., (1986). Solute clustering in supersaturated solutions. Chemical Engineering Science, **41**, 1285-1289.

Lu, G. W., Xia, H. R., Zhang, S. Q., Sun, X., Gao, Z. S., Wang, J. Y., (2001). Raman scattering investigation of the effect of EDTA additives on growth habit of KDP. Journal of Crystal Growth, **233**, 730-736.

Martins, P. M. and Rocha, F., (2006). The role of diffusional resistance on crystal growth: Interpretation of dissolution and growth rate data. Chemical Engineering Science, **61**, 5686-5695.

Martins, P. M., Rocha, F. A., Rein, P., (2006). The influence of impurities on the crystal growth kinetics according to a competitive adsorption model. Crystal Growth & Design, **6**, 2814-2821.

Meenan, P. A., Anderson, S. R., Klug, D. L., (2002). The influence of impurities and solvents on crystallization. In Handbook of Industrial Crystallization (2nd ed.), edited by Myerson, A. S. Boston : Butterworth-Heinemann.

Mohan, R. and Myerson, A. S., (1999). The effect of additives on the water activity of supersaturated solutions of beta-succinic acid. Journal of Crystal Growth, **206**, 99-108.

Mohan, R., Kaytancioglu, O., Myerson, A. S., (2000). Diffusion and cluster formation in supersaturated solutions of ammonium sulfate at 298K. Journal of Crystal Growth, **217**, 393-403.

Mohan, R. and Myerson, A. S., 2002. Growth kinetics: a thermodynamic approach. Chemical Engineering Science, **57**, 4277-4285.

Moolya, B. N., Jayarama, A., Sureshkumar, M. R. Dharmaprakash, S. M., (2005). Hydrogen bonded nonlinear optical γ-glycine: Crystal growth and characterization. Journal of Crystal Growth, **280**, 581–586.

Mullin, J. W., (1993). Crystallization**.** 3rd ed. London, Butterworths.

Mullin, J. W. and Sohnel, O., (1977). Expressions of supersaturation in crystallization studies. Chemical Engineering Science, **32**, 683-686.

Myerson, A. S. and Ginde, R., (2002). Crystals, crystal growth and nucleation. In Handbook of Industrial Crystallization (2nd ed.), edited by Myerson, A. S. Boston : Butterworth-Heinemann.

Myerson, A. S. and Lo, P. Y., (1991). Cluster formation and diffusion in supersaturated binary and ternary amino acid solutions. Journal of Crystal Growth, **110**, 26-33.

Myerson, A. S. and Izmailov, A. F., (1997). Relationship between diffusivity and viscosity for supersaturated electrolyte solutions. Journal of Crystal Growth, **174**, 369-379.

Na, H., Arnold, S., Myerson, A. S., (1994). Cluster formation in highly supersaturated solution droplets. Journal of Crystal Growth, **139**, 104-112.

Na, H., Arnold, S., Myerson, A. S., (1995). Water activity in supersaturated aqueous solutions of organic solutes. Journal of Crystal Growth, **149**, 229-235.

Natarajan, S. and Rao, J. K. M., (1980). Crystal Structure of bis(glycine)calcium(II)dichloride tetrahydrate. Zeitschrift fur Kristallographie, **152**, 179-188.

Natarajan, S., (1983). X-ray study and IR spectra of glycine calcium nitrate dihydrate. Zeitschrift fur Kristallographie, **163**, 305-306.

Ohgaki, K., Makihara, Y., Morishita, M., (1991). Solute clusters in aqueous citric-acid solutions. Chemical Engineering Science, **46**, 3283-3287.

Ohgaki, K., Hirokawa, N., Ueda, M., (1992). Heterogeneity in aqueous solutions: electron microscopy of citric acid solutions**.** Chemical Engineering Science, **47**, 1819-1823.

Öncül, A. A., Sundmacher, K., Thévenin, D., (2005). Numerical investigation of the influence of the activity coefficient on barium sulphate crystallization. Chemical Engineering Science, **60**, 5395-5405.

Ong, S. L., (2007). Experimental study on the effects of supersaturation on thermodynamic activity for ternary aqueous solutions. A Report of Final Year Project. Department of Chemical and Biomolecular Endginnering, National University of Singapore.

Ottens, M., Lebreton, B., Zomerdijk, M., Rijkers, M. P. W. M., Bruinsma, O. S. L., van der Wielen, L. A. M., (2004). Impurity Effects on the Crystallization Kinetics of Ampicillin. Industrial & Engineering Chemistry Research, **43**, 7932-7938.

Peng, C., Chan, M. N., Chan, C. K., (2001). The hygroscopic properties of dicarboxylic and multifunctional acids: measurements and UNIFAC predictions. Environmental Science & Technology, **35**, 4495-4501.

Phang, S. and Steel, B. J., (1974). Activity coefficients from e.m.f. measurements using cation-responsive glass electrode. NaCl+glycine+water at 273.15, 283.15, 298.15 and 323.15 K. The Journal of Chemical Thermodynamics, **6**, 537-548.

Piquemal, J. P., Perera, L, Cisneros, G. A., (2006). Towards accurate solvation dynamics of divalent cations in water using the polarizable amoeba force field: From energetics to structure. Journal of Chemical Physics, **125**, Art. No. 054511.

Prausnitz, J. M., Lichtenthaler, R. N., Azevedo, E. G., (1999). Molecular thermodynamics of fluid-phase equilibria. Printice Hall PTR. New Jersey. 4th ed. pp. 508 – 511.

Qin, Y. and Rasmuson, Å. C., (1990). Growth and dissolution of succinic acid crystals in a batch stirred crystallize. American Institute of Chemical Engineers Journal, **36**, 665 – 676.

Qu, H., Louhi-Kultanen, M., Kallas, J., (2006). In-line image analysis on the effects of additives in batch cooling crystallization. Journal of Crystal Growth, **289**, 286-294.

Rak, M., Eremin, N. N, Eremina, T. A., Kuznetsov, Okhrimenko, V. A., Furmanova, N. G., Efremova, E. P., (2005). On the mechanism of impurity influence on growth kinetics and surface morphology of KDP crystals—I: defect centres formed by bivalent and trivalent impurity ions incorporated in KDP structure—theoretical study. Journal of Crystal Growth, **273,** 577–585.

Rao, J. K. M. and Natarajan, S., (1980). Structure of tris(glycine)calcium(II) Dibromide. Acta Cryst., **B36**, 1058-1061.

Rard, J. A. and Platford, R. F., (1991). Experimental methods: Isopiestic. In Activity Coefficients In Electrolyte Solutions (2nd ed). CRC Press, Int. edited by K S Pitzer.

Roberts, R. M. and Kirkwood, J. G., (1941). The Activity of Glycine in Aqueous Solutions of Potassium Chloride, from Electromotive Force Measurements. Journal of American Chemical Society, **63**, 1373-1375.

Rodriguez-Raposo, R., Fernandez-Merida, L., Esteso, M. A., (1994). Activity coefficients in(electrolyte + amino acid) (aq). The dependence of the ion-zwitterion interactions on the ionic strength and on the molality of the amino acid analysed in terms of Pitzer's equation. The Journal of Chemical Thermodynamics, **26**, 1121-1128.

Robinson, R. A. and Stokes, R. H., (1961). Activity coefficients in aqueous solutions of sucrose, mannitol axd their mixtures at 25 °C. J . Phys. Chem., **66**, 1954-1958.

Roelands, C. P. M, Horst, J. H. T, Kramer, H. J. M., Jansens, P. J., (2007). Precipitation Mechanism of Stable and Metastable Polymorphs of L-Glutamic Acid. American Institute of Chemical Engineers Journal, **53**, 354-362.

Sakai, H., Hosogai, H., Kawakita, T. (1991). Transformation of α-glycine to γ-glycine. Journal of Crystal Growth, **116**, 421-426.

Sandler, S. I., (2003). Quantum mechanics: a new tool for enginnering thermodynamics. Fluid Phase Equilibria, **210**, 147-160.

Sangwal, K., (1996). Effects of impurities on crystal growth processes. Progress in Crystal Growth and Characterization of Materials, **32,** 3-43.

Sangwal, K., (1999). Kinetic effects of impurities on the growth of single crystals from solutions. Journal of Crystal Growth, **203**, 197-212.

Sangwal, K. and Mielniczek-Brzoska, E., (2001). On the effect of Cu(II) impurity on the growth kinetics of ammonium oxalate monohydrate crystals from aqueous solutions. Crystal Research and Technology, **36**, 837-849.

Scherier, E. E. and Robison, R. A., (1971). A study of free energy relationships in some amino acid-sodium chloride-water systems. The Journal of Biological Chemistry, **246**, 2870-2874.

Scott, C. and Black, S., (2005): In-line analysis of impurity effects on crystallization. Organic Process Research & Development, **9**, 890-893.

Shimon, L. J. W., Wireko, F. C., Wolf, J., Addadi, L., Berkovitch-Yellin, Z., Lahav, M., Leiserowitz, L., (1986). Assignment of absolute structure of polar crystals using tailor-made additives. Solvent-surface interactions on the polar crystals of α-resorcinol, (R,S) alanine and γ-glycine. Mol. Cryst. Liq. Cryst. **137**, 67-86.

Smith, E. R. B. and Smith, P. K., (1937a). The activity of glycine in aqueous solution at twenty-five degrees. The Journal of Biological Chemistry, **117**, 209-216.

Smith, P. K. and Smith, E. R. B., (1937b). Thermodynamic properties of solutions of amino acids and related substances. ii. the activity of aliphatic amino acids in aqueous solution at twenty-five degrees. The Journal of Biological Chemistry, **121,** 607-613**.**

Smith, P. K. and Smith, E. R. B., (1940). Thermodynamic properties of solutions of amino acids and related substances. The Journal of Biological Chemistry, **132, 5**7-64**.**

Sorell, L. S. and Myerson, A. S., (1982). Diffusivity of urea in concentrated, saturated and supersaturated aqueous solutions. American Institute of Chemical Engineers Journal, **28**, 772-778.

Sum, A. K. and Sandler, S. I., (1999). Use of *ab initio* methods to make phase equilibria predictions using activity coefficient models. Fluid Phase Equilibria, **158-160**, 375-380.

Sun, X., Garetz, B. A., Myerson, A. S., (2006). Supersaturation and Polarization Dependence of Polymorph Control in the Nonphotochemical Laser-Induced Nucleation (NPLIN) of Aqueous Glycine Solutions. Crystal Growth & Design, **6**, 685-689.

Tavare, N. S., (1995). Industrial Crystallization – Process Simulation Analysis and Design. Plenum Press, New York.

Thompson, C., Davies, M. C., Roberts, C. J., Tendler, S. J. B., Wilkinson, M. J., (2004). The effects of additives on the growth and morphology of paracetamol (acetaminophen) crystals. International Journal of Pharmaceutics **280** 137–150.

Tian, F., (2006). Kinetics Study on Crystallization of Polymorphic Crystals. A Report of Final Year Project. Department of Chemical and Biomolecular Endginnering, National University of Singapore.

Tjahjono, M., Guo, L., Garland, M., (2005). The development of a response surface model for the determination of infinite dilution partial molar volumes and excess volumes from dilute multi-component data alone. Implications for the characterization of non-isolatable solutes in complex homogeneous reactive systems. Chemical Engineering Science, **60**, 3239-3249.

Towler, C. S., Davey, R. J., Lancaster, R. W., Price, C. J., (2004). Impact of molecular speciation on crystal nucleation in polymorphic systems: the conundrum of γ glycine and molecular 'self poisoning'. Journal of American Chemical Society, **126**, 13347-13353.

Veverka, V., Sohnel, O, Bennema, P, Garside, J., (1991). Concentration Gradients in Supersaturated Solutions: a Thermodynamic Analysis. American Institute of Chemical Engineers Journal, **37**, 490-498

Weissbuch, I., Zbaida, D., Addadi, L., Leiserowitz, L., Lahav, M. (1987). Design of Polymeric Inhibitors for the Control of Crystal Polymorphism. Induced Enantiomeric Resolution of Racemic Histidine by Crystallization at 25 °C. Journal of American Chemical Society**, 109,** 1869-1871.

Weissbuch, I., Leisorowitz, L., Lahav, M., (1994a). "Tailor-Made" and Charge-Transfer Auxiliaries for the Control of the Crystal Polymorphism. Advanced Materials, **6**, 952-956.

Weissbuch, I., Popvitz-Biro, R., Leiserowitz, L., Lahav, M., (1994b). In The Lock and Key Principle; Behr, J. P., Ed.; John Wiley & Sons: New York, 1994: pp 173-246.

Weissbuch, I., Popvitz-Biro, R., Lahav, M., Leiserowitz, L., (1995). Understanding and Control of Nucleation, Growth, Habit, Dissolution and Structure of Two- and Three-Dimensional Crystals Using 'Tailor-Made Auxiliaries. Acta Cryst. **B51**, 115-148.

Weissbuch, I., Lahav, M., Leiserowitz, L., (2003). Toward Stereochemical Control, Monitoring, and Understanding of Crystal Nucleation. Crystal Growth & Design, **3**, 125-150.

Weissbuch, I., Torbeev, V.Y., Leiserowitz, L., Lahav, M., (2005). Solvent Effect on Crystal Polymorphism: Why Addition of Methanol or Ethanol to Aqueous Solutions Induces the Precipitation of the Least Stable b Form of Glycine. Angew. Chem. Int. Ed., 2005, **44**, 3226 –3229.

Zaccaro, J., Matic, J., Myerson, A. S., Garetz, B. A., (2001). Nonphotochemical, laser-induced nucleation of supersaturated aqueous glycine produces unexpected γ-glycine. Crystal Growth & Design, **1**, 5-8.

Zemaitis, J. F., Jr, Clark, D. M., Refal, M., Scrivner, N. C., (1986). Handbook of aqueous electrolyte thermodynamics. Design Institute for Physical Property Data sponsored by the American Institute of Chemical Engineers. New York.

Appendix A Solubility Test

An isothermal method was used to measure the solubility of an amino acid in a given electrolyte solution at 25 °C. There were three major stages involved in the method for solubility test: solid-liquid equilibration, determination of solution concentration and examination of crystal polymorphs. Solubilities of three amino acids, glycine, DL-serine and DL-alanine in various electrolyte solutions were tested at 25 °C.

A1. Equilibration between crystals and liquid

The equilibration may be either a dissolution process for crystals to dissolve or a solution desupersaturation process for the crystals to grow at the given temperature of interest. Either process eventually reaches the solid-liquid equilibrium at which the concentration of the solute of interest is the solubility.

A1-1 Equilibration via crystal dissolution

Sufficient excess of crystals of an amino acid was put in a given electrolyte solution (approximately 130 g) in a jacketed glass container (a 250 ml warming beaker). The suspension solution was agitated by a magnetic stirrer to allow the solid-liquid equilibrium to be attained fast, while the temperature of the solution was maintained at 25 °C using a water circulator (temperature readability of 0.1 °C). The crystals were dissolved into the solution till the solid-liquid equilibration was reached. The jacketed glass container was kept sealed throughout the experiment to avoid evaporation.

A1-2 Equilibration via solution desupersaturation

Sufficient excess of crystals of an amino acid was put in a given electrolyte solution (approximately 130 g) in a jacketed glass container (a 250 ml warming beaker). While the suspension solution agitated by a magnetic stirrer, it was first heated up to about 30 °C and maintained for approximately 2 hours to make the solution concentrated (higher than solubility at 25 °C); then the suspension solution was cooled down to and maintained at 25 °C using a water circulator for the crystals in the solution to keep growing till the solid-liquid equilibration was reached. The jacketed glass container was kept sealed throughout the experiment to avoid evaporation.

A2 Determination of solution concentration

A2-1 Measurement of solution density

After the solid-liquid equilibrium was reached via either crystal dissolution or solution desupersaturation, the agitation was stopped to allow the suspended crystals to settle. The clear supernatant saturated solution, withdrawn using a disposable syringe (B.Braun, 2ml), was injected into the Anton-Paar DMA5000 precise density meter to measure the solution density, through a disposable nylon syringe filter (FroFill, pore size 0.22μm). This density meter has a density accuracy of $\pm 10^{-6}$ g/ml. The temperature in the measuring tube of the meter was kept at 25.000±0.001°C, using the built-in temperature control system. The concentration of the saturated solution, i.e. the solubility, was then determined using a pre-determined correlation curve of solution density vs solution concentration at a given electrolyte molality (refer to Section A2-2 for correlation). Compared with the commonly used solution-drying method for

concentration determination (Khoshkbarchi and Vera, 1997; Ferreira, et al., 2005), using solution density has obvious advantages: no concern about thermal degradation of the sample; overcoming the uncertainty due to insufficient removal of the trapped solvent among the crystal particles. In fact, excellent reproducibility and high accuracy of concentration measurement using solution density have been reported (Lampreia et al., 2006; Tjahjono et al., 2005).

A2-2 Correlation of solution density vs solution concentration

For a given electrolyte solution (its density d_0 at 25 °C can be obtained using the density meter), standard solutions (at least 3) of an amino acid were prepared using the same electrolyte solution. The solution density of any of the standard solutions was measured, denoted as d. Data for a typical correlation of solution density deference Δd ($\Delta d = d - d_0$, g/ml) with glycine concentration c (g/100g H_2O) were shown in Table A-1 and plotted in Figure A-1. The obtained correlation was nicely straight, $\Delta d = 0.0020672385c + 0.0117321440$, with correlation coefficient $R^2 = 0.99996$. In fact, excellent straight correlation lines were also obtained for general systems of (electrolyte+amino acid+H2O) at 25 °C, with correlation coefficient R^2 of about 0.9999. These correlation curves were then used to determine the concentrations of an amino acid in given electrolyte aqueous solutions.

Table A-1 density of solution (glycine+2.5m NaCl) vs glycine concentration at 25 °C (Density of 2.5m NaCl, d_0 = 1.089194 g/ml at 25 °C)

glycine concentration (c, g/100g H_2O) of standard solutions	Density of (2.5m NaCl+glycine+H_2O), g/ml, at 25 °C	Density difference, $\Delta d = d - d_0$, at 25 °C
24.566	1.151697	0.062503
25.484	1.153624	0.064430
25.902	1.154478	0.065284
26.572	1.155860	0.066666
27.007	1.156745	0.067551

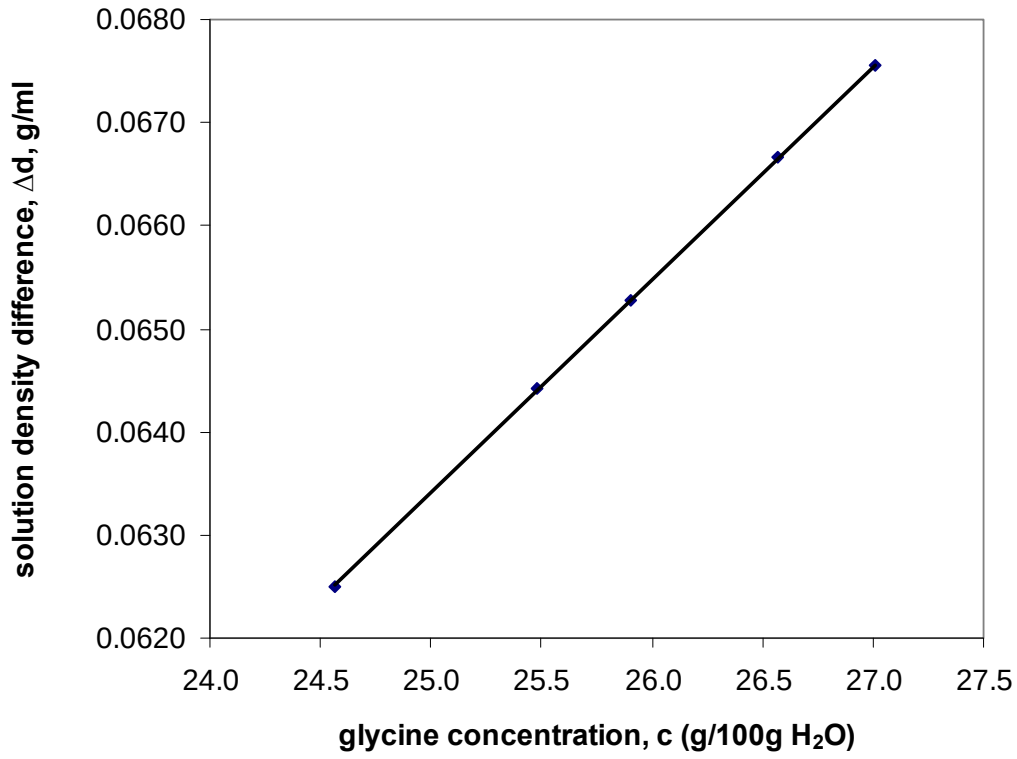

Figure A1 Correlation of solution density difference vs glycine concentration in 2.5m NaCl solution at 25 °C.

A3 Examination of crystal polymorphs

It should be pointed out that powder-XRD was performed to check the polymorphs of crystals of these amino acids (especially glycine) before and after the solid-liquid equilibration, as an amino acid may have different polymorphs which have different solubilities (Sakai, et al., 1991). It is necessary to examine the polymorphs of crystals before and after solid-liquid equilibration because the transformation from one polymorph to another may occur during solid-liquid equilibration. The polymorph should be controlled for reliable and accurate solubility measurement. XRD examination of the raw γ-glycine, DL-serine and DL-alanine and their crystals collected from the saturated solutions confirmed that there were no polymorph changes, which addressed the concern on polymorph transition.

A4 Discussion

It was found that it took about 24 hours for the crystals to dissolve and reach the equilibrium in an aqueous electrolyte solution. In order to ensure the equilibrium was reached, the equilibration lasted for at least 48 hours. As expected, excellent reproducibility of the solubility data was achieved, with a very small absolute mean deviation (less than 0.02g/100g H_2O). The uncertainty of solubility of an amino acid in an electrolyte solution increased (nearly linearly) with electrolyte molality. Generally, it was estimated that the uncertainty of the solubility in a concentrated electrolyte (e.g. 5m NaCl) solution was not bigger than 0.04g/100g H_2O.

It was also noted that dissolution and desupersaturation paths produced practically the same solubility data. As impurity incorporation could occur during crystal growth (here desupersaturation process), the negligible difference between solubility data produced by dissolution and desupersaturation would be another evidence suggesting that the incorporation (if any) of these electrolytes into amino acid lattices was insignificant.

It should be pointed out that, α-glycine is thermodynamically metastable and it can quickly converted into γ-glycine in many electrolyte solutions. Therefore, the solubility of α-glycine in these electrolyte solutions could only be approximately screened by dissolving α-glycine crystals in an electrolyte solution in a short period of time (about one hour rather than 24 or 48 hours) before the solution sample was taken for concentration determination. As the rate of α-glycine dissolution was fast, it was reasonably assumed that the solution concentration after one hour of dissolution was quite close to the solubility. The solubility of α-glycine obtained in this way was generally underestimated. Nevertheless, these screened solubility data of α-glycine were still useful for reliable study on glycine polymorphs from electrolyte solutions (**Chapter 6**).